Elastomer-based pneumatic device to measure the mechanical properties of cell monolayers

Thèse N° 9443

Francesca SORBA

2019

(EPFL

ÉCOLE POLYTECHNIQUE
FÉDÉRALE DE LAUSANNE

Acknowledgements

This research project would not have been possible without the help and support of many kind people around me.

Above all, I would like to express my deep gratitude to my supervisors Dr. Cristina Martin-Olmos and Prof. Herbert Shea for their guidance and advice throughout the thesis. I would like to heartily thank Cristina, who mentored me for the last four years and a half, since my master thesis. She gave me the opportunity to join the group in CSEM and work on this exciting project. Thank you for your availability, your constant scientific and human support, positivity and endless trust. I learned a lot from you and I deeply appreciate how you always encouraged me in taking new challenges and always believed in my success. I would like to thank my professor Herbert Shea, for the time he dedicated me and for guiding me throughout this project with great scientific expertise, constructive discussions and a lot of enthusiasm.

I am very thankful to my internal and external jury examiners Prof. Giovanni Boero, Prof. Philippe Renaud, Prof. Alexandra Kämpfer-Homsy and Dr. Jens Möller who kindly accepted to review and evaluate this thesis.

I would like to thank the current members of the group and current group leader Michel Despont who supported me and gave me several scientific advices throughout the work. Many thanks to Martine Jungo, Nemanja Niketic, Arno Hoogerwerf, Bane Timotijevic, Timothée Frei, Sarah Heub, Amir Ghadimi and Diane Ledroit. A special thank to Réal Ischer for his help in the design and construction of set-ups, to Gilles Weder for his advices on the biological applications of my work, Dara Bayat for his kind help with with Comsol simulations and for being a great office mate and to Jasmine Kernen for her advices in protocol preparation and fluorescence imaging. I am extremely grateful for the many experiments and work who would not have been possible without all of you and for the good time spent together. Also thanks for your trust and great work together on the Submarine project.

Things changed a lot since when I started working in CSEM. I would like to heartily thank my first group lead by Martha Liley and the group members who were not part of the team until the end of my thesis, Rita Smajda, Mélanie Favre, Silvia Angeloni, Patricia Schneider and especially Marta Giazzon for teaching me how to work with cells from the basics and for bringing her good mood everyday at work.

I owe particular thanks to my LMTS colleagues for the stimulating and pleasant working environment. Thank you Nadine Besse, Alexis Marette, Juan Zarate, Sam Schlatter, Bekir

Acknowledgements

Abstract

This thesis brings advances in the field of microsystems for mechanobiology by providing a miniaturized cell stretcher for measuring living cell monolayers Young's modulus over time. The presented device provides the first demonstration that standard mechanical testing techniques can be integrated within a miniaturized device and interfaced with living cells, opening the door for diagnosis and drug screening applications in mechanobiology.

Everyday life physiological functions such as breathing, muscle contraction, and blood circulation rely on the ability of single cells to organize into higher complexity structures, sustain and perform mechanical deformations. Cell monolayers are the simplest tissues in the body and play a critical role since the embryogenesis stage, when they drive differentiation into organs, to acting as physical barriers and partitioning organs in the adults. Because of their specific interface location, cell monolayers stabilize tissues by sustaining external physiological stresses. While it is known that altered elasticity from cells to tissues is closely related to anomalous behaviour and diseases, the advancements in the field are still quite slow. This is mainly due to the fact that current techniques for measuring cell and tissue mechanics rely on complex and bulky measurement platforms with low repeatability rate, difficult integration with standard cell protocols and limited measurement time-scales.

This thesis presents the development of the design, fabrication processes and biological tests of a compact device for measuring cell monolayers Young's modulus which overcomes the main challenges of existing techniques.
The measurements principle is based on planar deformation of cell monolayers by pneumatic actuation and strain optical read-out. Cell monolayers adhere to a deformable membrane specially designed to be soft ($\sim$ 30 kPa) and thin ($\sim$ 5-10 μm) as the layer of cells to achieve high sensitivity in measuring cell contribution to the overall membrane mechanical properties. The core of our technology is the use of differential strain measurements between a region of the substrate covered with cells and a bare region. During the actuation, the strains of both regions are optically measured by a pattern recognition algorithm. This allows to measure the mechanical properties of the adherent cell layer by subtracting the contribution of the membrane itself. Furthermore, the use of a differential read-out makes it possible to avoid complex force measurement equipment, thus making the whole device more compact and compatible with long time measurements in sterility conditions.

Abstract

We report measurements of the Young's modulus of two cell types. The results show that cell monolayer Young's modulus for both cell types is around one order of magnitude higher than in single cells (such as obtained by atomic force microscopy). This indicates the relevant contribution of cell anisotropy and conformation to their mechanical response.
In addition, changes in Young's modulus due to external additional chemical and physical stimulations have been explored. In particular, chemicals targeting precise proteins have been used to determine their contribution to the overall mechanical properties of the cell layer. Physical stimulation is also tested by cyclically stretching the cells for 1 hour and by decreasing the temperature to 33°C, both experiments resulted in an increase of the cell Young's modulus. This was a reversible modification, cell mechanical properties returned to their initial values after the restoration of the initial conditions.

This device can be easily adapted to perform measurement with several types of adherent cells. It provides highly repeatable Young's modulus measurements in the physiologically relevant range between 3 kPa and 300 kPa, over time and in cell culture conditions, thus allowing experiments over longer time scales. The obtained results altogether demonstrate the capability of measuring changes in cell mechanics over time and therefore the device potential for determining the effect of diverse stimuli and thus advancing our understanding of cell mechanics.

Key words: Cell stretcher, elastomers, cell monolayer Young's modulus, mechanobiology, cell population, pneumatic actuation.

Résumé

Cette thèse contribue à l'avancée du domaine des microsystèmes pour la mécanobiologie par le développement d'un actionneur en polymère miniaturisé pour mesurer les propriétés mécaniques des cellules humaines. Ce travail se veut être la première démonstration réussie d'une intégration d'essai standard de traction dans un dispositif miniaturisé pour des mesures du module de Young de cellules biologiques, ouvrant ainsi la porte à nombreuses applications dans le diagnostic et criblage de médicaments.

Les fonctions physiologiques de la vie quotidienne, telles que la respiration, la contraction musculaire et la circulation sanguine, dépendent de la capacité des cellules individuelles à s'organiser en structures plus complexes et à supporter des déformations mécaniques. Les monocouches de cellules sont les tissus les plus simples du corps et jouent un rôle essentiel dès le stade de l'embryogenèse, lorsqu'elles engendrent la différenciation entre organes, à leur rôle de barrières physiques ou encore en assurant la compartimentation des organes chez les adultes. En raison de leur nature d'interface, les monocouches de cellules stabilisent les tissus en supportant des contraintes physiologiques externes. Elles sont donc utiles pour caractériser les comportements cellulaires collectifs, les interactions cellule-cellule et la réponse mécanique collective à la déformation.
Bien qu'il soit admis qu'une altération de l'élasticité des cellules aux tissus est étroitement liée à leur détérioration et au développement de plusieurs maladies, les progrès dans le domaine sont encore assez lents. Cela est principalement dû au fait que les techniques actuelles de mesure de la mécanique des cellules et des tissus reposent sur des dispositifs de mesure complexes et volumineux, avec un faible taux de répétabilité, une intégration difficile avec les protocoles cellulaires et des échelles de temps de mesure limitées.

Cette thèse présente la conception, le développement des procédés de fabrication et des tests biologiques d'un dispositif compact pour mesurer le module de Young de monocouches de cellules, avec de nombreuses améliorations par rapport aux techniques existantes. Le principe de mesure est basé sur la déformation dans le plan des monocouches de cellules par actionnement pneumatique et mesure optique de la contrainte. Les monocouches de cellules adhèrent à une membrane déformable spécialement conçue pour être aussi souple (∼ 30 kPa) et mince (∼ 5-10 μm) que la couche de cellules, permettant ainsi d'atteindre une sensibilité élevée dans la mesure de la contribution cellulaire aux propriétés mécaniques

globales de l'ensemble. Le fondement de notre technologie repose sur l'utilisation de mesures de déformations planaires différentielles entre une région du substrat recouverte de cellules et une région vierge de cellules. Au cours de l'actionnement, les contraintes des deux régions sont mesurées optiquement par un algorithme de mesure de champs de déformation. Cela permet de mesurer les propriétés mécaniques de la couche de cellules adhérant à la membrane en soustrayant la contribution de la membrane elle-même. De plus, la lecture différentielle permet de s'affranchir d'équipements de mesure de force complexes, rendant ainsi l'ensemble du dispositif plus compact et compatible avec les mesures de longue durée dans en conditions stériles.

Nous rapportons les mesures du module de Young de deux types de cellules. Les résultats montrent que le module de Young de monocouches cellulaires pour les deux types de cellules est environ un ordre de grandeur supérieur à celui des cellules individuelles (comme par exemple celui obtenu par microscopie à force atomique). Cela indique une contribution importante de l'anisotropie et de la conformation des cellules à leur réponse mécanique. De plus, des modifications du module de Young dues à des stimulations chimiques et physiques externes supplémentaires ont été explorées. En particulier, des composés chimiques ciblant des protéines précises ont été utilisés pour déterminer la contribution de ces protéines aux propriétés mécaniques globales de la couche cellulaire. Deux types de stimulation physique ont été également testés : étirer cycliquement les cellules pendant 1 heure, et en abaisser la température à 33°C – les deux expériences aboutissant à une augmentation du module de Young de la cellule. Il s'agit d'une modification réversible : les propriétés mécaniques des cellules reviennent à leurs valeurs initiales après le rétablissement des conditions initiales.

Ce dispositif peut être facilement adapté pour effectuer des mesures avec plusieurs types de cellules adhérentes. Il fournit des mesures du module de Young hautement reproductibles dans une fourchette physiologiquement pertinente comprise entre 3 kPa et 300 kPa, et dans des conditions de culture, permettant ainsi des expériences sur des échelles de temps plus longues. Les résultats obtenus démontrent dans leur ensemble la capacité de mesurer les changements de la mécanique cellulaire dans le temps et le potentiel offert par le dispositif proposé pour déterminer l'effet de divers stimuli, et ainsi faire progresser notre compréhension de la mécanique cellulaire.

Mots clefs : Actionneur en élastomère, biocompatible, milieu de culture déformable, mono-couche cellulaire, module de Young, mécanobiologie, actionnement pneumatique.

Riassunto

Questo lavoro di ricerca descrive lo sviluppo di un microdispositivo per misurare le proprietà meccaniche di popolazioni di cellule in seguito a deformazioni esterne.

L'innovazione di questo lavoro consiste nella possibilità di interfacciare metodi standard per la misura delle proprietà meccaniche, come il test di trazione, con dei campioni biologici. Grazie alla sua versatilità e possibilità di monitorare l'evoluzione della risposta meccanica cellulare nel tempo, questo dispositivo apre le porte per nuove applicazioni della meccanobiologia in diagnostica e screening di medicinali.

Le funzioni fisiologiche della vita di tutti i giorni come la respirazione, la contrazione muscolare e la circolazione del sangue si basano sull'abilità delle singole cellule di organizzarsi in strutture con grado di complessità più elevato e rispondere in modo appropriato alle deformazioni meccaniche imposte dall'esterno. Le popolazioni cellulari, in particolare nella conformazione di singolo strato di cellule, sono i tessuti più semplici nel nostro corpo e svolgono un ruolo critico fin dall'embriogenesi, dove regolano il processo di differenziazione in tessuti e organi, fino all'adulto dove agiscono come barriere fisiche tra diverse zone interne o come ripartizione degli organi. Essendo la loro una posizione di interfaccia, i monostrati cellulari stabilizzano i tessuti sostenendo compressioni e tensioni.

I monostrati cellulari sono formati da cellule meccanicamente legate tra loro e possono quindi essere utilizzati come semplici modelli per studiare i comportamenti cellulari collettivi, le interazioni cellula-cellula e la risposta meccanica complessiva in seguito a deformazioni esterne. E' noto infatti che l'elasticità delle cellule e dei tessuti è strettamente correlata a numerose patologie, tuttavia i metodi attualmente disponibili per effettuare queste misure sono particolarmente complessi, voluminosi, con bassa ripetibilità e soprattutto di difficile integrazione con i processi normalmente usati in cultura cellulare. Questi metodi prevedono infatti la misura dell'elasticità cellulare in condizioni non fisiologiche per le cellule e su periodi di tempo limitati.

Questo dottorato presenta lo sviluppo del concetto, dei processi di fabbricazione e dei test biologici di un dispositivo compatto e miniaturizzato per misurare il modulo di Young di monostrati cellulari, che presenta numerosi vantaggi rispetto alle tecnologie esistenti.

In questo dispositivo, i monostrati di cellule aderiscono a una membrana deformabile appositamente disegnata per essere morbida (~ 30 kPa) e sottile (~ 5-10 μm) come l'aggregato di cellule stesso. Questo fa sì che la membrana sia molto sensibile alle deformazioni e permetta

di distinguere il contributo dovuto alla presenza delle cellule dalle proprietà meccaniche complessive. Il principio di misura si basa sulla deformazione planare della membrana e di conseguenza delle cellule mediante un'attuazione pneumatica. L'innovazione principale della nostra tecnologia consiste nell'uso di misure differenziali di deformazioni tra una regione della membrana coperta da cellule e una regione senza. Durante la misura, le deformazioni di entrambe le regioni sono quantificate attraverso l'uso di un algoritmo di riconoscimento di pattern su immagi ottiche del campione. In questo modo, le proprietà meccaniche della popolazione di cellule possono essere misurate sottraendo il contributo della membrana stessa. Questo metodo differenziale, consente inoltre di evitare complesse apparecchiature per misurare la forza esercitata durante la deformazione, rendendo così l'intero dispositivo più compatto e compatibile con misurazioni di lunga durata in condizioni di sterilità.

In questo lavoro, riportiamo misure del modulo di Young effettuate su due tipi di cellule. I risultati mostrano che il modulo di Young per entrambi i tipi di cellule e misurato sull'intera popolazione di cellule è circa un ordine di grandezza più alto rispetto a quello misurato su cellule singole (per esempio mediante microscopia a forza atomica). Questo risultato indica l'importante contributo dell'anisotropia cellulare (deformazione planare verso deformazione perpendicolare al substrato) e della conformazione delle cellule (singole o in aggregati) alle loro proprietà meccaniche.

Inoltre, riportiamo l'effetto di vari tipi di stimoli esterni chimici e fisici sulla risposta meccanica cellulare. Riguardo agli stimoli chimici, abbiamo usato sostanze chimiche che mirano a modificare precise proteine, così da determinare il loro contributo alle proprietà meccaniche complessive della popolazione di cellule. La stimolazione fisica è stata effettuata in due modi : deformando ciclicamente le cellule per 1 ora e diminuendo la temperatura a 33°C. Entrambi questi esperimenti hanno dimostrato un aumento reversibile (nel caso in cui le condizioni inziali siano reinstaurate) del modulo di Young.

Questo dispositivo e metodo di misura può essere facilmente adattato per misurare diversi tipi di cellule aderenti. Il modulo di Young della popolazione di cellule e il suo evolversi nel tempo può essere misurato nell'intervallo fisiologicamente rilevante tra 3 kPa e 300 kPa, e in condizioni di sterilità e compatibilità con i processi standard per la cultura cellulare. Questo fa sì che esperimenti su scale temporali più lunghe siano possibili. I risultati ottenuti dimostrano complessivamente la capacità del dispositivo sviluppato in questa tesi di misurare le proprietà meccaniche nel tempo, da cui il suo potenziale uso per determinare l'effetto di stimoli esterni e far progredire la nostra comprensione della meccanica cellulare.

Parole chiave : dispositivi dinamici per cultura cellulare, elastomeri, popolazione di cellule, modulo di Young, meccanobiologia, attuazione pneumatica.

Contents

Contents

List of Figures

List of Tables

1 Introduction

1.1 Background and motivation

In the human body, cells experience a complex mechanical environment that includes tensile, compressive and shear stresses [1, 2]. Mechanotransduction comprehends the processes used by cells to sense the mechanical stimuli of the neighbouring environment and accordingly respond by modifying their shape, differentiating, proliferating as well as programming apoptosis.

One of the main achievements in mechanobiology in the last decades consisted in the correlation between several pathologies and unusual mechanical properties of tissues [1, 3]. An example of this is given by tumours diagnosis by clinicians, often based on differences in tissue rigidity sensed by palpation. Further studies in mechanobiology have demonstrated that changes in cellular mechanics can lead in cellular malfunctions and even to pathological conditions [4]. Cell mechanical responses have been thus identified as a mean to evaluate the progression state of several pathologies. In the last decades a lot of effort has been made to advance in this field as it could provide new cues and in-vitro tools to understand diseases development and how to treat them.

Because of the high complexity and ethical issues in performing in-vivo experiments, researchers heavily rely on in-vitro studies. These, historically relied on culturing cells on hard substrates such as glass or polystyrene. Nowadays there is however an increased need of reproducing as close as possible the conditions felt by the cells within the body. For this, novel in-vitro platforms which includes cell mechanical stimulation by using soft deformable substrates, known as cell stretchers, are becoming more and more popular. Researchers in the field try to develop miniaturized device which can be easily used in parallel for higher measurement throughput and therefore better statistics [5].

However, cell stretchers are not easily interfaced with set-ups for measuring cell mechanics. While measuring cell mechanical properties is of high interest because of its correlation with diseases, this field is still not yet mature. Existing methods to measure cell mechanics

are mainly relying on very bulky set-ups and often perform measurements on cells outside their physiological morphology and environment [6, 7, 8]. It is indeed difficult to combine bulky systems with standard equipments such as incubators, microscopes and long term measurement because of the lack in sterility, and they lead to impractical parallelization when high-throughput measurements are performed. Furthermore, results obtained using different methods are rarely comparable because of the different approaches and cell configuration used in the measurements. There is therefore a great interest in developing miniaturized devices for measuring the mechanical properties of living cells that could be interfaced with standard cell culture protocols and equipments.

In this thesis, I focus on developing a novel device for measuring the mechanical properties of adherent cell monolayers combining in-plane stretching and therefore continuous optical monitoring of the sample with miniaturization of the set-up and high sensitivity to cell elasticity and its changes over time. The main challenge was related to the integration of actuating and sensing techniques with biology standard techniques and equipments. The other big challenge is due to the mechanical properties mismatch between cells and their substrate which makes it difficult to measure the effect of cells. In this work, I overcame these challenges by implementing a differential read-out between bare and cell covered regions of the membrane, which allows to avoid complex and bulky force measurement equipment. The final device is therefore compact and easily interfaced with cell culture environment. The sensitivity to cell mechanics was optimized by the use of a thin and soft membrane allowing to decouple cell mechanical response from the bare membrane one. The measurement method relies on pneumatic actuation within a miniaturized device which allows to deform in-plane a suspended membrane where cells are cultured. During the deformation, the strain is measured by pattern recognition analysis of the microscopy images.

This method has the advantages of low cost and ease of use, the miniaturization to chip dimensions and in performing real time optical observation during the measurements. Thanks to its small dimension, the device could be used to deform several substrates in parallel with the same strain profile thus allowing higher measurement throughput as well as the possibility to compare measurement of cells with different treatments or conditions at the same time.

1.2 Research objectives

My thesis was founded by a Swiss National Foundation grant (grant number 205321_153365) and the goal of the project was to develop a novel, sensitive, miniaturized measurement platform for cell mechanics studies. This project involved the cooperation between the 'Emerging micro and nano technologies' group at the Swiss Center for Electronics and Microtechnology (CSEM SA) whit strong expertise in Micro-Electro-Mechanical Systems (MEMS) and cell mechanics as well as biology facilities available, and the 'Soft Transducers Laboratory' (LMTS) group at EPFL with great experience in sensors and actuators development using elastomers and deformable materials.

The main objective of this thesis is to provide the first demonstration that cell tensile mechanical properties can be measured on chip over time and in physiological conditions. This study advances the knowledge in miniaturized systems for cell studies and provide a new tool with several advantages over state of the art techniques for further investigation of cell mechanobiology.

The concept of the miniaturized device for cell Young's modulus measurements is illustrated in Figure 1.1: the device can fit a standard cell dish, cells are cultured on a suspended elastomer membrane, and measurements are directly acquired on a computer. More in detail, the final device working principle relies on stretching cells in plane by pneumatic actuation while acquiring differential strain optical measurements between a region covered with cell and a bare region of the membrane.

Figure 1.1 – Final working principle of the device developed within this thesis: the device allows simple acquisition of the measurement directly on the computer, its working principle is based on pneumatic actuation combined with a differential strain optical read-out.

The final device I developed in this thesis is shown in Figure 1.2. It fits a 55 mm diameter cell culture dish which has been engineered for the pneumatic actuation connections while keeping the sample in sterile conditions.

Figure 1.2 – Picture of the final device developed within this thesis and placed in a 55 mm diameter Petri-dish for cell culture.

In order to ensure representative results and an interesting alternative to current measurement platforms, the device should meet the following requirements:

- The device must allow measurements in cytocompatible environment over few days at least. The materials must therefore be non-cytoxic and transparent for optical imaging.

- The device should allow to deform cells in-plane for ensuring continuous imaging, and with a range of deformation up to 10%-15%.

- The device must provide stable actuation and cell adhesion on the device during the deformation.

- It is highly desirable that the measurement approach could allow evaluation of cell mechanics over long time. This would represent an important step forward in respect to existing technologies.

In order to validate the technology and demonstrate its application it is necessary to demonstrate that:

- It is possible to measure the mechanical properties of cells. And these measurements should be validated by calibration of the device with known elasticity samples.

- It is possible to measure elastic modulus changes over time due to additional external stimulation such as drugs or physical changes.

1.3   Thesis outline and contributions

This thesis advances the micro-systems for mechanobiology field by developing and validating the first on chip measurement of tensile cell mechanical properties. In addition, it presents techniques for ultra-soft substrate fabrication, chemical functionalization for cell adhesion and patterning, and experimental response of cell Young's modulus to chemical and physical external stimulations. The main contribution of the thesis is to provide the first demonstration of interfacing tensile elastic measurements with cell culture environment. This opens the door to new possibilities in cell mechanobiology as it allows to perform experiments that were not feasible before such as adherent cell population Young's modulus monitoring over several hours in physiological environment combined with real-time optical imaging of the sample. This thesis is organised as following:

Chapter 1 introduces the thesis objectives and summarizes its challenges and contributions.

Chapter 2 covers the concept of cell mechanobiology focusing on cell mechanical properties measurements. State-of-the-art devices are presented discussing their key features, and analysing how well the measurement approaches represent the in-vivo environment felt by the cells.

Chapter 3 provides a proof of concept set-up demonstrating the feasibility of adhering cell Young's modulus measurements. The sensitivity requirements for measuring the Young's modulus of adherent cell populations are discussed. The substrate material characterization and the design optimization to meet the requirements are presented. The measurement concept is validated through a customized calibrated pull-test device used to assess the feasibility of cell measurements.

Chapter 4 summarizes the integration of the proof of concept set-up into a miniaturized device. The chapter also describes the choices taken in order to obtain a cytocompatible device, in particular allowing sterilization through ethanol, incubation, and immersion in cellular culture medium. The final fabrication process is described as well as the device characterization and calibration using known elasticity samples.

Chapter 5 presents cell measurements results. The mechanical adhesion between the cells and the membrane is experimentally validated. Also, the possibility to perform live-fluorescence monitoring of the cells is demonstrated. The Young's modulus values of two cell types measured 5% strain are reported.

Chapter 6 reports the results of additional external chemical and physical stimulations effects to cell Young's modulus. The changes in cell mechanics due to chemicals targeting known cellular proteins are used for validation purposes. Also, physical stimulation is performed in two experiments: (i) continuous mechanical deformation for 1 hour and (ii) by decreasing the temperature from 37°C to 33°C. Both stimulations have found to influence cell Young's modulus and to be reversible when the initial conditions are restored. All together, these results demonstrate the capability of measuring cell Young's modulus over time and thus the device potential for determining the effect of diverse and unknown physical and chemical stimuli on cell mechanics.

Chapter 7 concludes the thesis by summarizing the main achievements and giving a general outlook on the work with some propositions for the future work.

2 Introduction to mechanobiology

2.1 Summary

In this chapter, I introduce the concept of cell mechanobiology, an interdisciplinary field that focuses on how cells and tissues sense and respond physical forces as well as the contributions of cellular mechanical properties to cell fate. The origin of mechanobiology can be traced back to the early twentieth century with the publication of the book "On Growth and Form" describing how biological entities are shaped by developmental changes [9]. Since these first observations on cell shape deformation and force exertion during development and migration, the application of physics and modeling became an integral part of many biological studies [10, 11]. The interest in this field fostered the development of several tools to investigate the relationship between biological entities and the mechanical properties within their environment. In the next sections I will explain the main notions for single cell and cell population mechanobiology and discuss their relevance for significant modelling and understanding of the in-vivo behaviour. I will also discuss the limitations of current technologies as well as the need for new tools to advance in this field.

2.2 Introduction to mechanobiology

Mechanobiology is an field of science at the interface between biology and engineering that studies cellular mechanotransduction processes. It aims to elucidate how external mechanical stimuli as well as internal mechanical properties of cells are transduced into molecular and intracellular responses that govern cell health and behaviour. Cells are dynamic, complex structures that can generate and resist mechanical forces as part of their normal physiology [1]. Mechanobiology encompasses a very wide range of all these complex phenomena regulating cell behavior. An non exhaustive list of what mechanobiology comprehends, includes: cell force exertion [12], contractility [13], shape modification [14], cell rheological and elastic properties [15], interaction with neighbouring cells and the ECM [16], aging [17] and tissue regeneration [18]. In this thesis, I focus on the mechanical properties of cells layer, i.e. the

condition when cells are not only attached to a substrate but also interacting among each other through physical connections. This simple model can be used to adequately investigate the mechanical response of tissues in our body as well as their ability to sustain stress and deformations.

Our body is continuously subjected to mechanical stimulation: muscles exert tensile forces on bones during motion, blood flow exerts shear stresses on vessels, lung tissue is cyclically stretched when breathing etc... Through mechanotransduction, the mechanical forces are translated into biochemical signals that influence several cellular activities as differentiation, proliferation, migration and disease. In a similar way, chemical and physical signals are also known to influence the ability of cells to sense and sustain mechanical stimulation within their environment [2, 19, 20].
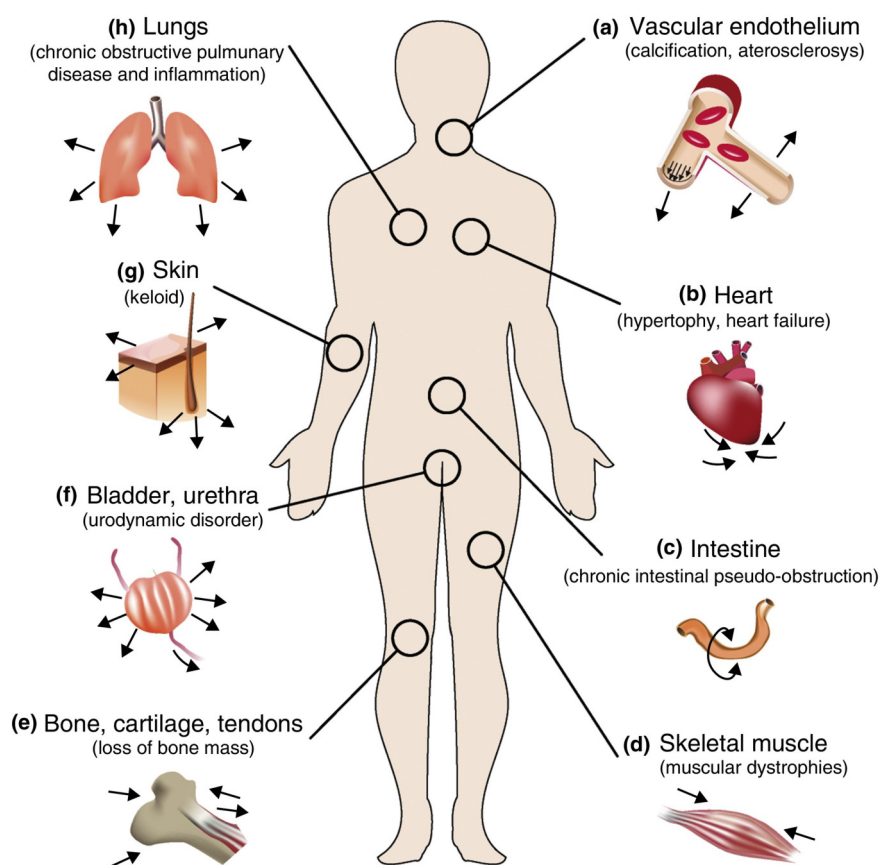
Figure 2.1 – Cells in the body continuously sustain complex mechanical loading. Impaired ability in sensing and responding to mechanical stimulation can lead to anomalous behavior and disease. The figure shows some the associated mechanical diseases to the most common internal mechanical stimuli in the human body (From [21]).

This mechanism play an essential role since tissues and organs embryogenesis to the maintenance of homeostasis in the adult organism [21]. It has been known since many years that appropriate mechanical stimulation leads to tissue growth and remodeling for preserving a

proper structural function. For example embryonic morphogenesis and differentiation results from rearrangement and deformation of cell layers subjected to forces; skeletal and cardiac muscles can respond to increased load such as intensive exercise by changing their shape, density and stiffness [22, 23] and in a similar way blood vessels are remodeled by changes in blood pressure and shear stress [24, 25]. On the contrary, abnormal mechanical stimuli or anomalous cell response to stimuli can alter the cell itself and the extra-cellular matrix (ECM) structure, eventually leading to tissue and organ pathologies as shown in Figure 2.1. Loss in contractility of the heart muscle cells can lead to heart failure, loss in compliance of the blood vessel walls is commonly related to hypertension and other cardiovascular diseases [26, 27], immobilization over time lead to muscle atrophy, glaucoma has been associated with increased cellular rigidity [28], whereas asthma has been linked to a reduced deformability of bronchial muscle cells [29]. Although in the past few decades it became more and more evident that cell mechanics and the mechanics of the environment around the cells are influencing the physiology and pathology of tissues, the fundamental mechanisms behind the mechanotransduction processes remain still unclear. This is even more complex because cells are living, dynamic entities and their structure depends on the environment they sense. There is therefore a great interest in the development of new tools for mechanobiology that are matching as much as possible the environment cells sense in the body for more significant measurements. In addition, miniaturized, high-throughput platforms are necessary to combine high accuracy with statistically relevant results. Advances in this field could lead to deeper understanding of the mechanotransduction mechanisms and therefore to better diagnosis and treatment of several pathologies.

2.3 Mechanical properties of living cells and tissues

In the body, cells and tissues exhibit specific mechanical properties that are determined by their function as well as the structure and tensions of their cellular components [30]. The ability of cells to resist deformation, is typically measured through the Young's modulus.
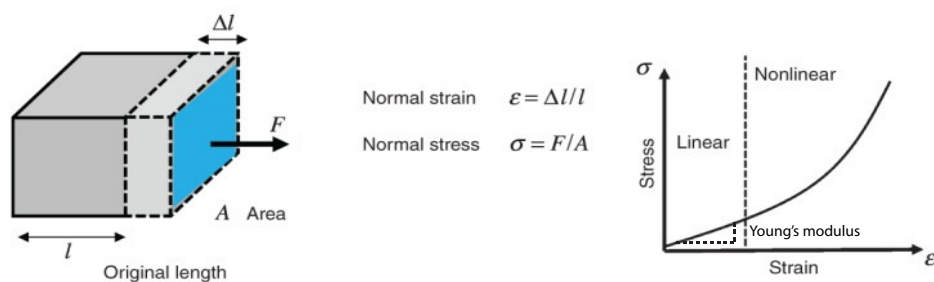
Figure 2.2 – Definition of the Young's modulus of a material. (a) Stress is defined as the force per unit area while the strain is the deformation per unit length. (b) The relationship between stress and strain defines the Young's modulus. Cells typically exhibit a linear stress versus strain relationship for small deformations, while for large deformations the relationship becomes non linear and the stress increases more rapidly. (Adapted from [1]).

The Young's modulus or elastic modulus is a fundamental property of solids determining their ability to sustain their shape in response to an applied stress (Figure 2.2). In the cells this function is mainly fulfilled by the cytoskeleton, an interconnected network of protein filaments that give to cells their structural rigidity [1]. However, because cell are complex heterogeneous material containing liquids as well as numerous filaments and organelles, they exhibit also viscous properties. When a viscoelastic material deforms, it stores and dissipates mechanical energy simultaneously. Typical viscoelastic response are stress relaxation, when stress in the material relaxes in response to constant deformation and creep response when strain increase over time at constant stress. Cells are known to be intrinsically viscoelastic, they display infact both elastic and viscous properties when a deformation is applied [1].
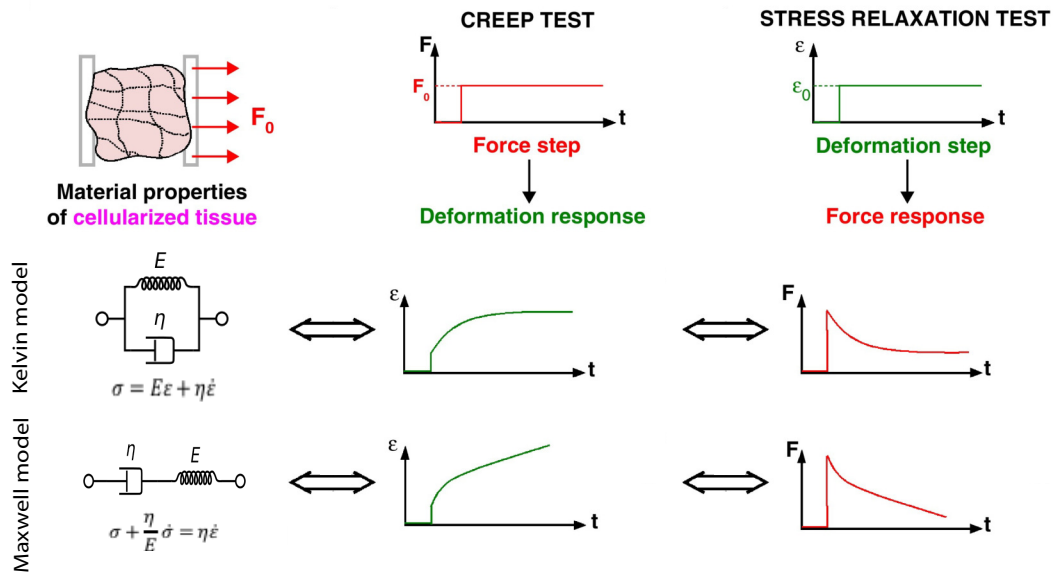
Figure 2.3 – Common rheorogical models for biological materials are represented accompanied by their characteristic equation and the creep and stress relaxation behaviour. (Adapted from [31]).

Several models have been proposed to take into account the elastic and the viscous components of the cells in a mathematical formalism. The basic elements are springs for the elastic components and dashpots for the viscous ones. The stiffness k of the spring set the force necessary to deform it and the deformation is fully reversible at the removal of the force. Dashposts are instead parametrized by their viscosity η that impose the rate at which they can be deformed, in this case the deformation is not fully recovered. Combinations of these two elements have been used to mathematically model cell or tissue dynamics. Every dashpot element introduces a time constant τ indicating the time need for the system to reach the equilibrium. The most common models are the linear solid model, the Maxwell and the Kelvin-Voigt models; these can be also assembled in power-law models corresponding to series of infinite viscoelastic solids (Figure 2.3).

Most of the biological cells are within tens to hundreds of μm in size, exhibit elastic modulus values in the range from a few hundred Pa to tens of kPa and a viscosity in the order of a few hundred Pa·s [1]. However, these values are significantly affected by the chemical and mechanical environment as well as cell–cell and cell–ECM interactions [32]. Furthermore, the sample size plays a significant role in determining the mechanical properties as they strongly depend on the inner structure of the sample.

A single cell is covered by a thin lipid bi-layer, the cell membrane, that forms a barrier dividing the interior of the cell from the extra-cellular environment. The interior of a cell is called cytoplasm and it is a fluid, crowded with organelles, that leads to cell rheological properties. The nucleus lies at the center of the cell and it also plays a role in mechanotransduction. Within the cytoplasm there is the cytoskeleton, a highly ordered network of filamentous proteins that allows the cells to sustain mechanical stress, move by modyfying their shape as well as transmit and generate cellular forces [1, 33]. The cytoskeleton is composed by three groups of protein filaments: actin microfilaments, microtubules and intermediate filaments as illustrated in Figure 2.4.
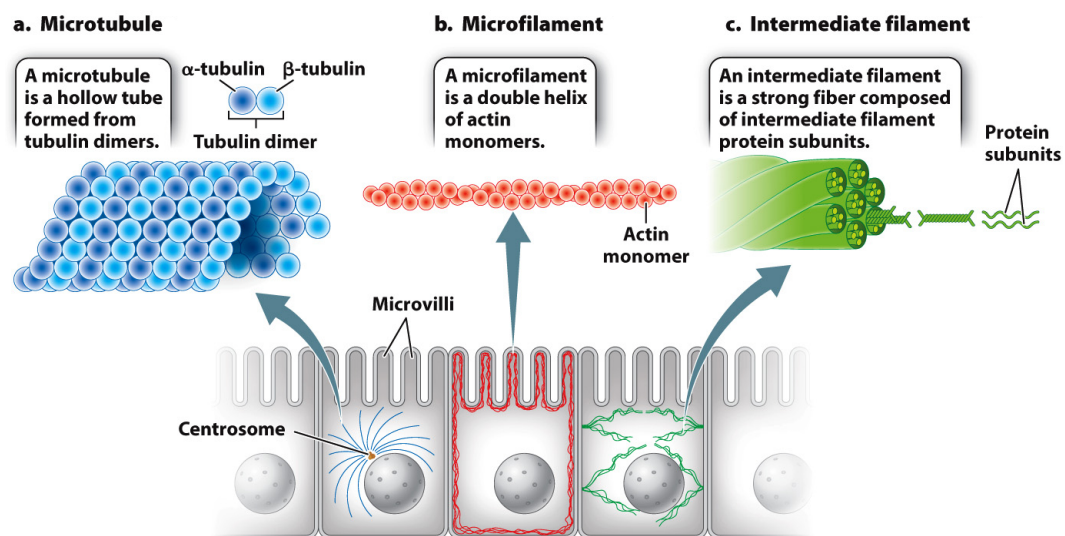
Figure 2.4 – The three types of cytoskeletal filaments and their localization inside a cell: (a) microtubule radiating from the centrosome; (b) actin microfilaments are found in many cell types just beneath the cell cortex to strengthen the membrane; and (c) intermediate filaments (Picture from [34]).

These protein filaments are highly dynamic and rapidly reorganize in response to external signals enabling cells to maintain shape by resisting tensions, contract and apply forces on the substrate to migrate. Also, they take part in cell adhesion to the substrate, stabilizing the organelles' position inside the cytoplasm and maintaining cell shape by resisting compression [35, 33]. The cytoskeleton capability in sustaining deformations is thus not only affected by the rigidity of the single filaments but it rises as a consequence of their forming structures at higher level and from interacting with the other filaments inside the cells [35].

Furthermore, cellular internal structure is strongly influenced by the external environment. In particular, isolated single cells exhibit a different structure than cells at higher organization level such as cells in a tissue or an organ. In fact in addition to cell-substrate coupling, neighboring cells form mechanical connections that make the mechanics of multicellular populations drastically different from single cells [36]. These junctions have critical mechanical functions in normal physiology as they can sustain tensile forces that would otherwise tend to tear the tissue apart. The strength and type of cell-cell contacts not only promote the mechanical adhesion among cells but also active communication through the exchange of chemical and electrical signals as well as force transmission modulation [33]. From this communication, collective cell behaviours can occur such as the organization of smaller sub-domains in tissues, collective migration, invasion to glass-like states in dense epithelial layers [37, 38].
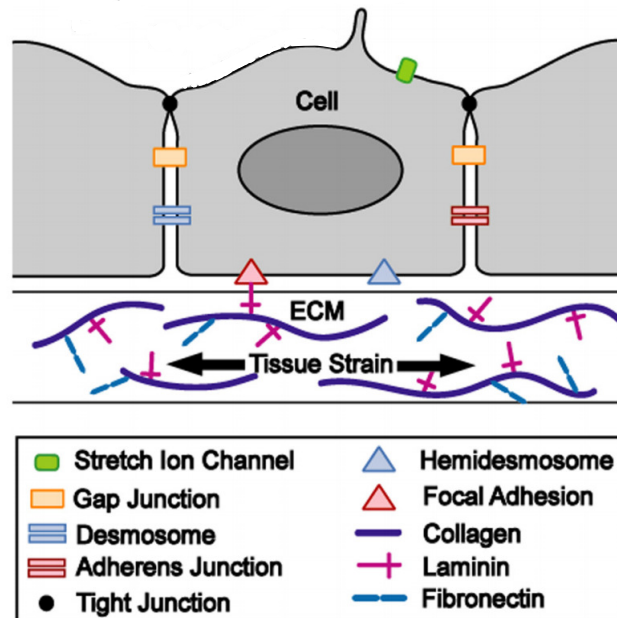
Figure 2.5 – In multicellular aggregates, cells are mechanically attached among each other through different types of intercellular junctions. Also, mechanical adhesion sites are present for bonding to the surrounding ECM through focal adhesion sites. The schematic represent the main types of of cell-cell and cell-substrate junctions (Adapted from [33]).

Cell–cell junctions that intracellularly connect two or more cells can be divided in three types: tight junctions, gap junctions, and anchoring junctions (Figure 2.5). The tight junctions are presents only in the type of cells that form barriers in the body such as epithelial cells. They act as barriers that regulate solutes diffusion between cell layers by forming a seal between neighboring cells. Gap junctions are pores that allow for direct chemical exchange between adjacent cells. Anchoring junctions promotes cytoskeletal connections among cells. Depending on the type of proteins they mechanically connect, it is possible to distinguish among: adherens junctions (connecting the actin filaments of neighboring cells), desmosomes

(joining cellular intermediate filaments), and hemidesmosomes (linking a cell's intermediate filaments to the extracellular matrix through integrins) [33].

Research in mechanobiology in the last decades have dealt with the mechanics of biological samples at different scales from cellular proteins [39, 40, 41], single cells [42, 43, 44] to tissues [45, 30, 23] and organs [46, 47]. In general it has been shown that there is a trend for elastic properties of biological components to decrease when considering larger structures. The protein fibers that form cell cytoskeleton are significantly stiffer than tissue assemblies which in turn are significantly stiffer than bulk tissue sample as shown in Figure 2.6.
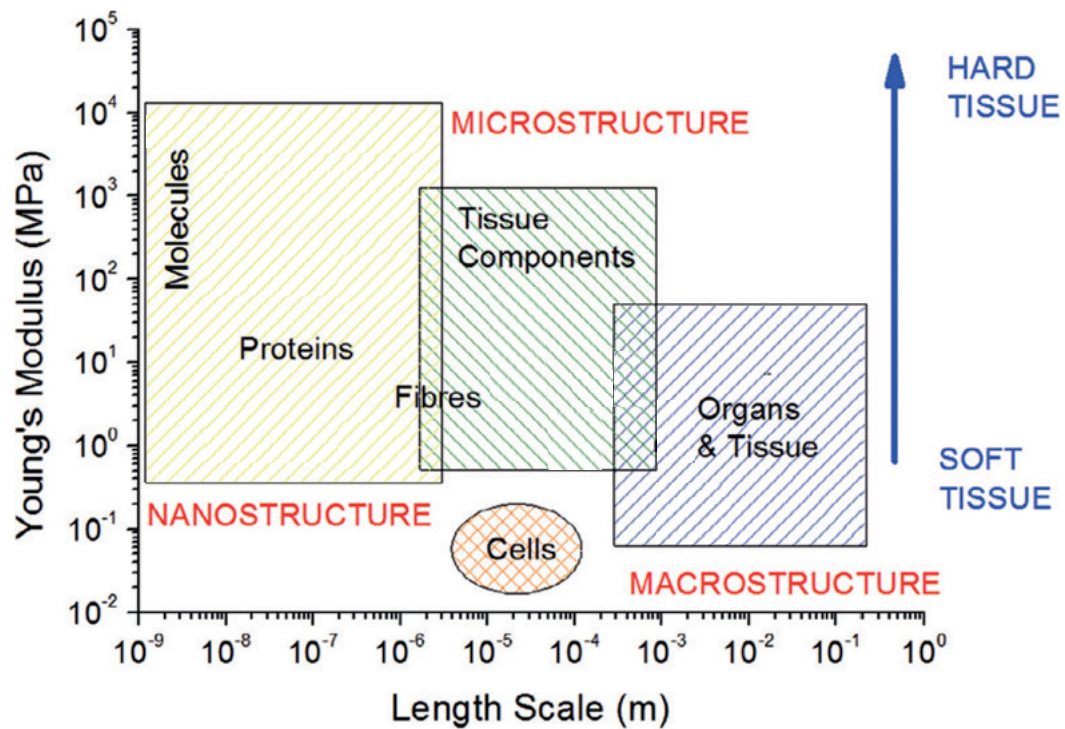
Figure 2.6 – Mechanical properties of biological components at different length scales. The graph summarizes experimental data from previous studies showing that there is a clear decrease in Young's modulus when passing from the micro to the macro scale of the sample. (Picture adapted from [48])

The Young's modulus of single cells ranges from values as low as few hundred Pa (for example in glial or neuronal cells) [49] to tens of kPa (such as in human thrombocytes) [50]. With this high variability single cells partially follow this trend as they are altogether softer than the proteins that compose them, however they are also softer than tissues and organs [48]. Cells are much softer than the protein filaments that compose them because these filaments are folded inside the cells and only partially unfold upon cell deformation. The higher Young's modulus of tissue compared to cells can be explained by the presence of cell-cell interactions that give a higher structural rigidity. While, when considering bulk samples a large part of the sample volume is occupied by the soft ECM matrix surrounding the cells which dominates the overall mechanical properties.

2.4 Mechanical properties as hallmark for disease

The importance in sustaining mechanical forces and stress at different scales, from the intracellular filaments to the tissue level, is even more evident when considering pathologies that arise because of inadequate elasticity of cells and tissues [1, 3].

Several studies have shown that in many diseases cell cytoskeleton exhibit abnormal features. For example, sickle cell anemia and malaria involve the disruption of actin filaments as well as actin binding to the red blood cell membrane leads to anomalous cell shape and compromised function [41, 51]. On the other hand, the excessive presence of F-actin inside the cells results in increased cellular viscosity and impairing cell duplication [52]. Also, diseases such as Bullosa Simplex are often associated to genetic mutations of intermediate filaments leading to increased tissue fragility [53]. At the tissue level, the mechanical functions of cell layers is particularly evident where pathogens or mutations affect cell-cell junctions resulting in increased fragility of tissues [54]. Also, cell layer mechanics is particularly critical during embryogenesis as it can results in the failure of proper embryo development [46, 55]. During embryogenesis, altered mechanics of cell layer such as the disruption of intercellular adhesion or impairment in cellular contractility results to anomalous tissue morphologies and congenital diseases such as issues of neural tube, abnormal alveolar structures and pulmonary hypoplasia [56, 47]. Another example is the impairment of ephitelium cell-cell junctions that can hinder their barrier function such as in exacerbations in asthma [57]. Also, fibrotic diseases such as pulmonary fibrosis, systemic sclerosis, and cardiovascular disease involve the hyperproliferation of fibroblasts and excessive ECM secretion. This also happen in wound healing, where it is very common that damaged tissue is replaced by highly fibrous one because of increased ECM deposition and crosslinking. In the pathological case of hypertrophic scars it is well know the formation of fibrotic masses called keloids. Depending on where this scar stiffening occurs, it can have consequences on normal cellular behavior [46], for instance limiting joints movements, fibrotic cardiac disease [58] or for scarring of the central nervous systems it can seriously impair tissue function [59, 60]. Aging is another factor that alter tissue mechanical properties and therefore may disrupt tissue homeostasis [46, 48, 17]. For example, the muscle ECM structure becomes stiffer with age because of highly crosslinking [61], blood vessels have also been observed to become stiffer (arteriosclerosis) with increased cardiovascular risk factors [62] while bones or cartilage become more fragile as in osteoarthritis [63]. One of the most studied disease associated with mechanical properties of cells and cell aggregates is cancer. Although increased stiffness is a hallmark feature associated with cancer development [46], cancer cells and in particular metastatic cells are characterized by increased deformability and elasticity [64]. It has been suggested that increased cell deformability correlates with the ability of metastatic cells to squeeze through the surrounding tissues and spread within the body [65, 66].

Mechanical properties measurements have thus emerged as a potential method to characterize diseases and even determine their state [4]. In the next two sections I will explain some of the most common methods to asses the mechanics of biological samples. Even if the vast majority

of these platforms and experimental protocols are custom-made, few commercial devices exist [67, 68, 69, 70]. However, their use is quite limited as there are still several challenges to be met before their use in clinical applications such as providing high throughput measurements performed in a configuration resembling the in-vivo environment.

2.5   Single cell mechanobiology

Most of the mechanical tests on cells up to now have been performed on single cells, either adherent or in suspension. Single-cells mechanical stimulation has been used for studying mechanotransduction [71, 72] as well as characterizing the mechanical properties of cells [73, 74]. In these measurements, the elasticity of the cells is measured by typically stretch or squeeze cells and by quantifying the deformation for a known applied stress. For small deformations (up to 5% strain) the response is within the linear regime and it is dominated by actin and intermediate filaments [75, 76]. When larger deformations are applied, between 5% and 25% strain, cytoskeleton behavior can result in nonlinear responses which depend on the type of cells involved [77, 78]. Even larger deformations are sustained by microtubules, and nuclear mechanics comes into play when cells are forced to move into narrow channels or are highly compressed. [79, 6].

The most common techniques for investigating the mechanics of single cells in-vitro are grouped in Table 2.1 with their main advantages and drawbacks. In general, single cell techniques have lead to great advancements in our understanding of the mechanics of whole cells and sub-cellular components. However, these approaches have the main disadvantages of being quite invasive (e.g. surface functionalization for beads attachment) and to measure cell mechanics in configurations that are quite different from the state in-vivo (cells are suspended in a fluid or weakly adherent to the substrate). All these factors significantly influence cell response and behavior [37]. Furthermore cells considered as single entities have different mechanical response than when they are interacting with other cells as happens in the body making it difficult to put these results into context. Few techniques have been developed to overcome this limitation and allow studies on cell populations and aggregates, as I discuss in the next paragraph.
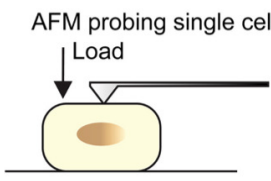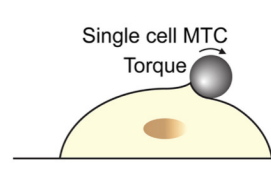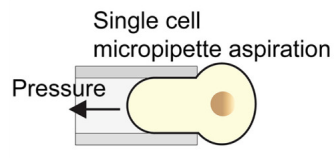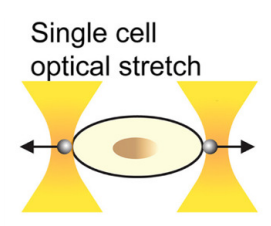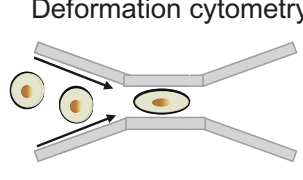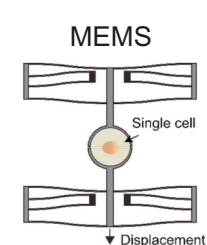
Technique	Advantages	Disadvantages	References
AFM probing single cell Load	• Force sensing resolution: 10–10^5pN • Spatial resolution: 1–10^5nm	• Substrate and measurement location influence • Low throughput	Cytoskeleton [80, 81], whole cells [82, 83, 84, 85],disease [86, 87, 64]
Single cell MTC Torque	• Torques applications • Bead adhesion to specific receptors	• Not-uniform stress • Invasive technique	Single cell [88, 89, 90], DNA [7, 91], receptors [92, 93, 94]
Single cell micropipette aspiration Pressure	• Seconds to hours timescales • Inexpensive, simple	• Low accuracy • Low throughput (long sample preparation)	Single cell elasticity [95, 44, 96]
Single cell optical stretch	• pN resolution • Can probe cells' active responses	• Photodamage and local heating • Suspended cells	Membrane tether [97], whole-cells [43, 42, 98, 99], proteins [40, 39]
Deformation cytometry	• Device miniaturization • High throughput (thousands cells/s)	• Limited observation time (ms) • High flow rate instabilities	Whole cell [100, 101], nuclei [102]
MEMS Single cell Displacement	• Integration of electronic circuits • Miniaturization	• Lack transparency • Complex design	Cell forces [103, 104], cell elasticity [105, 106, 107]

Table 2.1 – Comparison among the most common measurement techniques for single cell mechanics, advantages and drawbacks are also summarized [37, 33, 32].

2.6 Cell population mechanobiology

In tissues and organs, cells do not exist as isolated entities but they are surrounded by other cells as well as by the ECM. Because of the radical difference in cytoskeletal organization due to the mechanical coupling with surrounding cells, it is not possible to have information on cell populations mechanical behavior from single cell experiments [8]. In general, collective dynamics is not simply the sum of individual response, instead cells coordinate their movements by actively interacting with each other [36]. Cell monolayers can be considered as the simplest tissues in the body and the easiest model for studying the mechanical response of cell populations allowing to obtain results that are more representative of the in-vivo environment. Cell monolayers are present in several cavities in of the human body, acting as physical barriers to partition organs. Because of this specific interface location, they have to withstand external physiological stresses (stretching of the skin, peristalsis motion in the gastro-intestinal tract, urothelium stretching due to hydrostatic pressure etc...).

In recent years, there has been a huge increase in the development of cell stretcher devices to study the response of cell populations to cyclic dynamic loading over time [5, 108, 109, 110]. However, very little is known about their mechanics. For example how tissue-scale mechanical properties such as elasticity and tension are affected by intercellular junctions formation, or the contribution of each type of cytoskeletal junction to monolayer mechanics [45]. Including elasticity measurements into state of the art cell stretchers is not straightforward because of the significant difference between the elasticity of the cell population and the substrate. In the next section I review the most common techniques for cell stretcher devices and the few existing ones that have been cleverly modified to allow mechanical properties measurements.

2.6.1 Cell stretcher devices for cell population mechanical studies

Scientists have mainly relied on cell stretchers devices to study the mechanical response of cell populations. They consist in deforming a layer of adherent cells by stretching their substrate. The deformations imposed on the cells mimic their physiological mechanical environment within the body and depending on the experiment can be applied in one, two or all directions (uniaxial, biaxial or equiaxial strain) as shown in (Figure 2.7). Cell stretchers are generally used to determine the effects of controlled mechanical stimulation on several properties of the cells, for example: morphology, metabolism and anomalous behaviour [111, 112, 113].

Devices for stretching a layer of cells are mainly custom made set-ups for laboratory research, however a few exist that are commercially available. For example Strex USA proposes systems consisting in elastic chambers that are linearly pulled by a linear motor for uniaxial strain of the cell culture (Figure 2.8a). Flexcell International Corporation, on the other hand sells a system where cells are cultured on deformable membranes located on the top of pneumatic chambers. The membrane can slide on a central loading post when vacuum is created below the membrane leading to around 20% radial in plane deformation of the suspended membrane (Figure 2.8b). These devices are however difficult to integrate within standard cell culture
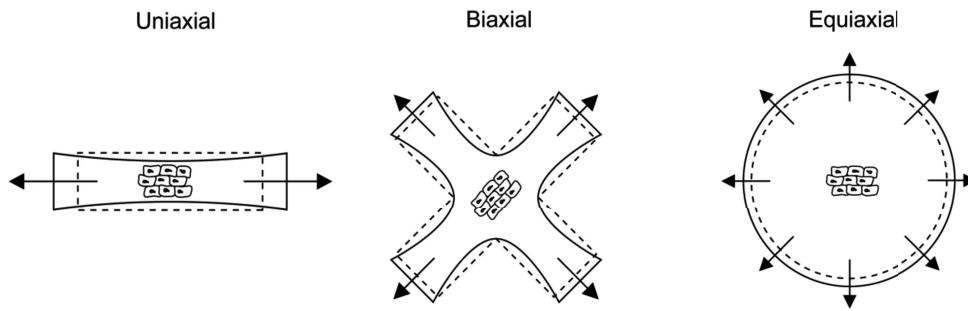
Figure 2.7 – Schematic of the different types of strain applied to cells by cell stretcher devices: (a) uniaxial strain exhibiting compressive strain in the transversal direction, (b) biaxial, with deformation induced on two perpendicular directions and (c) equiaxial where a radial force is applied (Adapted from [114]).

Petri-dishes and have low throughput which limits their use and wider applications. In order to overcome those limitations, significant effort to miniaturize cell stretcher devices has been made over the last years. The main approach for miniaturized devices is to use pneumatic actuation to stretch a thin suspended membrane where cells are cultured. For example, a device for organ-on-chip has been first developed by the Wyss Institute at Harvard University to recreate the in-vivo mechanical stimulation of the alveolar-capillary interface in the lung (Figure 2.8c). When the pressure is decreased in the two pneumatic side-chambers, the membrane is deformed in uniaxial strain configuration. Variations of this design have been proposed to reproduce other organ-on-chip [115, 116] or to induce biaxial strain to the cell population [109].

The main limitation of the cited cell stretcher devices is the fact that because of their design and working principle they do not allow to measure the mechanical properties of the cell population under study. The main challenge is to be able to extract information of the cell layer mechanics alone decoupled from the substrate. While the cell layer form a very thin (few μm) and soft layer (few Pa to kPa), the substrate used in the presented devices are mainly made of few mm thick silicone material. The are easily deformable but still 1-2 orders of magnitude stiffer (hundreds of kPa to MPa) than the cell layer cultured on them. Therefore, the mechanical properties of the substrates are dominating the mechanical response, making it very difficult to measure the stiffness of the cell layer [119, 120]. A second challenge is how to precisely measure the force exerted by the substrate during the deformation to be able to obtain stress-strain curve for the cell monolayer. Few approaches have been proposed to overcome this challenge. Some of these are based on bulge tests, making use of out of plane deformations [121, 122], others use unsopported cell monolayers [8, 123, 124]. In general, the cell stretcher devices allowing measurements of cell population mechanical properties can be divided in two main groups: the ones relying on out-of plane deformation and the one employing in-plane deformations in a uniaxial tensile test configuration.
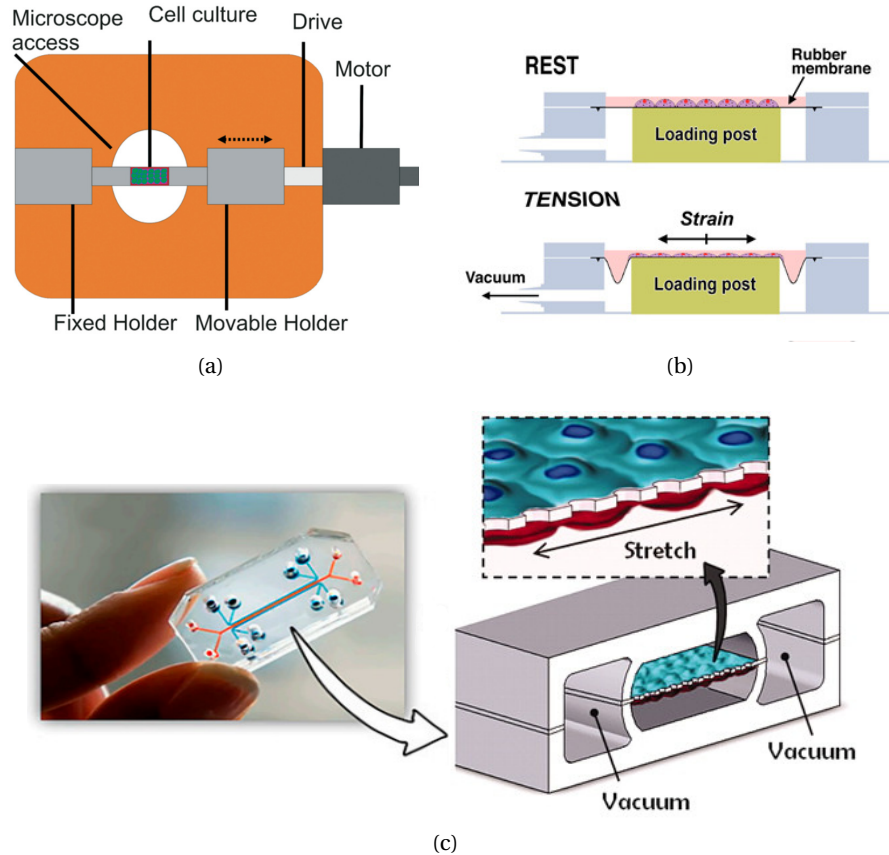
Figure 2.8 – Schematic representing different types of cell stretchers designs: (a) Motor-based uniaxial cell stretcher produced by STERX (From [108]), (b) Vacuum-based cell stretcher, commercial device from Flexcell (From [117]) and (c) Microfluidic cell stretcher device for lung-on-chip experiments (Adapted from [118]).

Bulge test based approaches for measuring cell layer elasticity

The bulge testing technique is a well-known method mainly used to measure the mechanical properties of thin metals through out-of-plane deformation [125]. In a classic bulge test experiment, inflation pressure is applied to a free-standing thin film which has clamped boundaries. The resultant deflection is recorded using a non-contact method such as laser interferometer. Knowing the geometry, the applied pressure and the associated deformation it is possible to estimate the Young's modulus value of the material. Thanks to the low out-of-plane rigidity of thin suspended material, the bulge test a suitable method to detect even very low changes in Young's modulus of the suspended membrane.

This method has been successfully adapted to measure the mechanical properties of cell monolayers cultured on thin deformable silicone membranes which are clamped at their edges. This design has been adapted to either strech [121, 122, 126, 127] or compress a cell layer [128]. A first design and experimental apparatus was proposed in 2007 for measuring

(a)

(b)
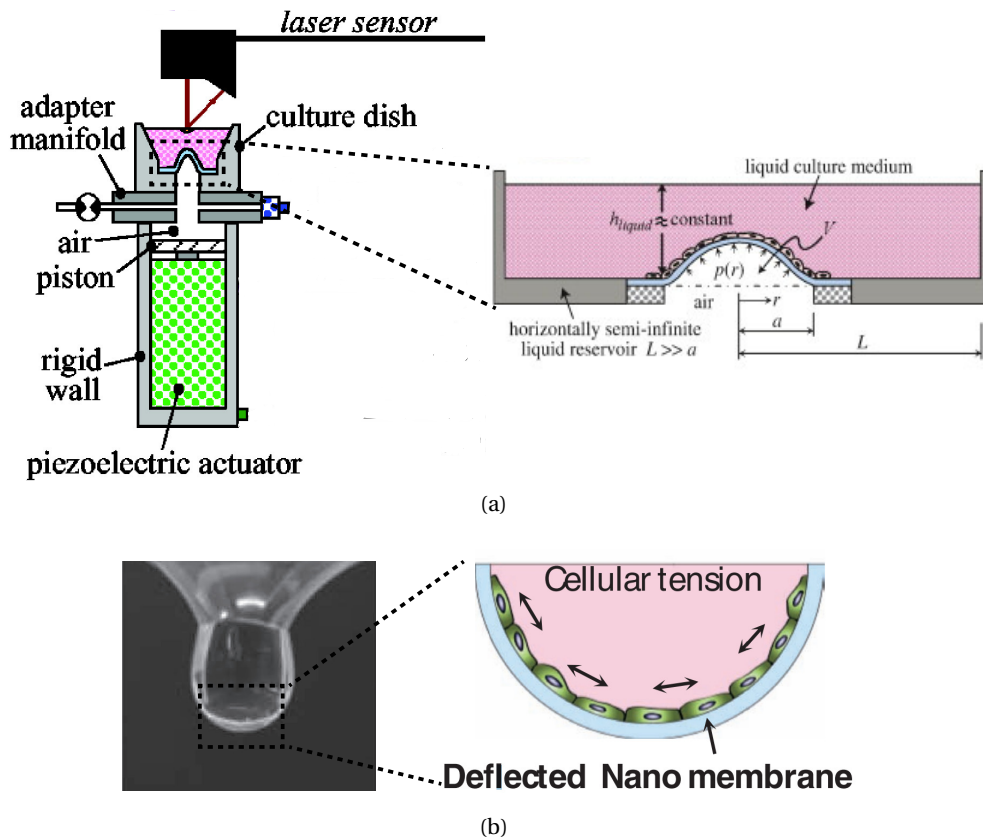
Figure 2.9 – Schematic of two devices designed for measuring the mechanical properties of a cell monolayer through the bulge test approach: (a) The membrane where cells are cultured is deformed by increasing the pressure below the membrane, the deflection is measured through a laser sensor (Adapted from [121]) and (b) the membrane stretching is induced by adding cell medium on top of the membrane, the deformation in the vertical direction is optically measured (Adapted from [122]).

a layer of ephidermal keratinocytes [121]. Gas pressure is applied on the bottom of a membrane where cells are cultured and the deformation is measured using a laser displacement sensor (Figure 2.9a). A similar approach was also shown in 2013 [122], where the membrane is deformed by adding a defined volume of medium on top of a nanometer-thick membrane (Figure 2.9b). More recently the same method has been proposed with the addition of electrical strain read-out [126, 127]. In one approach, the membrane deflection caused by pressure applied above the membrane is measured as a change in conductivity in an ionic liquid-filled microfluidic channel placed below the membrane [126]. The deforming membrane is integrated within a microfluidic chip and sandwiched between the electrofluidic channel (on the bottom) and a pressure channel (on the top) (Figure 2.10a). Another study [127] propose the integration of carbon nanotubes-based strain sensors in the deformable membrane (Figure 2.10b). The addition of electrical strain read-out allows to miniaturize the testing platform and even to parallelize the tests [129].

20

(a)

(b)
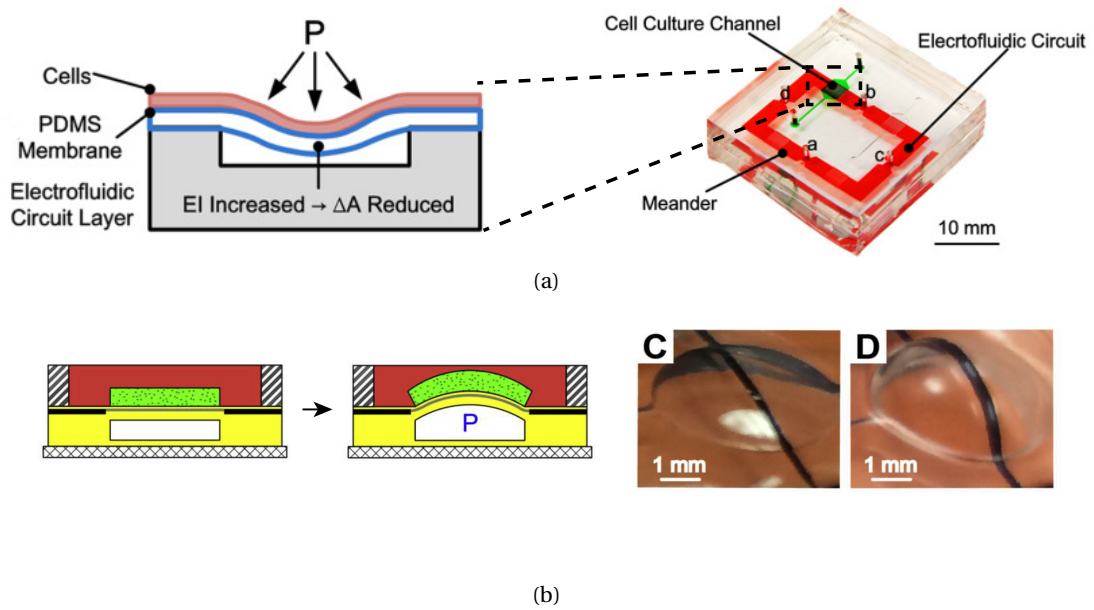
Figure 2.10 – Schematic of two devices combining bulge test approach with electrical strain read-out: (a) pressure is applied above the membrane, the deformation is measured through a change in resistance in the ionic liquid filling a channel below the membrane (Adapted from [126]) and (b) strain sensors (represented in black) made of carbon nanotubes (CNT) and PDMS composite are placed in the membrane hosting the cells (From [127]).

Bulge test has the advantages of having a membrane fully clamped which increase the robustness of the test even when using very thin or soft membranes. Also, cells' contribution to the total rigidity can be measured quite easily and without imposing too many constraints on the membrane itself. A range of membrane stiffnesses for out of plane deformations allowing to see the effect of cells mechanical properties, can be defined by compromising the elasticity of the material with the membrane thickness. Substrates up to 100 times stiffer than the cells can be used if they are thin enough [122]. On the other hand, the use optical read-out of the vertical deflection result in bulky set-up, while the addition of electrical strain sensors makes the sample non-transparent and can have stability issues for long time measurements in humid environment. In addition, because this method is based on vertical deflection, it has the intrinsic drawback of making it quite difficult to observe the sample during the experiment. This is a critical limitation for biological applications where optical inspection of sample morphology during the experiment is essential to assess its well-being and therefore the validity of the measurements.

Uniaxial tensile test based approaches for measuring cell layer elasticity

In a uniaxial tensile test (or pull-test) the mechanical properties of a material are measured by pulling the sample in-plane in a controlled way while measuring the force exerted during the deformation normally using a load cell. This type of test is commonly used for testing metals [130], polymers [131] and has also been used for biopsies [119, 132]. Adapting this

measurement technique to living biological samples is desirable because thanks to the in-plane movement, it is possible to monitor cells during the stretching. However its application is not trivial due to the low stiffness values at stake. Normally, motorized stages are used to apply a known strain to the sample through custom-made connector that allows the sample to be placed in liquid. The forces to be measured are in the order of sub-mN to few mN, making it quite difficult to find a reliable and sensitive enough commercially available force sensors. Because of this, custom solutions based on optically monitoring calibrated structures to extract the stress from the observed deformation have been proposed (Figure 2.11b). The main critical point is the selection of material properties and geometry along with their fabrication feasibility so that the substrate does not fully dominate the mechanical response [120]. The only works published on measuring cell in plane elasticity overcome this latter challenge by using completely suspended cell layers, i.e. without substrate. Harris et Al [133, 133] managed to obtain a fully suspended cell monolayers between two rods by removing an hydrogel substrate through enzymatic digestion. One of the rod is then displaced to obtain a certain deformation of the cells while the force is measured by monitoring the deflection of calibrated rod of known elasticity attached to the fixed side 2.11a.
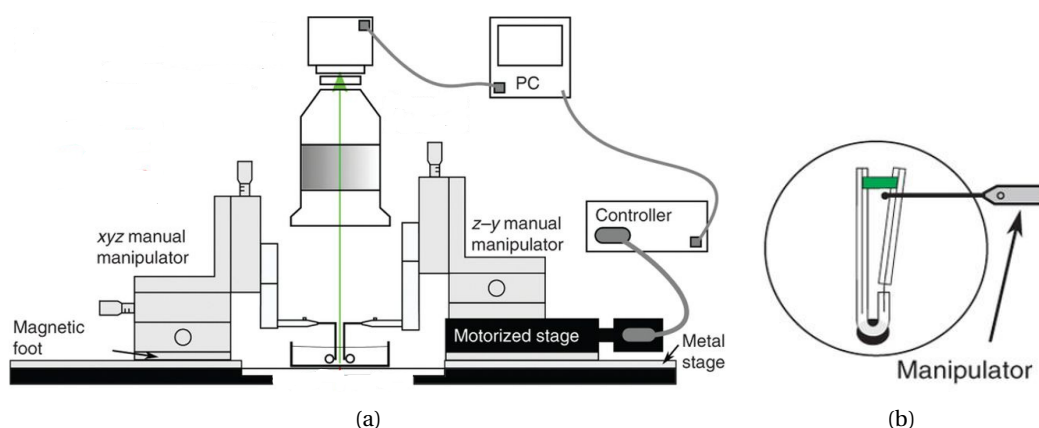
Figure 2.11 – Schematics of the measurement set-up for investigation of the mechanical properties of cell monolayers. (a) The suspended cell monolayer is placed under a camera for imaging and it is suspended between one fixed rods and one moving rods used to deform it. (b) Schematics of the operating principle for force sensing, the rod is characterized so that by knowing the defletion itis possible to retreive the exerted force. (Pictures from [8])

A more recent publication report measurement of suspended vascular smooth muscle cell monolayers Young's modulus using a Hall-effect based force sensor [124]. Cells are cultured on thermo-responsive polydimethylsiloxane (PDMS) substrates and carefully detached from the it after 7 days culture by just placing the samples at room temperature. The cell sheets are then glued to mounts on the tensile stretcher. The force sensor they developed combining a cantilever with a Hall-Effect sensor as well as magnets for measuring the force with a range of measured forces ranging from the μN to the N.

These two approaches described above, are the only two uniaxial-based techniques to measure
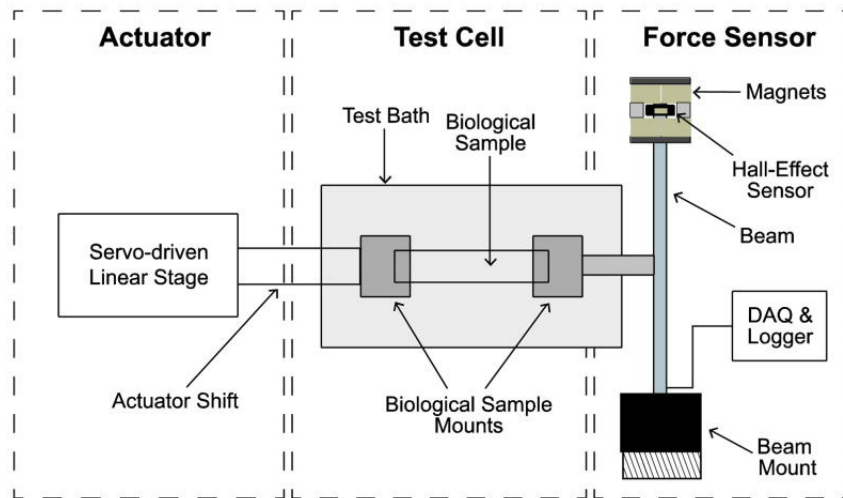
Figure 2.12 – Hall-effect based uniaxial tensile tester schematic. The uniaxial tensile tester is composed of three subparts: the linear actuator, the test cell consisting in an acqueous bath for the sample and the force Hall-Effect sensor (Picture from [124]).

in-plane cell elasticity that have been published so far. Their advantages over bulge approach rely in the possibility to continuously monitor the sample during the stretching and to apply uniaxial deformation instead of equiaxial. The latter point is particularly important because of the anisotropy of cells, the elasticity measurement is in fact influenced by the direction of the force exerted on the sample. In addition using a suspended cell monolayer allow to perform direct measurement with high sensitivity without the need to subtract the substrate influence. This, however, comes with several limitations in terms of fragility and difficult repeatability. Furthermore, the significance of the results can be questioned because of the difference in cytoskeletal conformation compared to adherent cells. Also these techniques cannot be used over prolonged time periods because of the suspended layer low stability over time as well as the fact that none of these set-up are compatible with a biological incubator.

2.7   Conclusion

In this chapter, I explained the relevance of mechanobiology at different scales, from proteins to tissues, in understanding healthy and diseased states. Also, I focused on the importance of recreating an environment similar to the one experienced in-vivo to rely on more significant results. For this it is particularly important to take into account that most of the cells in our body are chemically and mechanically connected to each other to form higher hierarchy structures. However most of the techniques to study cell elasticity up to now are single-cell based. Because of the numerous challenges to extend elasticity measurements to cell populations, only few techniques have been proposed. As I discussed in Section 2.6.1, there are still several improvements that can be made to improve the significance, versatility and impact of this measurements.

The next chapters of the thesis focus on the contribution I brought to this field by overcoming the main limitations of current cell stretcher for cell elasticity measurements. As described in detail in Chapter 4, by integrating in-plane stretching in a microfluidic device and differential strain optical read-out, I have developed the first miniaturized device for measuring in-plane adherent cell monolayers mechanical properties over time. Being based on in-plane stretching, my device allows continuous monitoring of the sample, and it is at the same time compatible with cells adhering on a substrate. This opens new possibilities for longer time investigation of cell mechanics.

3 Measuring adherent cell mechanics - Substrate design and validation

3.1 Summary

Measuring the mechanical properties of cell layer adhering to a substrate is highly desirable because of the resemblance with the in-vivo environment. The main challenge consists in decoupling cell and substrate contributions to the overall mechanical response. Existing techniques use out-of-plane displacement to take advantage of the lower rigidity compared to tensile deformations. However, this results in bulky set-ups and the difficulty in continuous imaging of the sample.

In this chapter, I explain how I designed a device which combines for the first time, mechanical properties measurements of cells adhering to a substrate using in-plane deformations. I present the theoretical calculations and experimental validation of uniaxial tensile measurements performed on adherent cells. I first explain the sample modelling and the critical parameters that influence the capability to measure cell's mechanical contribution. I then show the characterization and choice of the materials as well as the geometry optimization to increase the measurement sensitivity. I finally detail the assembly of a uniaxial tensile apparatus allowing measurements in liquid and the experimental verification by measuring calibration samples and cells.

3.2 Measurement method

In an uniaxial tensile measurement, the sample is deformed along a single axis and the force is measured during the deformation. By cyclically stretching the sample, stress-strain curves are obtained. The relationship between stress and strain allow to calculate the Young's modulus of the sample. As shown in Figure 3.1a, I designed an uniaxial tensile apparatus that allows to perform measurements of thin and fragile materials such as a cell layers. The method consists in sticking the sample on a substrate with carefully engineered properties and then comparing the stress strain response of the bare substrate and of the composite made of the substrate and sample to be measured. I apply this concept for adherent cell layer measurement, by

comparing the mechanical response of a bare substrate with the one obtained after culturing a cell layer to the same substrate. The substrate plays thus a crucial role in the feasibility of this measurement. In order to be able to see a change in the composite elastic modulus when cells are present, it is necessary that the substrate has an elastic constant that is comparable or even smaller than the one of the cell layer. If the measurement substrate is properly designed, the slope in the stress-strain graph increases when cells are adhering to the membrane, as a consequence of the higher Young's modulus (Figure 3.1b).

<center>(a)　　　　　　　　　　　　　　(b)</center>
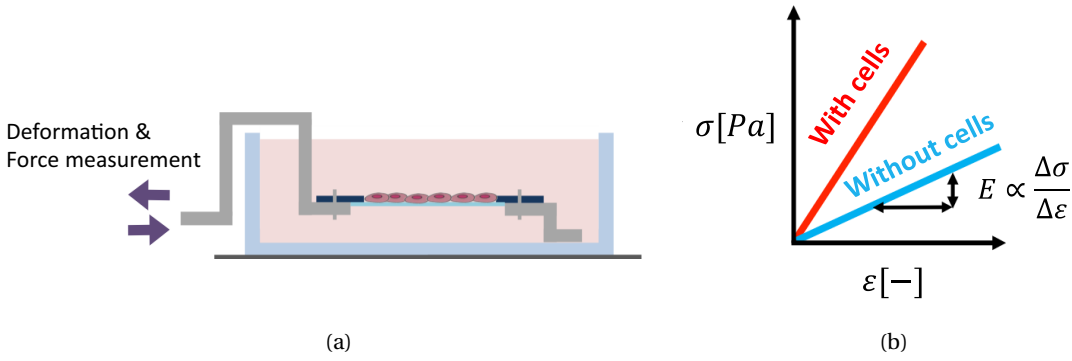
Figure 3.1 – Schematics representing the customized uniaxial tensile test and the expected measurements: (a) standard uniaxial tensile test is adapted to perform measurement in liquid by mean of customized holders; (b) the slope in the stress-strain graph increases when cells are present indicating a higher Young's modulus. In this chapter, I show the optimization of the substrate so that it is possible to see a clear difference in the slope when cells are present on the membrane.

This method is highly versatile and can be generally used when the sample is too thin or cannot be handled and measured on commercial set-ups. This was demonstrated by the fact that the same set-up was also used within two other projects at LMTS Laboratory at EPFL for measuring the mechanical properties of thin stretchable electrodes [134, 135].

3.3 Design and optimization

3.3.1 Model of the sample and sensitivity requirements

We consider an adherent confluent cell layer that fully covers a deformable substrate. Assuming that the cells strongly adhere to its surface, the composite made of the adhering cells and the elastic substrate itself can be considered as two materials perfectly glued to each other as schematically represented in Figure 3.2.

In the simplest case when the cells fully cover the surface the two materials deform together as two springs in parallel when an external deformation is imposed. This model requires two assumptions: (i) perfect adhesion of the cell layer to the substrate and (ii) full coverage by the cell layer.
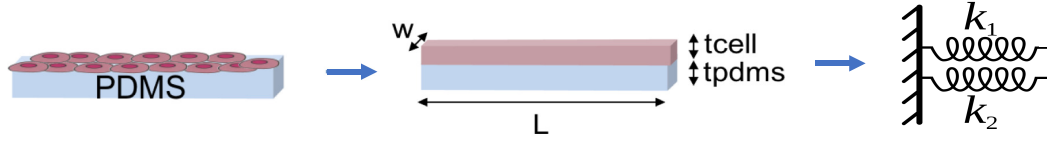
Figure 3.2 – Schematic of the cell layer on the membrane and its modelling as two layers bonded together. The configuration of two parallel springs is used for better visualization of the composite behaviour: the strain is the same for both material while the force is shared between the two, according to their individual spring constant.

Being in iso-strain the conditions:

$$\varepsilon_1 = \varepsilon_2 \quad \Rightarrow \quad \frac{\sigma_1}{E_1} = \frac{\sigma_2}{E_2} \tag{3.1}$$

Where E is the Young's modulus, σ the stress and ε the strain. As the stress is force per unit area, the total stress can be calculated from the stress within the individual regions and their respective dimensions as:

$$\sigma_{tot} = \sigma_1 f + \sigma_2 (1 - f) \tag{3.2}$$

Where f represents the volume fraction of layer 1 and 1-f the volume fraction of layer 2. Combining together Equations 3.1 and 3.2 it is possible to obtain the rule of mixture that can be used to calculate the mechanical properties of composite materials [136]:

$$E_{tot} = E_1 f + E_2 (1 - f) \tag{3.3}$$

Assuming that cell uniformly cover the membrane, the only difference in geometry is given by the difference in thickness between the two layers, and Equation 3.3 can be simplified to:

$$E_{tot} (t_{substrate} + t_{cells}) = E_{substrate} t_{substrate} + E_{cells} t_{cells} \tag{3.4}$$

In order to see the contribution of cells to the mechanical response of the composite, the two factors on the right side of Equation 3.4 should be in the same order of magnitude. To increase the sensitivity of the measurement, the product of the Young's modulus and the thickness of the substrate should therefore be comparable or lower than the cell layer one. Cell monolayer

thickness ranges from few μm to tens of μm depending on the cell type. Regarding cell layer Young's modulus, the few sources available in literature report values between 20 kPa, for kidney epithelial cell monolayer [8, 122], to 155 kPa for vascular smooth muscle cells [124].

In the next sections I detail the material characterization and modelling to optimize the substrate material and geometry for adherent cell mechanical properties measurements.

3.3.2 Material mechanical properties characterization

Ideally the substrate Young's modulus should be as low as possible to increase the measurement sensitivity. However, the material should be chosen taking into account the trade-off between sensitivity and fabrication feasibility. This means that the substrate material should be soft but it should also have a certain degree of mechanical rigidity to sustain deformation and transfer them to the cells cultured on top.

In the range of few kPa to hundreds of kPa Young's modulus we can find hydrogels and polymers. Hydrogels have become very popular thanks to their unique properties such as tunable low Young's modulus (few tens of kPa down to hundreds of Pa), biocompatibility and high water content that make them closely resemble natural living tissues [138, 139]. However, because of their lack in structural integrity they are quite difficult to be given an accurate shape. Polymer typically used in cell analysis applications can be divided into two major categories: thermoplastics and polydimethylsiloxane (PDMS). Thermoplastics (poly(methyl methacrylate) (PMMA), polycarbonate (PC), polystyrene (PS) to cite a few) have high biocompatibility andlow water-absorption however, their Young's moduli in the order of 1-3 GPa makes them much stiffer then the cells and difficult to deform [140]. Polydimethylsiloxane (PDMS) is nowadays the most used material in microfluidic devices thanks to its standard fabrication process, biocompatibility, high optical transmissivity and gas permeability. Furthermore, it combines a low Young's modulus ranging between tens of kPa to few MPa as well as mechanical stability, characteristics that makes PDMS an ideal material for the cell substrate.

Given the importance of the substrate mechanical properties, I performed the mechanical characterization of different PDMS formulations and investigated the relationship between the mechanical properties and the membranes' thickness. 10 μm thick suspended PDMS membranes were fabricated following a casting process developed at the Soft Transducers Laboratory (EPFL, Switzerland) [67]. Briefly the uncured PDMS solution is casted on a Polyethylene terephthalate (PET) foil (Figure 3.3a) on top of a water soluble sacrificial layer (Poly(acrylic acid), PAA). After heat curing, the membranes are released from the PET foil by simple immersion in water and gentle peel-off, which allows to fabricate very thin membranes with high yield. Membranes are attached on PET laser-cut frames using double side tape prior to membrane suspension to keep the desired shape (Figure 3.3b).

I selected few commercially available PDMS formulations and characterized thin membranes' mechanical properties using a commercial pull-tester (3340 Single Column Universal Testing

(a)

(b)

Figure 3.3 – (a) PDMS uncured solution is spread at the desired thickness on a PET foil using a blade caster. This method allow to have relative big area covered with PDMS [and high reproducibility of the membrane thickness. After curing in the oven, the membranes are suspended on PET frames as holders by water immersion. (b) Picture of a 1:6 aspect ratio suspended membrane.

System from Instron, Figure 3.4a). The following silicones were selected:

- Sylgard 186 (S186, Dow Corning®), the standard PDMS used in most microfluidics and devices for cell studies

- MED4901 (NuSil), medium stiffness silicone that can be used in medical implants

- MED4086 (NuSil), a very stiffness and low viscosity silicone elastomer used in medical implants

I fabricated suspended membranes of the selected silicones following the producers' instructions and I suspended them on custom-made frames compatible with our commercial pull-tester as illustrated in Figure 3.4b. The membranes were 10 μm thick and had 1:10 aspect ratio to minimize the necking at the edges during the deformation.

Force versus elongation curves were obtained for the three materials at a strain rate of 6 mm/min with deformations up to 20%. I chose a deformation rate of 6 mm/min so that the samples deform very slowly in a quasi-static regime. In this case the acceleration is very small and can be neglected so that inertial forces due to acceleration do not affect the measurement. The force and elongations data are then converted into stress versus strain. As the stress is defined as the force over the cross-sectional area, it is essential to calculate the modification in thickness and width during the deformation. PDMS is in fact a non compressible material (Poisson's ratio $\nu \approx 0.5$) which means that its volume remains constant during the deformation. In the 1:10 aspect ratio configuration used for the experiment, I considered negligible the inwards compression at the edges and assume that the membrane width (w) remains constant.

(a)

(b)
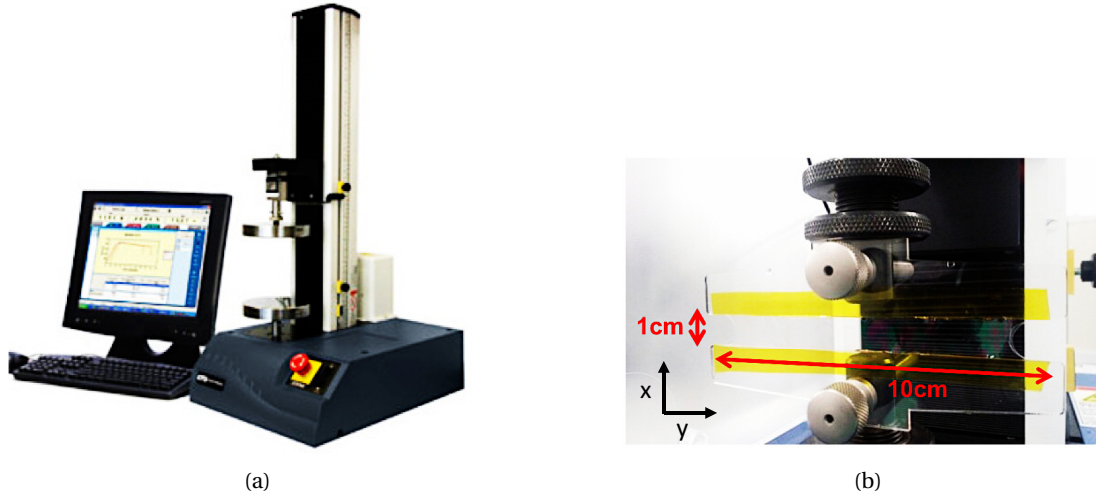
Figure 3.4 – (a) Commercial set-up for mechanical properties measurement used for characterizing the substrate Young's modulus. (b) 1:10 aspect ratio membrane placed on the instrument during a test. Customized PMMA holders are used to hold the sample on the instrument.

As a consequence, when the length (l) is stretched of λ_l, the thickness (t) change accordingly to keep the volume constant:

$$V_0 = V_f \quad \Rightarrow \quad l_0 t_0 w_0 = l_f t_f w_f, \quad \text{where:} \quad w_f = w_0, \quad l_f = l_0 \lambda_l \quad \text{and} \quad t_f = t_0 \lambda_t \quad (3.5)$$

Where λ_l is the applied stretch to the material length and λ_t the resulting stretch in thickness due to volume conservation. We can therefore calculate the change in cross sectional area as [141]:

$$V_0 = V_f = \frac{l_f t_f w_f}{l_0 t_0 w_0} = 1 = \lambda_l \lambda_t \quad \Rightarrow \quad \lambda_l = \frac{1}{\lambda_t} \quad \Rightarrow \quad S_f = t_f w_f = t_0 \lambda_t w_0 = \frac{S_0}{\lambda_l} \quad (3.6)$$

Stress versus strain curves are therefore obtained taking into account the cross sectional area change during the deformation, the results for the selected PDMS are shown in Figure 3.5.

As the membrane deformation is limited along the y direction (the frame constraints the width, see Figure 3.4b), a stress is exerted on the membrane in that direction. Therefore the Young's modulus cannot be simply calculated as the slope of the stress-strain graph which is the case when the only applied stress is the one along the impose deformation direction (in this case along x). Using the generalized Hook law in 3D (Equation 3.7) and imposing that ε_y=0, σ_z=0 and v=0.5 it is possible to find that in this configuration, the Young's modulus is 3/4 of the

stress-strain graphs' slope.

$$\varepsilon_x = \frac{\sigma_x}{E} - \nu\frac{\sigma_y}{E} - \nu\frac{\sigma_z}{E}$$
$$\varepsilon_y = -\nu\frac{\sigma_x}{E} + \frac{\sigma_y}{E} - \nu\frac{\sigma_z}{E} \qquad (3.7)$$
$$\varepsilon_z = -\nu\frac{\sigma_x}{E} - \nu\frac{\sigma_y}{E} + \frac{\sigma_z}{E}$$
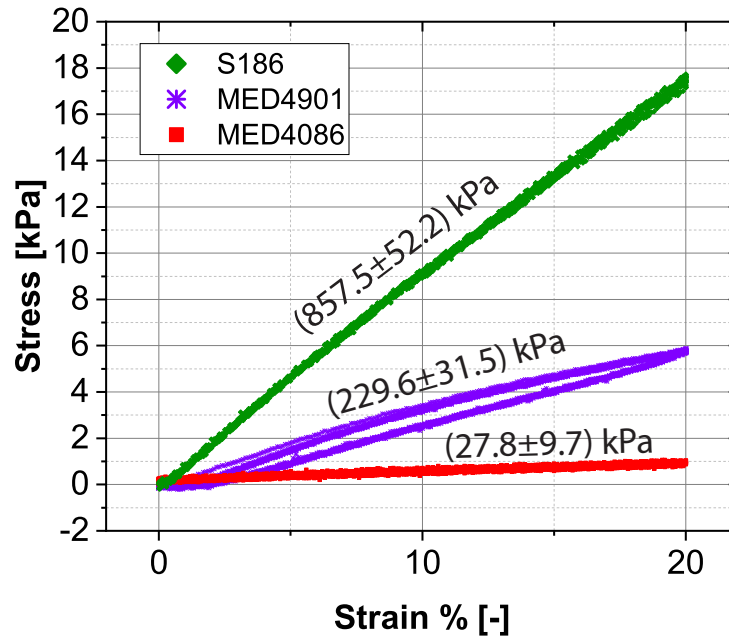
Figure 3.5 – Comparison among different type of commercially available silicones strain stress curves (3 cycles per PDMS formulation). Their slopes indicate the considerable difference among their mechanical properties. MED4086 is chosen as the substrate material for its low elasticity in the orders of 30 kPa (The Young's modulus is calculated as 3/4 of the slope as explained in the text).

The resulting Young's modulus values averaged over 5 samples per each material are: (857.5 ± 52.2) kPa for S186, (229.6 ± 31.5) kPa for MED4901 and (27.8 ± 9.7) kPa for MED4086. The hysteresis in the MED4901 stress-strain curves (Figure 3.5) also shows that this material has higher viscosity than the other two silicones. The variability in Young's modulus, is mainly due to small variability in the fabrication process or in the measurement sample preparation. From these results, MED4086 was selected because of its low Young's modulus which is comparable to the one expected from the cell monolayer [8]. Another possibility to have low Young's modulus silicone was to modify the material crosslinking ratio by changing the amount of curing agent in the liquid silicone mixture [142]. However, we decided not to use this method

as it may lead to mechanical instability, difficult reproducibility of mechanical properties as well as for the cytotoxicity of the residual uncured silicone [143].

3.3.3 Thickness versus Young's modulus characterization

As explained in Section 3.3.1, the requirements for a high sensitivity substrate are: low Young's modulus as well as using thin membranes. I therefore characterized the Young's modulus at different membrane thickness from 750 nm to 20 μm. The results show that the mechanical properties are constant down to 3.5 μm, and then rapidly increase when the thickness is further diminished (Figure 3.6).
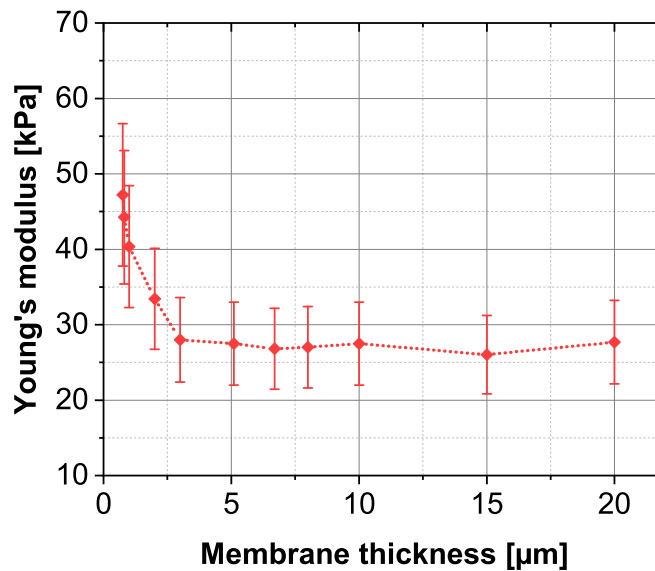
Figure 3.6 – The relationship between Young's modulus and membrane thickness for MED4086 reveals that around a critical thickness of 3 μm there is a transition from the bulk material properties to the surface properties with an increase in Young's modulus (measurements averaged on 3 samples per point).

This is in agreement with previous results [144, 145] and can be explained by the fact that when lowering the surface to volume ratio, as when decreasing the thickness, surface effects are dominating the mechanical properties. Because of the higher cross-linking ratio and the different the polymer chains arrangement at the surface [145], the Young's modulus increases when decreasing the thickness. There is therefore no advantage in lowering the thickness of the PDMS membrane below the 3-4 μm range. The thickness is therefore fixed in a range between 5 and 10 μm which allows to combine low Young's modulus with low thickness and thus increase the measurement sensitivity. In this way, the substrate contribution in Equation 3.4 is very similar to the cell layer one and cell mechanical contribution should be distinguishable from the bare substrate response.

3.3.4 Geometry optimization

The membrane geometry was chosen taking into account the following factors: limiting the lateral necking on the sides during deformation, strain uniformity and miniaturization of the membrane and the set-up. By increasing the membrane aspect ratio, it is possible to minimize the lateral necking and obtain a good strain uniformity. On the other hand, high aspect ratio membranes can be challenging to fabricate because of the very small length and also to integrate in miniaturized measurement device. The surface strains at different membrane aspect ratio were compared using COMSOL Multiphysics FEA (Finite Element Analysis) simulations. Rectangular membrane of 1:2, 1:3 and 1:5 aspect ratios undergoing a 10% deformation were considered (Figure 3.7). We concluded that a 1:5 aspect ratio can combine strain uniformity and dimensions compatible with standard equipment. Better uniformity could be achieved by using even higher aspect ratio membranes at costs of having a more challenging fabrication process and difficulty to integrate the membrane with standard equipments (sample dishes size, optical imaging field of view...). In the rest of this thesis, unless mentioned otherwise, (3x15)mm membranes are used.
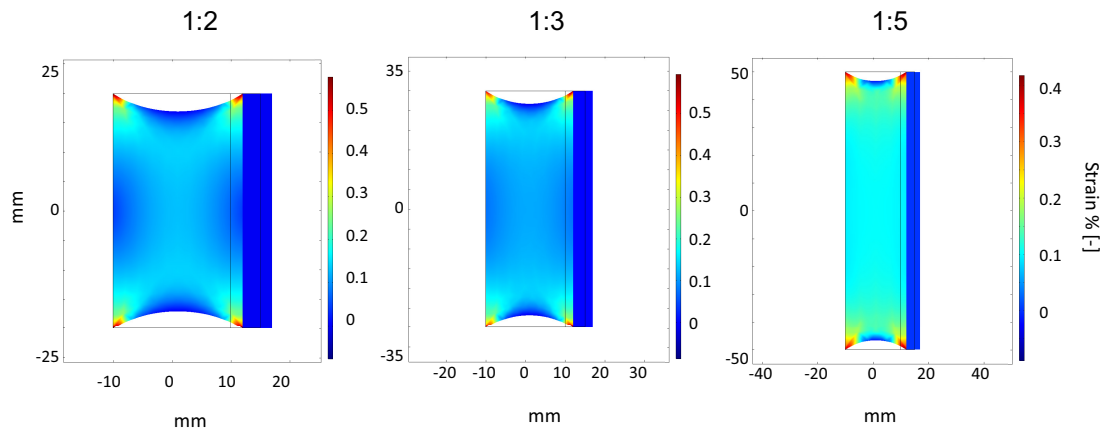
Figure 3.7 – Membrane geometry design comparison using COMSOL Multiphysics FEA structural mechanics module simulations. Different aspect ratio are compared in terms of their surface strain uniformity (first principal strain is showed in the figure) when a 10% deformation is applied. The 1:5 design was selected as optimal geometry because of the strain homogeneity combined with fabrication feasibility.

3.4 Apparatus assembly

I explain here the assembly of the tensile set-up used for the substrate design and to validate the feasibility of the measurement. The need for building this set-up came from the specific requirements necessary for my measurement. The set-up should in fact allow measurements of small forces in liquid environment, it should be compatible with inverted optical microscopy and it should ideally be compact enough to allow displacing it for measurements inside the incubator. As no commercially available instrument was found with these characteristics, the

device was built in-house. This pull test device was therefore assembled by carefully choosing the different components and the configuration to fulfil the mentioned requirements.

The final set-up is shown in Figure 3.8a. It is composed of a linear motor (Linear motor UAL from Saia-Burgess) to apply the desired deformation, a load cell (Futek LSB200, capacity 10g) for measuring small forces during the deformation and the sample holder. I chose that load cell for its high sensitivity below the mN. Also, I developed a LabView code to control the motor and to acquire the elongation and force data over time.

A customized piston structure made of Teflon and stainless steel is used to connect the motor and the load cell to accurately constrain the movement in the horizontal direction. The sample holder consists of a xzy manual stage for the alignment with a Petri-dish on top where the sample is placed during the measurement. Customized PMMA holders have been designed and fabricated with a computer numerical control (CNC) machine for holding the sample inside the Petri-dish: one is glued inside the Petri-dish's surface and another one is screwed to the force sensor outside the Petri-dish Figure 3.8b. Plastic pins are used to fix the membranes' frame on the holders. Before the measurements, the frame is laterally cut on the sides to allow the stretching of the membrane. When placing the membrane on the holder it is important to align it using the xyz stage so that it is perfectly horizontal during the deformation. After the measurement, it is possible to remove the membrane for future use by attaching a new frame around it and carefully removing the pins from the holders.

This apparatus allows thus to perform pull-test experiments in liquid environment and thanks to its small dimension it can be easily displaced. For example it can be placed under an inverted optical microscope for imaging the sample or placed inside the incubator for measurements at physiological conditions.

I used this set-up throughout my thesis to mechanically characterize the PDMS membranes for cell culture, and to validate the measurement approach. In addition, I also used it in two other projects collaborating with colleagues from LMTS Laboratory for measuring the elasticity of thin stretchable electrodes used for dielectric elastomer actuators (DEA). As the electrodes are too thin and fragile to be used as pull-test samples themselves, we characterized them using the same approach as for the cells. By measuring bare membranes and membranes coated with the electrodes, we were able to measure the Young's modulus of the electrode alone. Within the first project together with my colleague Xiaobin Ji, we measured the Young's modulus of carbon nanotubes monolayer electrodes deposed on PDMS membrane through Langmuir-Schaefer process and the results have been published in Sensors and Actuators Journal [134]. In the second project I collaborated with my colleague Samuel Schlatter and use the set-up I developed to measure the Young's modulus of inkjet printed carbon black electrodes for dielectric elastomer actuators [135].
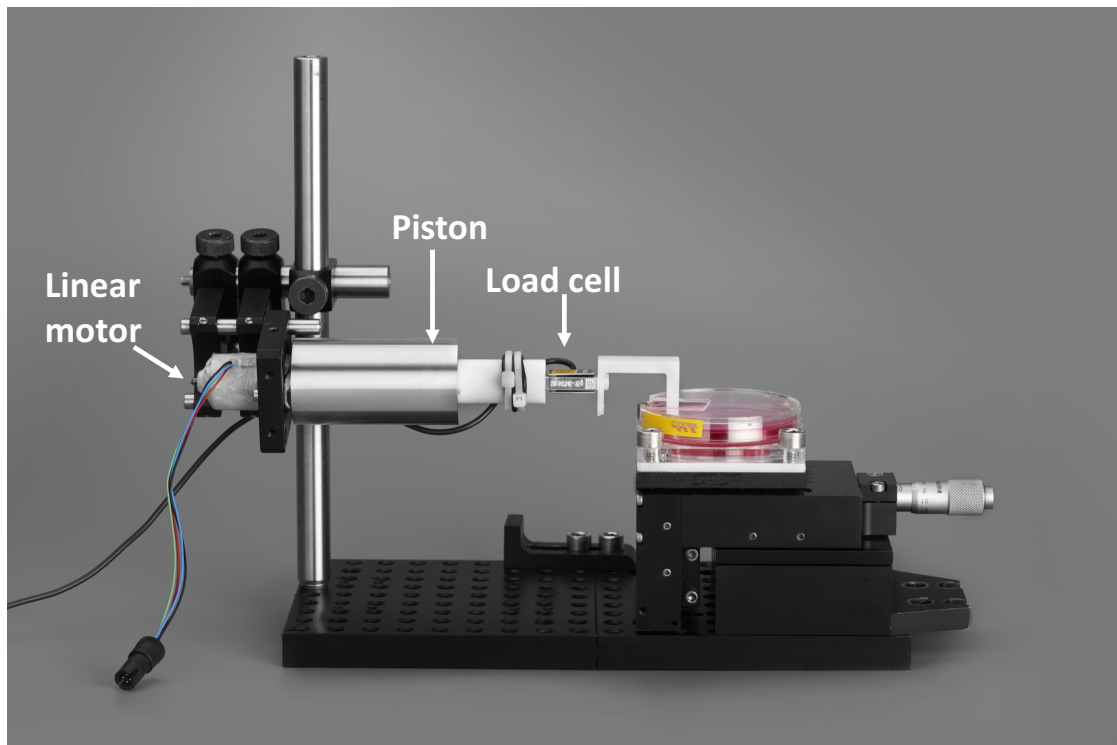
(a)
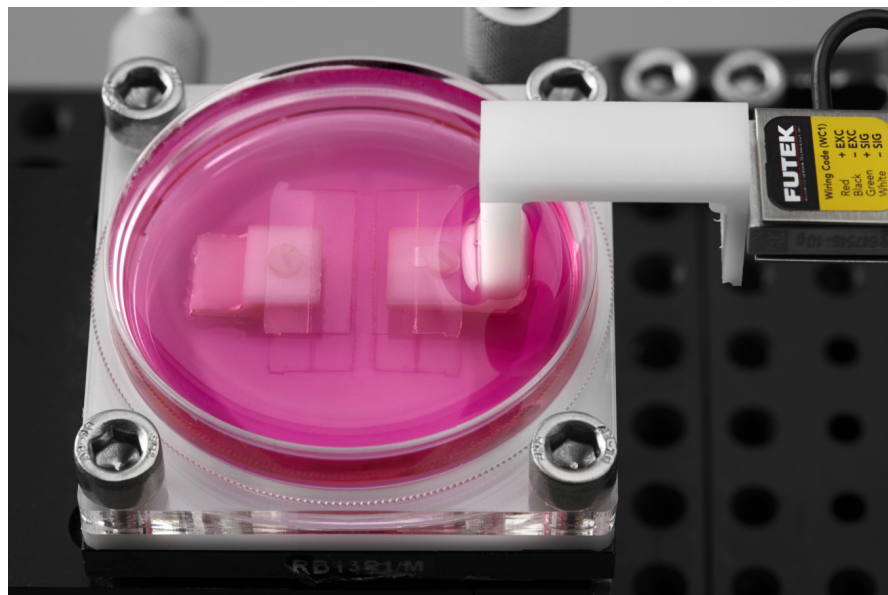
(b)

Figure 3.8 – Pictures of the pull-test device designed and assembled. (a) Final apparatus comprising a load cell and linear motor screwed to each other and to a connector holding the sample inside a liquid bath. The sample is placed inside a Petri-dish for containing the cell medium (b) on a xyz micro manipulator used for aligning the two connectors.

3.5 Experimental validation

The set-up has been first calibrated using known-elasticity samples and then tested to measure cell monolayer elasticity. In the next paragraph, unless otherwise specified, a measurement with the set-up consists in at three or more cycles up to 10% strain at a 0.6 mm/min strain rate. The Young's modulus values are calculated from the force displacement data as explained in Section 3.3.2.

3.5.1 Measurement validation through calibrated samples

In order to validate the measurement approach, calibrated samples with known Young's modulus have been used. The Young's modulus measured using my approach was then compared to the one measured using the commercial pull-test device.
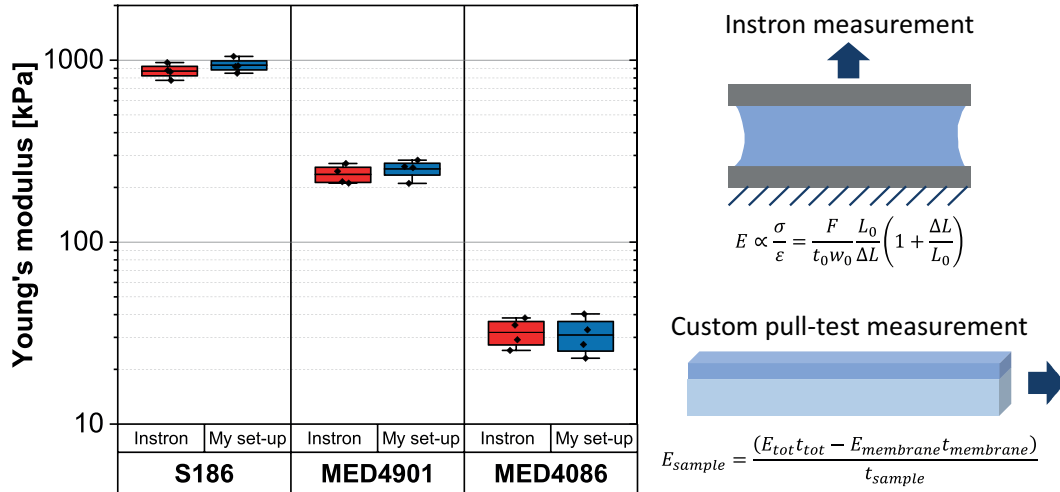
Figure 3.9 – Calibration samples measurement results. The Young's modulus measured using the composite membrane approach I developed is compared to the one measured through a commercially available pull-test device. The results obtained for three PDMS formulations show that the two methods give comparable results within the error bar and thus validate the proposed approach. (The graph represents the results obtained over 4 samples per condition.)

As calibration samples, I used membranes with known elasticity attached to the measurement membrane. Two groups of suspended membranes were prepared from the same PDMS casted foil, one group of membranes was mechanically characterized on the commercial device and the other was used on my set-up in place of the cells using Equation 3.4. The same parameters such as speed and deformation strain where used in both tests. Within my set-up, the calibration samples have been attached to the measurement membrane by simply adding a small ethanol drop before bringing the two surfaces into contact. After two hours drying the two membranes show strong adhesion between them. The calibration sample Young's

modulus is then measured from the composite (measurement membrane+calibration sample). This procedure was repeated for three PDMS formulations with different stiffness in order to test our method on several orders of magnitude. The results for S186, MED4901 and MED4086 are shown in Figure 3.9.

The obtained results show the reliability of my method as the Young's modulus is comparable to the one measured using a commercial instrument within the error bar. These results validate the proposed measurement approach within the tested range ~20 kPa - 800 kPa. In order to test the set-up for lower stiffness samples, hydrogels (Young's modulus tunable between hundreds of kPa and hundreds of Pa) could be used. However this was not feasible because of the difficulties in shaping hydrogels as thin membranes, making them adhering to the PDMS surface and having a standard method for results comparison.

3.5.2   Cell Young's modulus measurement

The experimental procedure with living cells consists in comparing the elasticity measured before seeding the cells on the surface, after cell adhesion and then after detaching the cells from the substrate. In these experiments sarcoma osteogenic cell line (SaOS$_2$) was used. Osteoblasts-like cells, such as SaOS$_2$ are found on the bone surface to isolate the mineralized internal structure from the external body fluids. Because of their structural function, osteoblast layers Young's modulus is an essential property for sustaining bone deformations during movement avoiding bone damage [146]. The choice of these cells was done because of the expected high Young modulus in respect to other cell lines (based on AFM-based measurements on single cells).
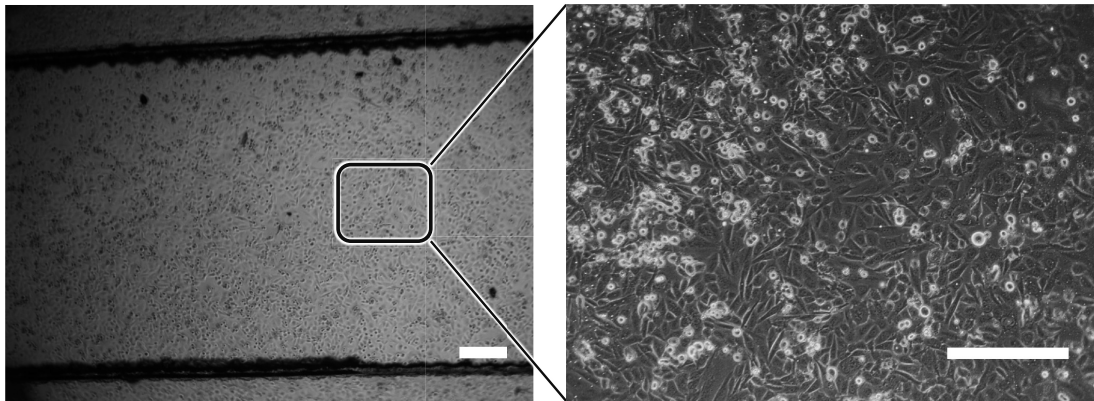
Figure 3.10 – SaOS$_2$ cells adhering on the membrane after 3 hours culture at 5x and 10x magnifications. Thanks to the surface functionalization and high concentration of seeded cells, it is possible to achieve a good cell coverage on the membrane. (scale bar is 200 μm)

All experiments were done within one day because of the difficulty in keeping the sample sterile when placed on the measurement set-up. Because of the holder presence, in fact, it is difficult to ensure good sealing of the sample. Temperature control during the experiment

was achieved by placing the Petri-dish with the sample inside a portable incubator (Stage Top Incubator from Okolab) compatible with inverted microscope imaging.
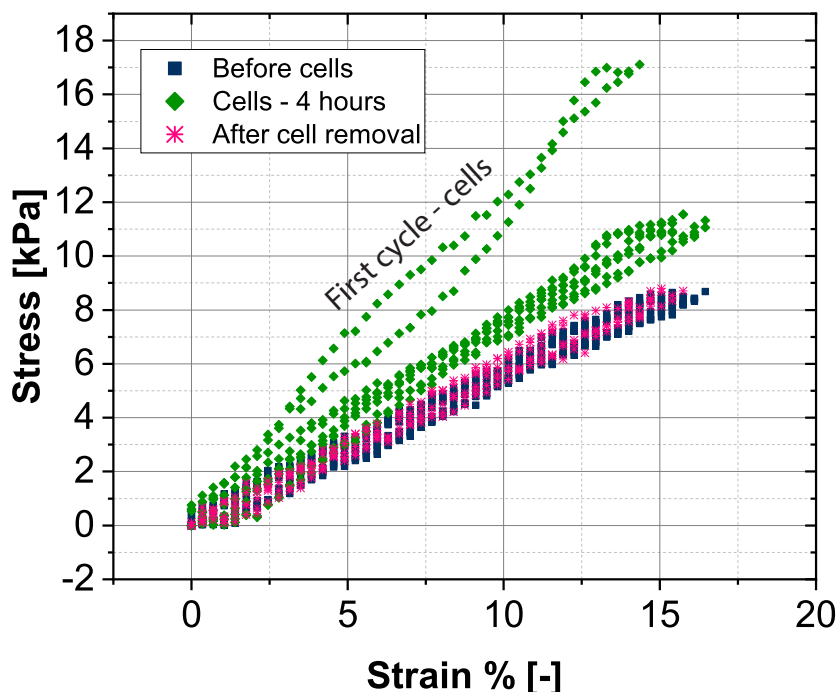
Figure 3.11 – SaOS$_2$ tensile measurement results at a 0.6 mm/min strain rate. Typical stress-strain curves of the three measured conditions: after membrane functionalization, after cell adhesion and after cell removal. The first stretching cycle with cells is considerably different from the following ones, where the response stabilizes at slightly higher slope than the non-cell measurements. This can be due to an adaptation of the cells to the imposed deformation after the first stretching cycle.

The set-up is carefully sterilized with ethanol using tissues and placed under an inverted microscope. A membrane of known thickness is placed on the set-up and the lateral frames are cut to allow it to deform (details on the membrane fabrication can be found in Section 4.5). The Petri-dish is then filled with ethanol for sterilization purposes, and washed three times with DI water. The surface is chemically functionalized for 1 hour by incubating 1 mg/ml human fibronectin (Corning) solution in HEPES 10 mM to facilitate cell adhesion and spreading on the surface. The surface is then washed three times in DI water, then the Petri-dish is filled with complete cell medium (McCoy 5A, Sigma) and the first measurement is performed. The cell solution (3 10^5 cells/ml) is prepared by collecting cells with 0.25 % trypsin-EDTA (Gibco) from a flask, and few drops of the cell solution are placed on the membrane to cover it. The cells are let 2 hours to adhere, medium is then added all around in the Petri-dish. After another hour, and provided that the cells are forming a confluent layer on the surface (Figure 3.10), a measurement is performed. The medium is then removed from the Petri-dish and trypsin

solution is added for 5-10 minutes to detach the cells. After complete removal of cells from the surface, the Petri-dish is again filled with medium a final measurement is performed. The measurement results are shown in Figure 3.11.

A clearly different response is measured when cells are adhering on the membrane. Also, as shown in the graph the curve goes back to the initial response after removing the cells. These measurements clearly indicate that it is possible to see the cell contribution to the total mechanics of the membrane and that the membrane was successfully designed. The first cycle of the cell measurement significantly differs from the following ones where the curve stabilizes. This may be due to an initial higher resistance of cells to deformation followed by their adaptation to the stretching that makes the following cycles very repeatable. In Figure 3.12 the Young's moduli measured in the three conditions are compared. From these measurements the Young's modulus of the cell monolayer itself is (66 ± 12) kPa assuming the osteoblast cell thickness to be 10 μm [146].
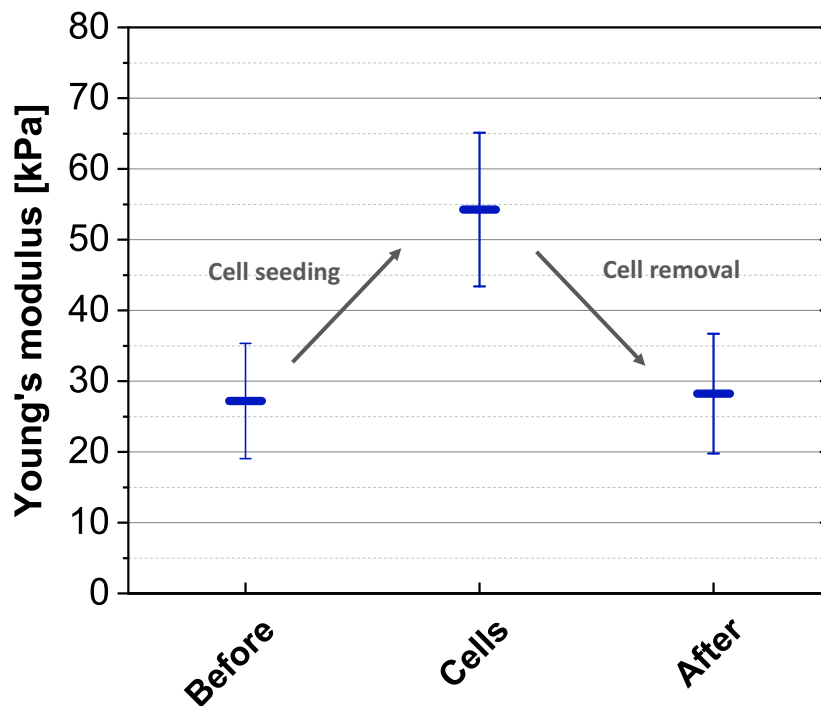
Figure 3.12 – The measured Young's modulus increases when cells are adhering to the surface and goes back to initial value after cell removal. The measurements are performed on ~ 5μm and 5 samples per point are averaged. The reversibility of the measurement allows to prove that the increase in stiffness is actually due to the cell presence.

These measurements allowed to successfully validate the design of the membrane and that measurement of adhering cells to an appropriately designed substrate are feasible. However, reliable values of the Young's modulus could not be measured because of the lack of a fully

mature cell monolayer on top of the membrane. Due to the difficulty in assuring a good sterility of the sample overtime we decided to limit the experimental time to few hours so that there was any influence from possible contaminations of the sample.

3.6 Conclusion

In this chapter, I showed that by carefully choosing the substrate mechanical properties and design so that its elastic constant is in the same order of magnitude as the cell monolayer's one, it is possible to measure the stiffening effect of cells adherent to it. This measurement is performed by comparing the mechanical response of the substrate covered with cells with the bare membrane response. The proposed Young's modulus measurement approach was validated through calibration and then cell measurements. The ability to measure the cells contribution from the overall mechanical response clearly indicates that the design of the membrane was successfully achieved. The material and thickness choices explained in the previous sections result in a substrate that is sensitive enough to allow cell measurements. Also, when removing the cells from the substrate, the response goes back to the one before cell seeding. The reversibility of this test confirms that the stiffening effect is due to the cell presence.

The possibility to measure in plane Young's moduli of adherent cells is a considerable improvement in respect to state of the art techniques [8, 124] based on tensile test which were limiting the measurement exclusively to suspended cell monolayers. Our approach, not only is more robust and easier to implement but also allows to measure the mechanics of adherent cells, i.e. in a similar configuration as would be found in the body.

Although this set-up is very sensitive and versatile, it has two main limitations associated to the sample sterility and measurement throughput. Because of the difficulty in keeping the membrane in sterile conditions, measurement could not be performed over long time-scales. Also, measurements can be performed only in a sequential way, thus limiting the impact and the possibilities of using this device outside the research environment. These limitations could have been overcome by small changes in the set-up design. However, as the key concepts and measurement feasibility were validated, I preferred to take a step further and miniaturize the elasticity measurement down to chip-scale dimensions as I will explain in the next chapter.

4 Miniaturized device for cell layer mechanics - Design and fabrication

4.1 Summary

In this chapter, I detail the conception and development of the miniaturized device to measure the Young's modulus of adherent cell population (Figure 1.2). The results validated in Chapter 3 are here applied on a more advanced stage by miniaturizing the measurement set-up. Thanks to its novel working principle and miniaturization, the proposed device overcomes most of the limitations of state-of-the-art devices such as bulky equipment, repeatability, measurement time limitation, difficulty in continuous sample observation etc. In the next paragraphs, I will show the design and fabrication steps I have developed to build this device. I first summarize the operating principle highlighting the novel approach that allows to combine in-plane deformations within a miniaturized measurement set up and I explain how the mechanical properties are measured. I then justify the design choices in order to meet the targeted stretching and read-out requirements. I finally present the final fabrication process I developed and the performance characterization of the device.

The potential of measuring cell elasticity on-chip is demonstrated by the capabilities of measuring Young's modulus and its variations over time as presented in Chapter 5. The heart of the technology I developed is the combination of the high sensitivity membrane (Chapter 3), differential strain read-out and actuation on-chip. Cells are cultured on suspended membranes and are exposed to tensile strain applied by pneumatic actuation. The core of the proposed approach is to measure the force exerted on the composite (membrane+cells) by monitoring the deformation of part of the membrane itself where cells are not present. As the membranes' mechanical properties are known, it is possible to extract the Young's modulus of the cell monolayer by just measuring their elongation. In this way, the force measurement is integrated within the measurement device making the miniaturization possible.

Part of the sections on the operating principle and processes have been presented at the MicroTas conference 2018 [147]. Additional information on the design fabrication and characterization methodology are provided in this chapter.

4.2 Requirements

The main requirements for the miniaturized device for measuring cell layer elasticity are summarized in Table 4.1. The measurement platform must be cytocompatible and optically transparent, it should be easily kept and used in a sterile environment and apply physiological range strain to the cells. Regarding the cytocompatibility, the material should not affect cell physiology, it should sustain standard cellular culture protocol such as sterilization and incubation and its properties should not be affected by ethanol or cell media. Transparency is necessary to optically monitor the sample during the measurement to asses cell viability. Compatibility with standard inverted microscopy and ideally with fluorescence microscopy implies that the cells should be placed at a distance compatible with the working distance of standard objectives, and they also should remain in the same focal plane during the measurement. To keep the sample in a sterile environment, the easiest approach is to make it compatible with standard Petri-dishes. Regarding the strain range, commercially available cell stretchers normally allow deformations up to 20% strain with frequencies up to 5Hz [117]. We chose to fix the strain between 5% and 10% in order to avoid active modification of the cell monolayer due to the imposed strain. Also, in order to ensure measurements within the elastic regime we chose to have low frequency deformations.

Parameter	Requirement
Biocompatibility	Essential
Compatibility with sterilization	Essential
In-liquid operation	Essential
Physiological & sterile environment	Essential
Optical transparency	Essential
Miniaturization	Highly desirable
Easy parallelization	Highly desirable
Strain type	Uniaxial tensile strain
Strain amplitude	$5\% - 10\%$
Deformation frequency	Below 0.1 Hz
Working lifetime	2 h to 24 h

Table 4.1 – Key requirements summary for the cell elasticity measurements device.

4.3 Choice of the operating principle

The choice of the operating principle is important because it determines the possibility to miniaturize the device. Young's modulus measurements require to quantify deformation and force at the same time.

Regarding the actuation, the most common techniques used in cell stretcher devices are pneumatic actuation, piezoelectric actuation, electromagnetic actuation and dielectric elas-

tomer actuators (DEA). The most crucial parameters considered in the choice of the actuation are summarized in Table 4.2. Pneumatic actuation combines a simple set-up without any direct contact with the biological sample or the cell culture medium, that is essential to avoid contamination. Also it can be easily miniaturized and parallelized. Piezoelectric actuation has the key advantage of the precision and wide range of controllable strains while electromagnetic actuators provide high precision and programmability. However, piezoelectric such as electromagnetic actuators actuators require a direct physical contact with the biological entities, which is severely limiting its applications [108]. Furthermore, electromagnetic actuators may include heating and contamination through lubrication. While electromagnetic and piezoelectric techniques have been excluded because of the difficulty in keeping the sterility of the sample, DEA and pneumatic actuations do not have these limitations. However, DEA may have stabilities issues and failures when operated in liquid environment over long time. Also as the electrodes are incorporated within the cell culture substrate, it is quite difficult to combine material optimization for both actuation and cell mechanics measurements. We therefore chose to implement pneumatic actuation.

Property	Actuation technique			
	Pneumatic	Piezoelectric	Electromagnetic	DEA
Miniaturization	✓	✓	~	✓
Parallelization	✓	~	✗	✓
Long term in-liquid measurements	✓	✗	✗	~
Substrate choice	✓	✓	✓	✗

Table 4.2 – Crucial requirements among the most common used method for cell-stretcher actuators are compared. For cell mechanical properties measurements it is important that the substrate can be designed to be as sensitive as possible, that measurements can be performed inside the incubator maintaining the sterility. Also miniaturization and possible parallelization are important parameters for future development stages of the device.

While actuation can be easily implemented, the force measurement is not straightforward. Most of force sensing methods are based on measuring deformations of components with known Young's modulus for example cantilevers [148], pillars [149] or beads embedded into a matrix (as in traction force microscopy, TFM) [150]. Forces can also be measured as the change in resistance when the resistive path is deformed as in strain gauges. Force sensors that are based on resistance measurements can be easily miniaturized but are very sensitive to temperature and humidity variations and they need to be insulated [151] to be used within cell culture platforms. As PDMS is a permeable material, it is very difficult to integrate strain gauges and assure their stability in liquid over time. I chose therefore to base the force measurement on optical deformation tracking thus removing any influence of temperature and humidity.

I chose to use part of the membrane dedicated to cell culture also for the force measurement. By making cells adhering only on part of the membrane, it is possible to monitor the deforma-

tion of the remaining part in order to measure the force exerted. Membranes' Young's moduli are in fact characterized for every device before experiments with the cells. Measuring the force from the deformation of the cell membrane allows to miniaturize even more the device. This approach results in a differential measurement between the membrane with and without cells which allows to subtracts effects due to the membrane itself and comparing in-real time the response of the two conditions.

The final working principle of the device is illustrated in Figure 4.1. The pneumatic actuation relies on the deformation of a thin wall in contact with the suspended membrane were cells are cultured. In contrast to already published stretching devices where pneumatic actuation is used to stretch cells over two sides or even radially [118], the membrane is stretched only on one direction, keeping the other side of the membrane fixed. This choice was done to assure a precise and uniform stretch over the membrane surface. It can in fact be quite difficult to obtain exactly the same stretching on both sides of the membrane: even if the pressure is changed in both chambers at the same time, the deformation on the two sides can slightly differ because of small differences from the fabrication or assembly processes. The deformation of the two regions is continuously monitored optically by placing the device under a microscope during the measurements.
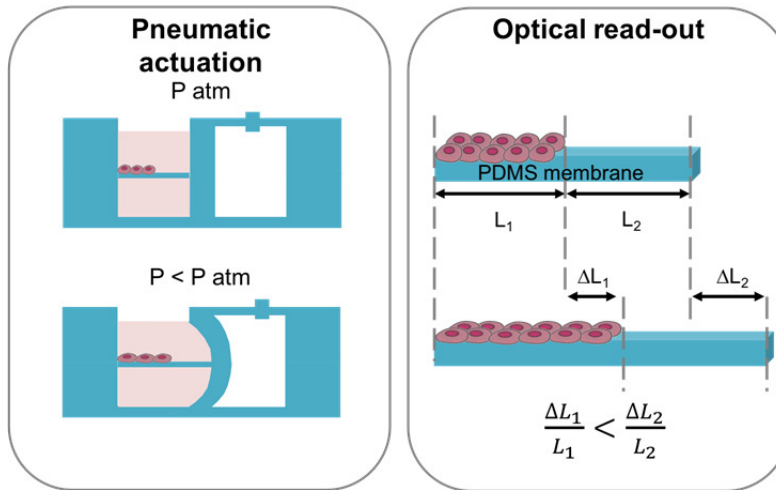
Figure 4.1 – Schematic of the device showing the chosen actuation and sensing approaches. Controlled negative pressure in the right chamber of the fluidic device allows in plane stretching of the confluent cell monolayer. The relative elongations of the cell and bare regions are optically monitored during the stretching. The strains of the two regions differ because of the cell presence increasing the stiffness.

Using the differential strain configuration, the bare and cell regions of the membranes can be modelled as two springs in parallel, of which, the one comprising the cells consists of two parallel springs as detailed in Chapter 3 (Figure 4.2).

When a negative pressure is applied and the membrane is deforming in plane, the two regions (bare and composite) sustain the same force. By equating these two forces and rewriting the

44
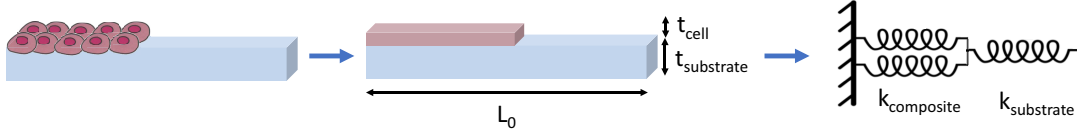
Figure 4.2 – Schematic of the cell layer and substrate model in the differential approach: the same force is exerted on both regions as in two springs in series, they therefore deform of different amount depending on their Young's modulus.

formula in terms of stress and strain it is possible to obtain:

$$F_{bare} = F_{composite} \quad \Rightarrow \quad \sigma_{bare} t_{bare} = \sigma_{composite} t_{composite} \tag{4.1}$$

$$\varepsilon_{bare} E_{bare} t_{bare} = \varepsilon_{composite} E_{composite} t_{composite} \tag{4.2}$$

Substituting then Equation 3.4 for the composite region, the following formula to measure the Young's modulus of the cell monolayer is obtained:

$$E_{cell} = \left(\frac{\varepsilon_{bare}}{\varepsilon_{composite}} - 1 \right) E_{bare} \frac{t_{bare}}{t_{cell}} \tag{4.3}$$

Where the strain of the two regions are measured during the stretching, while the other parameters like the thickness and the PDMS Young's modulus are characterized prior to the measurement.

4.4 Stretching design and modelling

The device has been modelled using COMSOL (structural mechanics module) to optimize its dimensions and geometry for the desired strain range. As the deformation should happen only at the interfacing wall, I decided to use a stiffer type of PDMS (S186) to fabricate the device and design its geometry to make different regions more or less easily deformable. The modelled design is quite simple, a suspended membrane (MED4086) is fixed on one side and attached to a deformable wall (S186) on the other. Negative pressures down to 100 kPa are applied over the whole wall surface (Figure 4.3a) and the deformation of the membrane is measured when varying its thickness. Figure 4.3b reports the modelling results, comparing the membrane strain when different pressures are applied and for a range of thickness varies between 100 μm and 1 mm. The thinnest the wall, the higher deformation is possible at lower pressure,

nevertheless fabrication constraints should be taken into account. The desired strain range is between 5% and 10 % strain, we decide therefore to use a wall thickness of around 500 μm that would combine ease of fabrication and desired strain range. I also analysed the influence of the wall length on the membrane strain uniformity. In general, it is in fact preferable to have some space laterally for a more uniform deformation. A length or around 50% of the membrane width is added on each side to make the wall longer and therefore its deformation in the central area more uniform.

(a) (b)
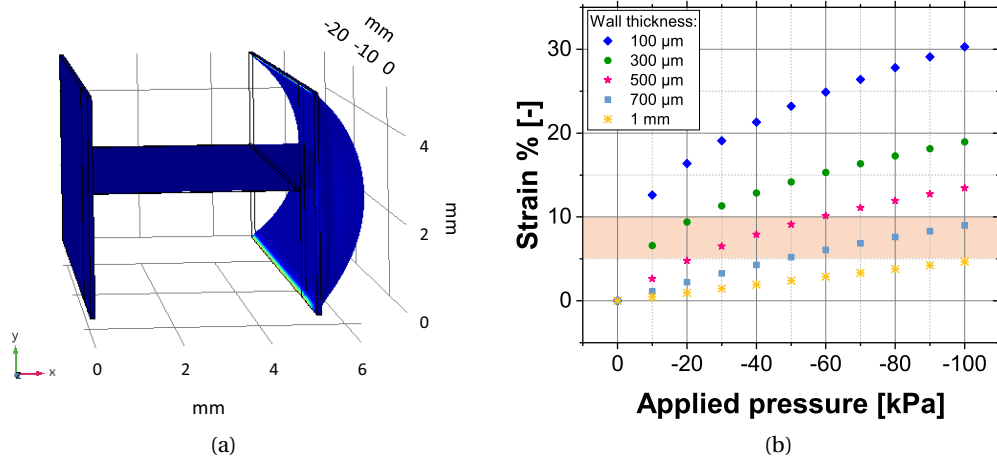
Figure 4.3 – FEA was performed to design the device geometry for pneumatic actuation. The schematics report the surface stress when pressure is imposed on the vertical deforming wall. Half of the suspended membrane connected to the deforming wall is used for the study taking advantage of the system symmetry. The parameters taken into account are the membrane thickness and the lateral wall length. (b) The strain is plotted for different applied pressure and wall thickness, the configurations suitable for 5% − 10% strains are taken into account and among them the 500 μm thick wall is chosen for its fabrication ease.

4.5 Fabrication process

In this section, I detail the finalized device fabrication process, which consists in three steps: the device molding, the membrane fabrication and the final assembly.

The device moulding, this is done by curing the PDMs formulation S186 in a custom mould to shape the bottom and top parts of the device. A single device is fabricated by assembling and glueing a bottom and a top piece together. Custom moulds shown in Figure 4.4a are fabricated in Teflon using a CNC milling machine (Step-Four CNC Basic 540 from Laumat). They consists of a layer with extruded adjacent channels giving shape to the middle wall. The mould has also an intermediate layer used to define the piece thickness. The different components of the mold are tightly fixed together using screws. S186 is mixed in a 1:10 ratio in a planetary mixer (Thinky mixer, ARE-250), the liquid mixture is then poured inside the

closed mould and then placed inside a desiccator to remove any bubbles from the mixture. After degassing, the pieces are placed inside the oven at 80°C for at least three hours. Thanks to the hydrophobic properties of Teflon, the PDMS can be easily removed from the mould once it is cured. Channels defining a middle wall of 500 μm width and 2 mm thickness were easily fabricated as shown in Figure 4.4b.

(a)　　　　　　　　　　　　　　　　　(b)

(c)　　　　　　　　　　　　　　　　　(d)
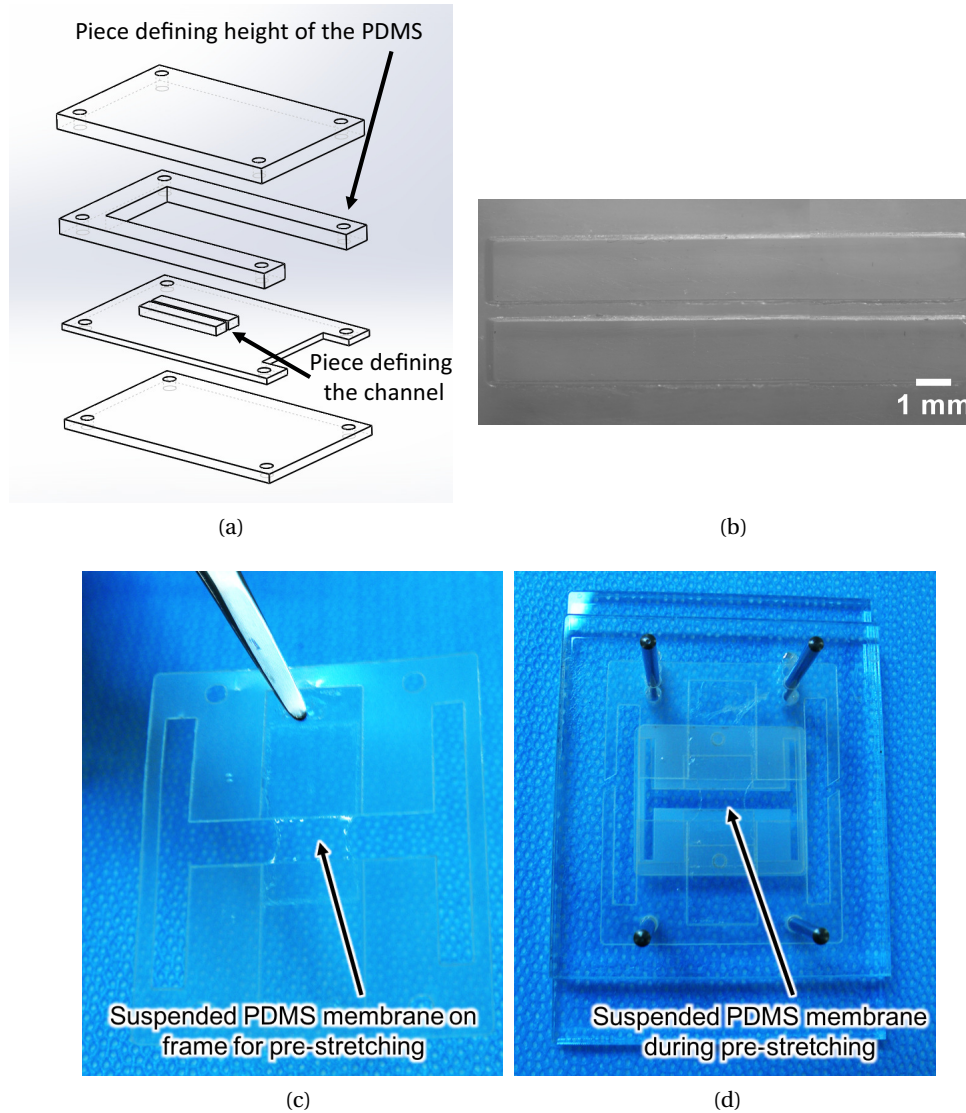
Figure 4.4 – Schematics and pictures from the fabrication process: (a) SolidWorks exploded view of the mould, (b) Picture of the molded bottom part of the device with the two channels parallel channels defining the cell and pressure chambers, (c) Suspended PDMS membrane on a frame designed especially for the pre-stretch, and (d) Picture of the pre-stretching step which is performed by uniaxial elongation of the membrane on a customized membrane stretcher. A new frame is then glued to the membrane to maintain the tension.

The membrane is made of the PDMS formulation MED4086 and is fabricated using a casting process developed in LMTS [152]. After curing of the membrane on the PET foil, (3x15)mm

rectangular shapes are cut and attached to custom laser-cut frames as shown in Figure 4.4c. The membranes are then pre-stretched of 1.5 stretch (50% strain) to keep them in tension and avoid sagging. The pre-stretch is also necessary for the cells to better adhere and spread on the surface. This pre-stretching step is performed on a customized membrane stretcher allowing to elongate uniaxially the suspended membrane of a precise amount (Figure 4.4d). After the pre-stretch, a new PET frame is attached to the suspended membrane to keep it in tension. The mechanical characterization of the pre-stretched membranes show that the Young's modulus does not vary from the non-pre-stretched membrane as it is still in the linear region of the stress versus strain curve (Figure 4.5).
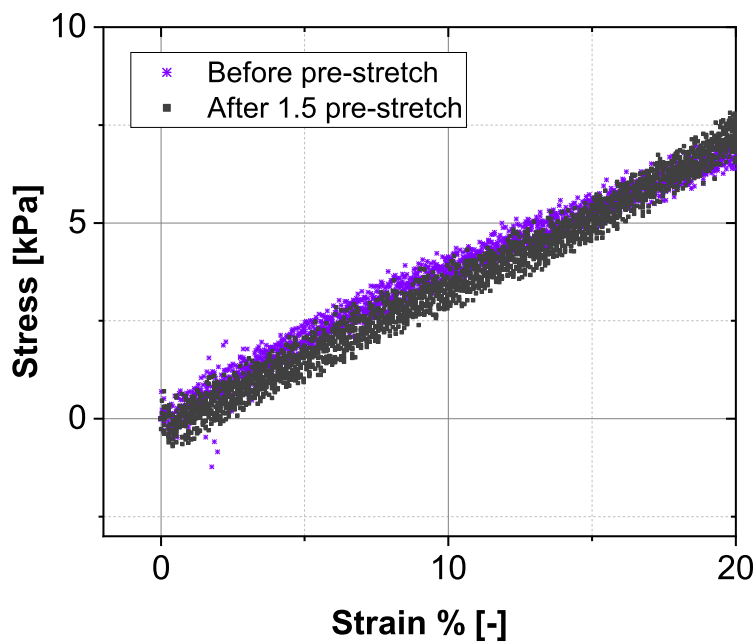
Figure 4.5 – The stress versus strain response is analysed for the membranes before and after the pre-stretch. The resulting curves show that the mechanical properties remain the same.

Each membrane is mechanically characterized using the custom set-up presented in Section 3.4 and their thickness is measured using a custom spectrometer developed within the LMTS laboratory at EPFL. Membranes are then glued to the bottom part of a device using a cytocompatible silicone glue RTV (Room-Temperature-Vulcanizing silicone, E43 from Elastosil) and are left in the incubator for one night as the glue cures in high humidity conditions. After this time, the lateral sides of the frame can be carefully cut leaving the membrane suspended within the cell culture channel. Few features were included to optimize the fabrication and measurement process and are shown in Figure 4.6. First, the frame holding the membrane was designed so that it is also partially suspended within the channel. This has two advantages: minimize the possibility that the glue is spread on the suspended part of the membrane which would interfere with the elasticity measurement, and second it allows to have an easily visible

line to track during the strain measurement even during the wall deformation. Another feature was to add laser-cut reference lines on the frame border to facilitate the positioning when the sample is observed at high magnification and therefore the membrane is not entirely visible.
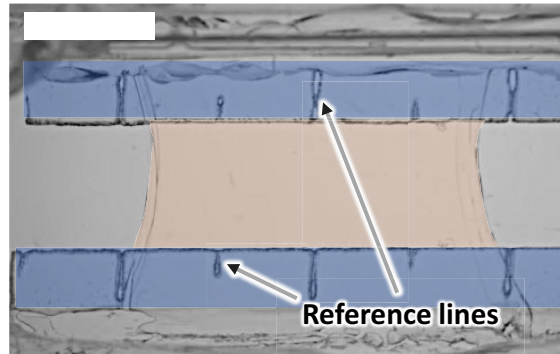
Figure 4.6 – Top view of the membrane for cell culture within the device. The fabrication process has been optimized by suspending the membrane (light pink zone) within a frame (light blue zone) to avoid glue to be in contact with the membrane; also reference lines are added to make it easier to locate the position at high magnification. (scale bar is 2 mm)
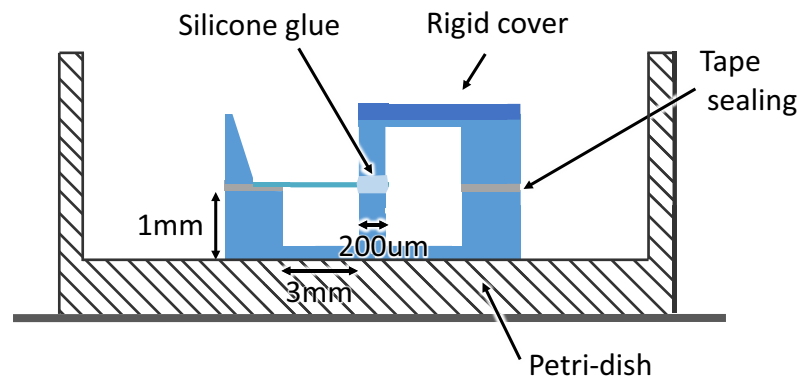
Figure 4.7 – Cross-section of the final device. The assembly consists in sealing the bottom and top molded pieces with the suspended membrane in the middle. Silicone glue is used to ensure the sealing during the deformation. Glass cover-slips are attached to the bottom and top surface to avoid their deformation during the actuation.

After gluing the membrane on the bottom part of the device, the top part is glued using both double side tape and RTV glue. The use of the glue is especially important for the two parts of the deforming wall to avoid leakage. The final assembled device is shown in Figure 4.7. In order to avoid deformation of the bottom or top surfaces when negative pressure is applied, glass cover-slips are attached using optically clear double side tape (ARclear 8932EE, from Adhesive Research). This was done so that the bottom piece could be thin enough to allow high magnification microscopy without deforming. Also a laser cut reservoir is added on top to contain more liquid and a hollow needle is inserted into the sealed chamber to have a tube connection towards the pressure control set-up.

4.6 Experimental set-up

The experimental set-up used during the elasticity measurement is shown in Figure 4.8a.

Pressure regulator   **Pressure sensor**

(a)
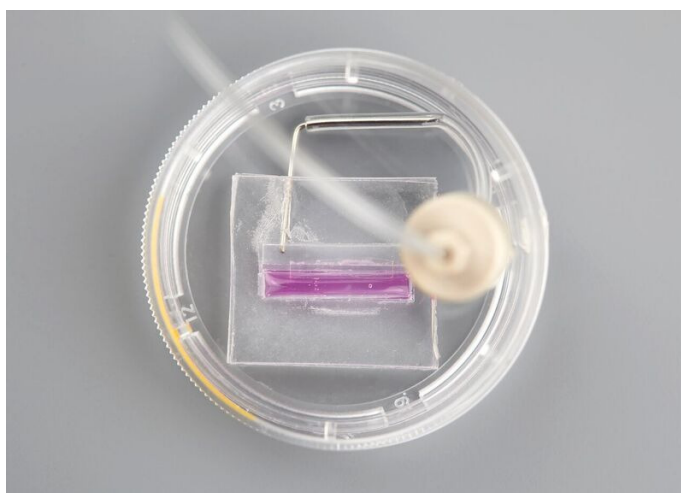
(b)

Figure 4.8 – Pictures of the experimental set-up used during the measurements. (a) A microscope compatible with imaging inside the incubator is connect to the computer outside the incubator, while the device is connected by a tube to an external pressure controller and sensor, these are controlled through a LabView interface. (b) Zoom-in on the device inside a standard cell culture dish with the engineered connectors for the tube to the outside.

The device is placed inside a standard Petri-dish (60 mm or 35 mmm are normally used in this work) and under an inverted microscope. The inverted microscope (Etaluma^{TM}, LS460) has been chosen for its compatibility with incubator environment over long time scales so that the sample can be kept in physiological conditions for the whole measurement. The Petri-dishes containing the device are engineered with connectors for the negative pressure tube (Figure 4.8b), thus assuring sample sterility. The tube connects the device to a pressure sensor (general fluids pressure sensor, PSE560 from SMC) and a pressure controller (electronic vacuum regulator, ITV009 from SMC) placed in series. The negative pressure source used was either the building vacuum supply or a portable pump (DS27 pump, D3K series from TCS micropumps). The pressure controller and sensor are controlled through a data acquisition card and a LabView program that I developed to apply a cyclic deformation over time. Also, the microscope is connected through a USB port to the computer for image acquisition. During the measurement pictures are acquired at 10 frames/second rate.

The whole set-up is quite simple, very versatile and portable. It allows to keep the samples inside the incubator while controlling the stretching and the imaging from the outside, without the need to open the incubator during the measurement.

4.7 Device performance characterization

The final device was characterized before starting experiment with the cells. In the next paragraphs I report the results from the strain versus applied pressure response and the creep behaviour characterization. Finally, I validated this measurement approach by using calibration samples in a similar way as in Chapter 3. All the presented characterization tests are performed when the cell culture chamber is filled with liquid and inside the incubator. The strain measurements are optical and based on a pattern recognition algorithm as detailed in Section 5.3.2.

4.7.1 Strain versus pressure response

The relationship between strain and the applied pressure is characteristic of each device as it highly depends on the fabrication process. This characteristic curve is measured for each device and defines which pressure should be applied to obtain a certain strain. I perform this characterization on each device prior to cell culture. In fact the response may considerably change depending on small fabrication details such as the amount of silicone glue added during the device assembly or the alignment between the two pieces.

An example of curve is shown in Figure 4.9 where the strains in the central and lateral regions of the membrane each over 3 cycles are reported. In the graph only the way up of the curve are compared. The obtained results show that for every applied pressure the resulting strain is comparable among the central and the later regions of the membrane, indicating the uniformity of the strain over the surface. Also, the response is the same over several cycles

(here only 3 are shown for simplicity) demonstrating the response repeatability.
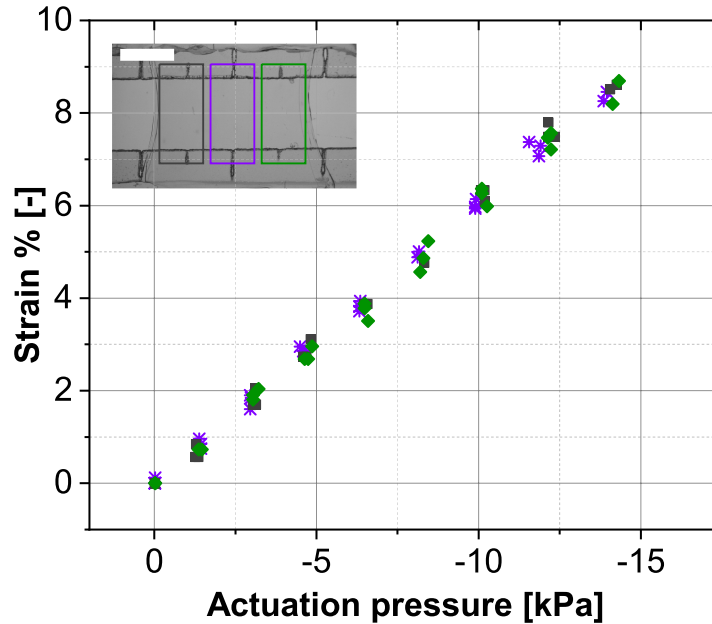
Figure 4.9 – The graph reports the results of the strain response of the device at different applied negative pressures. The strain is optically measured in 3 different parts of the membranes over 3 cycles each. The resulting curves demonstrate the uniformity and repeatability of the applied deformations. (scale bar is 2 mm)

4.7.2 Creep response

The device response over time was also characterized through creep experiments. For this, a pressure step is applied and then kept constant while optically measuring the membrane strain. The obtained results show a stable response of the device over up to 30 minutes (Figure 4.10). The device's response was compared with and without the membrane inside the device to investigate its effect. As expected, when the membrane is not present the device has a very similar response with just higher strain for the same applied pressure because of the decreased stiffness. As PDMS is intrinsic viscoelastic, it is possible to observe that the strain does not instantaneously reach its maximum level after a change in pressure. A rising time of 3 seconds is needed before the strain reaches its maximum value. It is important therefore to wait at least this time during the experiment so that the final strain is exerted on the cells.
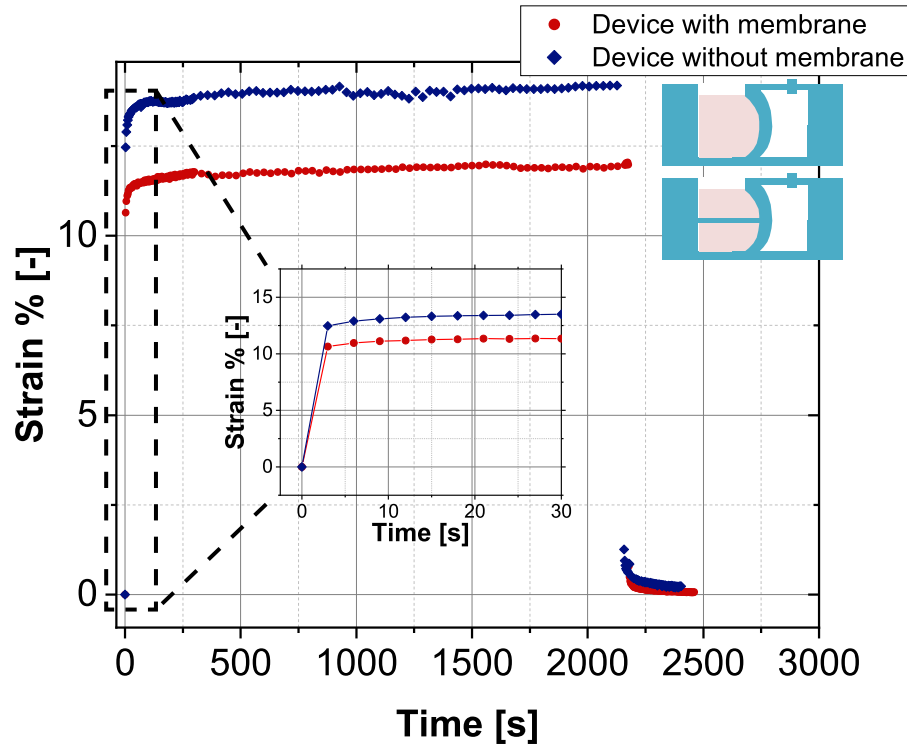
Figure 4.10 – The graph shows the strain evolution over time when a step in pressure is applied. Because of the viscoelastic properties of the material, the strain reaches its maximum value after a 3 seconds rising time. The membrane presence has the only effect to decrease the exerted strain for the same applied pressure as its presence increase the rigidity of the deformable parts of the device.

4.7.3   Set-up validation using calibrated samples

The measurement approach was validated in a similar way as presented in Section 3.5.1 using samples of known Young's modulus. In this case the calibrated samples were attached only on half of the membrane by carefully aligning the known membrane elasticity sample in a way that it covers only part of the measurement membrane (Figure 4.11a). Calibration samples' (MED4086) Young's modulus was measured over 3 stretching cycles using Equation 4.3 and compared with the commercial pull-tester device (3340 Single Column Universal Testing System from Instron). The results indicate that the two methods are comparable within 15% of their mean value (Figure 4.11b). This is comparable with the error of the measure and therefore validate the differential approach for measuring elasticity of samples adherent to the membrane.
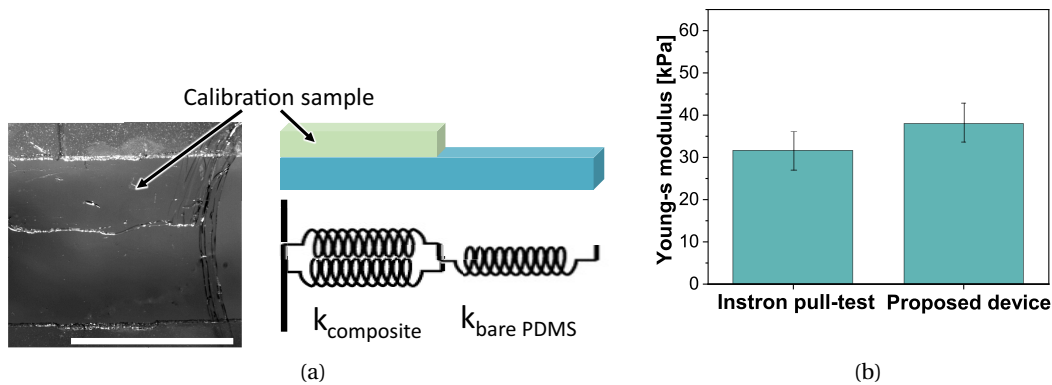
Figure 4.11 – Picture and schematic representing the known-elasticity thin membranes that are used as calibration samples instead of the cells. (a) The sample can be modelled as two springs in series, one representing the bare membrane and one the composite (in this case measurement membrane plus known elasticity membrane) (scale bar is 2 mm). (b) The measured values of the Young's modulus at 5% strain between the differential strain read-out I propose and a commercial pull-tester device are comparable within 15% of their mean value thus validating our approach (measurement on 5 devices each).

4.8 Conclusion

In conclusion, in this chapter, I presented the design for a compact cell stretcher allowing measurements of cell mechanical properties. The high sensitivity membranes developed in Chapter 3 are combined with a careful design of the actuation and sensing methods allowing miniaturization of the measurement. The main challenges in performing mechanical properties measurement with cells are discussed. Pneumatic actuation is chosen for its simplicity, scalability and compatibility with sterile measurements. Tensile uniaxial strain above 10% can be exerted with the presented device, however I chose to limit the strain to 5% during the Young's modulus measurements in order not to actively modify cells' morphology.

The design of the stretching device and its fabrication process have been detailed. The final device is made of cytocompatible and transparent materials, it can be easily sterilized and used with cell medium over several weeks. Table 4.3 summarize the fulfilment of the previously defined requirements.

The reported measurement approach, based on differential strain read-out, allows to avoid complicated force sensing methods and to miniaturize the device to chip-scale dimensions. This comes along with several advantages such as versatility, portability, compatibility with most of cell culture analysis platforms and techniques. Furthermore, using a differential approach makes the system independent of many variables (surface covered by the cells, pressure variations) that would otherwise significantly affect its precision. In addition, as the read-out is based on optical methods, there are no limitations in terms of stability or sensitivity

Parameter	Requirement	Result
Biocompatibility	Essential	Achieved
Compatibility with sterilization	Essential	Achieved with ethanol
In-liquid operation	Essential	Long-term (days-weeks)
Physiological, sterile environment	Essential	Long-term (days-weeks)
Optical transparency	Essential	Achieved
Miniaturization	Highly desirable	Achieved
Easy parallelization	Highly desirable	Feasible, not demonstrated
Strain type	Uniaxial tensile strain	Unixial strain profile
Strain amplitude	$5\% - 10\%$	$2\% - 15\%$
Deformation frequency	Below 0.1 Hz	0.025 Hz - 0.25 Hz
Working lifetime	2 h to 24 h	Several days

Table 4.3 – Key requirements summary and obtained results for the cell elasticity measurements device.

when performing measurements inside the incubator.

Thanks to the miniaturization of the device, it is therefore possible to perform investigation of cell monolayer mechanical properties over time in physiological environment. This represents a major step forward towards more representative of the in-vivo conditions investigation, to date in fact most of the mechanical measurements are performed in ambient conditions, thus being relatively far from those felt within the in-vivo physiological environment [1].

5 Measurements of cell mechanical properties

5.1 Summary

In this chapter, I demonstrate the successful application of the miniaturized device presented in Chapter 4 for measuring the mechanical properties of cells in vitro.

I first demonstrate that the strain imposed to the membrane is entirely transferred to the cells by tracking cellular strain during the actuation. The linear correlation between cellular and monolayer strains indicates that cells tightly adhere to the substrate and deform together with it. This is also confirmed by the spreading of focal adhesions imaged through confocal microscopy, indicating that cells homogeneously form bonds with the PDMS membrane. Furthermore, I show that it is possible to perform live cell imaging by staining the nuclei of living cells and tracking their deformation during the stretching. The elasticities of two cell lines are then quantified by cyclically exerting 5% tensile strain at 0.01 Hz on the cell population and measuring their Young's modulus using the differential strain read-out. Finally, I report the creep response results showing that the cell rheological behaviour is distinguishable from the PDMS one. For this, I analyse the creep response of the bare membrane and the membrane with cells by fitting the experimental curves with a Kelvin-Voigt model. The time constants of both regions are measured and show a clear difference between the cell and bare regions. This indicates the feasibility in quantifying the rheological properties of cells as well using this device.

All together, the results showed in this chapter provide the first demonstration of adherent cell mechanical properties measurements on-chip.

5.2 Epithelial cells

Epithelium is one of the primary tissue types in animals along with connective, muscle and nervous tissues. Cells within the epithelium form cohesive sheets and can be arranged in a single layer of cells or in a stratified conformation. Their main function is the lining of the inner

57

and outer body surfaces and cavities such as in skin, guts and ducts. Also, they chemically separate different physiological environments thanks to the tight association between cells through mechanical junctions that stabilize the tissue.

Because of their role as interfacing surfaces throughout the body, epithelial cells are continuously subjected to mechanical deformations. By sustaining tensile and compressive stresses and transmitting the mechanical information over several cell diameters, epithelial cells ensure proper organ stabilization since morphogenesis [21]. Understanding epithelial cell mechanotransduction processes in terms of forces, displacements and their time evolution is a key issue in mechanobiology. It is known that applied stress within short time-scales (around 1 minute) and below 10% strain, elastically deform the cellular sheet while preserving its integrity [153]. These deformations are elastic and reversible. On the other hand, when stress is applied over long time scales (tens of minutes or more), the cell layer exhibits a so-called fluid behaviour where cells move in a similar way as particles diffusing within a liquid [154]. One of the most common model for mammalian epithelial cells are Madin-Darby Canine Kidney (MDCK) cells. These cells are used for a wide variety of studies in research such as cell polarity, cell-cell adhesions, collective cell dynamics as well as self-assembly into 3D structures [155].

5.3   Materials and methods

5.3.1   Cell culture protocol

Prior to cell culture, the PDMS membrane is chemically functionalized to allow cell patterning, the process is illustrated in Figure 5.1a. The device is placed inside a Petri-dish and sterilized with ethanol. After three washing steps with DI water, a rectangular shaped Mylar piece, is carefully aligned on to the suspended membrane inside the device. This step is quite challenging because of the fragility of the membrane and the difficulty in manually reaching it. Fibronectin solution (50 μg/ml) in HEPES 10mM is incubated for 1 hour at room temperature to promote cell adhesion. The membrane is then washed and the Mylar membrane carefully removed. Pluronic F-127 diluted in DI water at 0.4% w/v is then added to the surface and let to incubate for 1 hour. The pluronic functionalizes the surface where fibronectin is not present and thus creates two regions on the surface with different chemical functionalization. MDCK cells (NBL-2, ATCC®, CCL-34^{TM}) are cultured following the manufacturer protocols [156] and seeded on the chemically functionalized membrane at a concentration of 250 000 cells/ml. The device is incubated at 37°C for 1 hour. Within this time, cells adhere only to the regions functionalized with fibronectin (Figure 5.1b). Unattached cells are therefore removed by gentle washing of the membrane surface with PBS. When the patterned is not needed, the membrane is simply treated with fibronectin for promoting cell adhesion on the whole surface. The cell culture chamber is then filled with cell culture medium (Eagle's Minimum Essential Medium (EMEM) supplemented with 1% streptomycillin and 10% inactivated fetal bovine serum), and the device is placed again inside the incubator for 4 hours. Thanks to

the high cell concentration, the cells form a confluent monolayer within around 5 hours of incubation at 37°C, 5% CO_2 and 95% relative humidity. The pluronic and fibronectin coatings on the membrane has been experimentally proved to not affect the mechanical properties of the membrane itself (Figure 5.2).

1. Fibronectin incubation using a mylar mask   2. Pluronic solution incubation   3. Cells seeding

■ PDMS   ■ Fibronectin   ■ Mylar mask   ■ Pluronic   ■ Plastic frame

(a)

2mm

200 μm

(b)
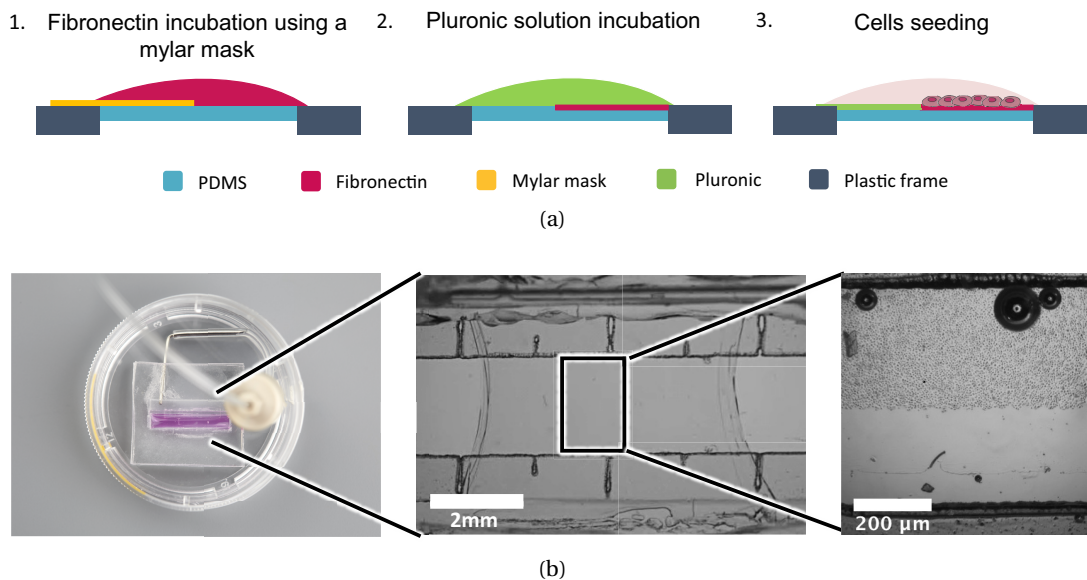
Figure 5.1 – Cell patterning protocol: (a) schematics of the protocol steps to obtain a double surface functionalization; (b) obtained patterning of MDCK on the suspended membrane.
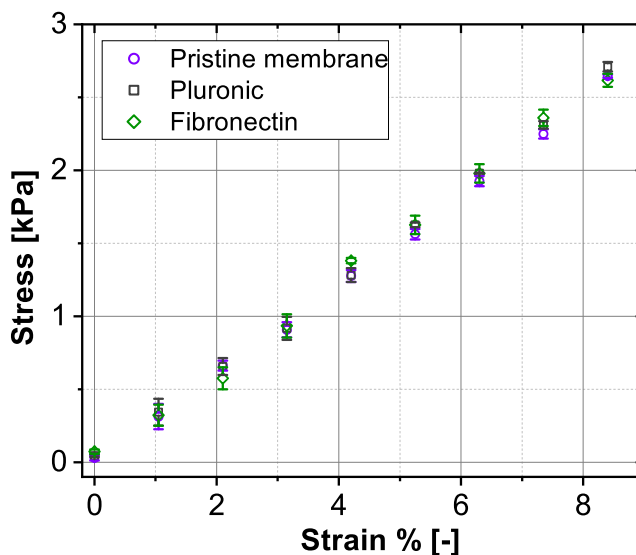
Figure 5.2 – Stress versus strain graph comparing the mechanical response of the pristine membrane and after protein functionalization (3 samples each). The effect of both pluronic and fibronectin to the membrane mechanical properties can be considered negligible.

5.3.2 Mechanical stimulation and strain optical read-out

All the measurements are performed in liquid and inside the incubator after a 30 minutes conditioning time to let the device and liquid adapt to the temperature and humidity levels. A measurement consists of three consecutive pressure cycles. The applied pressure is chosen after the device calibration to reach a membrane strain of around 5%. Each cycle consists in decreasing the pressure and keep it constant for around 30 seconds before returning to the initial position. During each of these steps, pictures are continuously taken at 10 frame/s. The pictures are then analysed using a pattern recognition algorithm using Vision Assistant software (from National Instruments). Briefly, regions of interest to be tracked are defined on one image and then a batch process is run to analyse the whole series of images from the measurement. This allows to automatically obtain the strain of the whole membrane and of the individual regions (bare and cell regions) over time. The Young's modulus is measured from the ratio of the bare and cell regions' strains using Equation 4.3. For this, the strain values at constant pressure are used and values are averaged over 3 cycles.

5.3.3 Staining and microscopy

The immunostaining protocol consists of the following steps. Cells are treated with 0.4% Triton-X, 0.4% formaldehyde solution for 3 minutes. They are then fixed in 4% formaldehyde for 20 minutes, permeabilized in 0.4% Triton X-100 for 10 minutes and finally blocked in 5% BSA (bovine serum albumin) for 2 hours. The primary antibody is added (α-Vinculin or α-ZO-1 produced in mouse) at 1:100 concentration in blocking buffer (5% BSA, 0.01% Triton X-100 in PBS) and incubated overnight at 4°C. The secondary antibody is then incubated (α-mouse, 1:500) for 2 hours and after that Phalloidin-488 at a concentration of 1:20 in blocking buffer is added for 45 minutes. The membranes are then mounted on glass slides using DAPI mounting medium for long term storage. Images were taken at a confocal microscope (Leica TCS SP5) and a fluorescence microscope (JPK Microscope Axiovert 200, Zeiss). The obtained images were processed using ImageJ software.

5.3.4 Cell layer thickness measurements

Cell thickness measurement is needed for the Young's modulus measurement (see Equation 4.3). For this, MDCK layer thickness was measured when cells are cultured on the suspended PDMS membrane by confocal z-stack analysis. A confluent cell layer patterned on half of the membrane was fixed and stained for actin, ZO-1 and DAPI.

I acquired confocal images of the layer at different sample heights in a z-stack configuration. The group of images were then combined and analysed with ImageJ software to obtain a 3D image of the monolayer and to measure its thickness. The resulting images, show that after an incubation time of 5 hours, cells homogeneously cover the membrane surface. The height is calculated as an average among different regions and results in $(8.25 \pm 0.3)\mu$m which
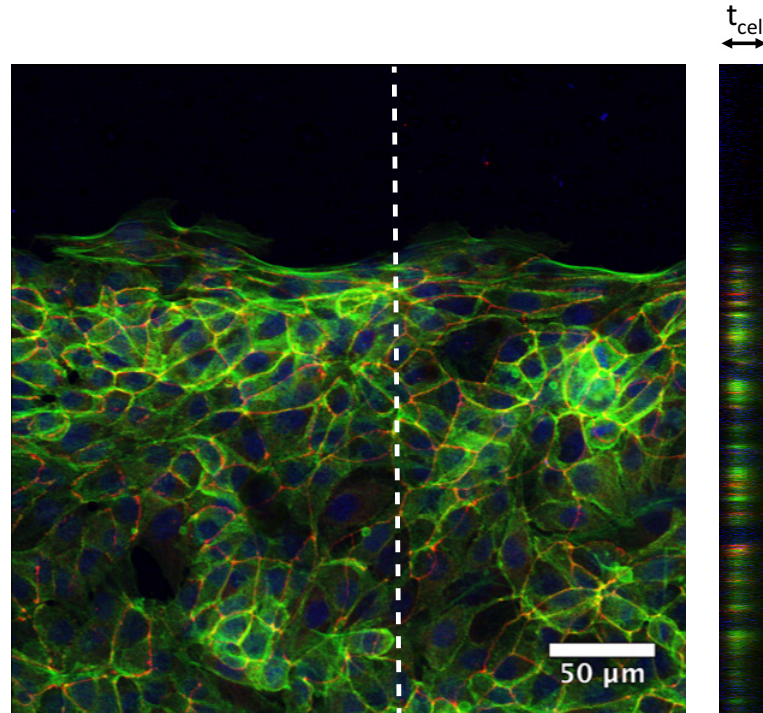
Figure 5.3 – Confocal imaging (20x magnification) of the cell layer on the membrane. A z-stack is acquired and its projection is used to measure the thickness of the cell layer. In the picture MDCK layer is shown with green staining for Alexa-488, red for tight junction protein ZO-1 and blue for DAPI. Performing a linear cut of the z-stack allows to estimate the thickness of the layer which results in $(8.25 \pm 0.3)\mu$m.

correspond well to previously reported literature values [157].

5.4   Cell layer adhesion on the membrane

Cell adhesion is an essential requirement for the Young's modulus measurement approach I developed. Cells need to well adhere to the PDMS suspended membrane also during the deformation so that the imposed strain is transferred to the cell layer.

5.4.1   Focal adhesion immunofluorescence imaging

As a first proof that cells adhere to the PDMS surface, I imaged their focal adhesion sites on the suspended membrane. Cells were cultured on a suspended membrane but not inside the device because of the difficulty in doing high magnification confocal imaging on the membrane when this is inside the device. Figure 5.4 shows the resulting imaging of focal adhesion after 5 hours incubation time. Focal adhesions are showed as the red dots, which are quite homogeneously distributed over the surface indicating the proper spreading of cells on the surface and their mechanical adhesion to it. This indicates that thanks to the protein

functionalization of the PDMS, cells can form adhesion sites in a similar way as they would do on standard cell culture substrates.
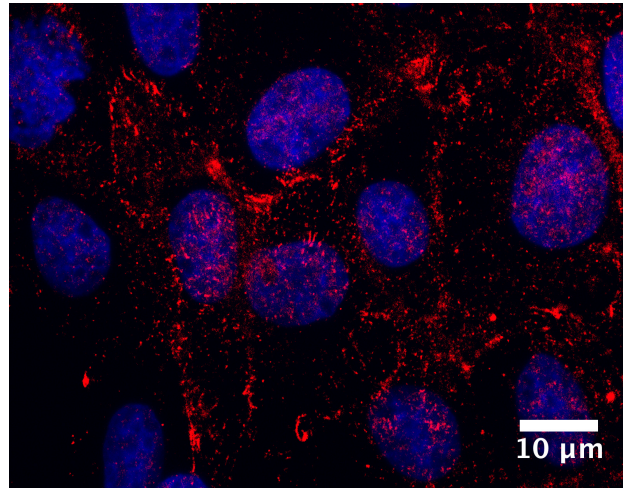
Figure 5.4 – Focal adhesion immunostaining (Leica confocal microscope, 60x magnification) on MDCK adhering to the PDMS membrane (Vinculin in red; DAPI in blue). The distribution of focal adhesions (in red) indicates the proper adhesion of cells on the surface.

5.4.2 Cellular strain versus monolayer strain characterization

In order to asses the quality of the cellular bond to the membrane, I correlate the strain of single cells within the monolayer to the whole monolayer one. For this, a suspended membrane inside the device was fully coated with fibronectin and then cells so that the whole surface was covered by a confluent cell layer. In this configuration, the membrane strain is the same as the cell monolayer strain. Cyclic deformation was applied and the monolayer strain was compared to the strain measured for single cells within the monolayer itself. The cells were imaged using a 5x objective to observe the whole monolayer deformation and then using a 10x objective to allow observing single cells deformations. In both cases, the recorded images were then analysed using the pattern recognition algorithm as explained in Section 5.3.2 to track both the monolayer and the cells deformations. The results are illustrated in Figure 5.5 and show a linear correlation between cell and monolayer strain up to 10% membrane strain. This confirms that the strain applied to the membrane is successfully transmitted to the cells in the range of strain used during the measurement.

Single cell strain within the monolayer was also measured in the direction perpendicular to the actuation (Figure 5.6). Along the actuation direction, the cell strain averaged on 8 cells within the monolayer is 5.21±0.43 and matches tightly to the whole monolayer strain which was measured as 5.12±0.13 averaged on 4 consecutive cycles. Along the transversal direction, cellular strain is tightly close to zero with a value of -0.22±0.24 averaged on 8 cells within the monolayer. The small negative value of strain in the transversal direction, indicates a small compression of the cells. However, this is negligible compared to the deformation along the

actuation axis. During actuation, cells are therefore deformed with an almost pure uniaxial strain.
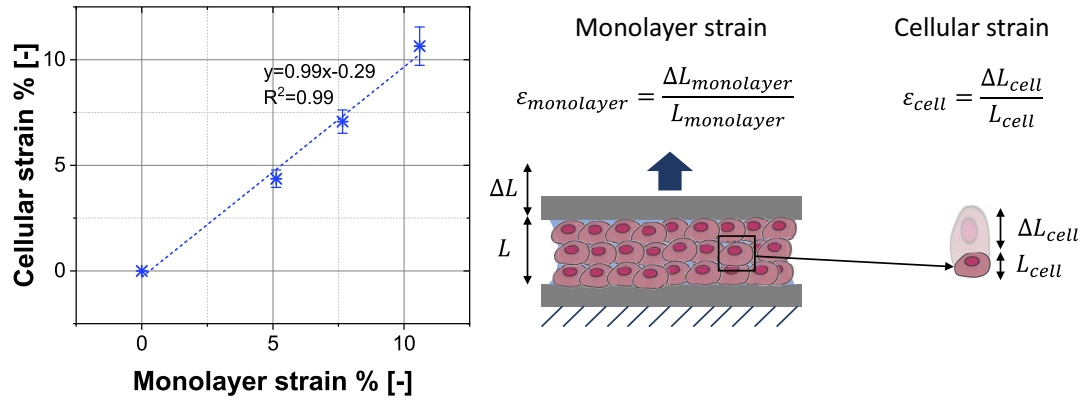
Figure 5.5 – Linear correlation between cellular and whole monolayer strain indicates that the cells deform together with the substrate. The strain is completely transferred from the membrane to the cells resulting the same deformation for both.
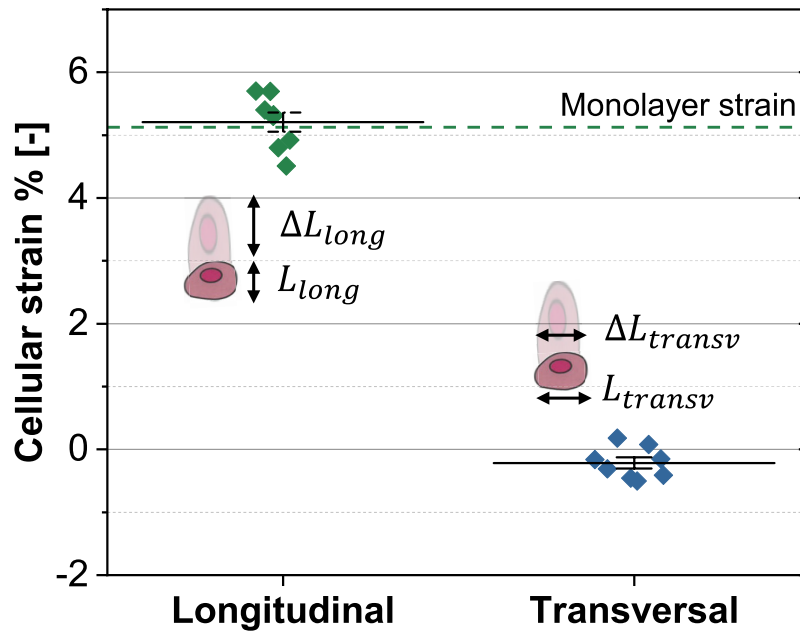
Figure 5.6 – The individual cell deformation happens in the same direction of the imposed strain in this case 5%, and it is almost zero in the transverse direction. This confirms that cells undergo uniaxial strain during the actuation.

5.4.3 Living cells fluorescence tracking during mechanical stimulation

Live cell fluorescent imaging is interesting for the possibility to image in real-time cellular protein variations [158] and correlate them with the elasticity measurements. I demonstrate here that the developed device is also suitable for living cell fluorescence imaging during the stretching by tracking living cell nuclei deformations. A device with the membrane fully covered with cells was incubated with NucBlue reagent (Hoechst 33342 from ThermoFisher), a cell-permeable nuclear stain for 20 minutes in the incubator. Then the device was placed under the fluorescence microscope and the nuclei images were taken at 6% and 12% membrane strains. Nuclei relative displacement was measured on several cells and in both cases it well correlates with the whole membrane strain as shown in Figure 5.7.
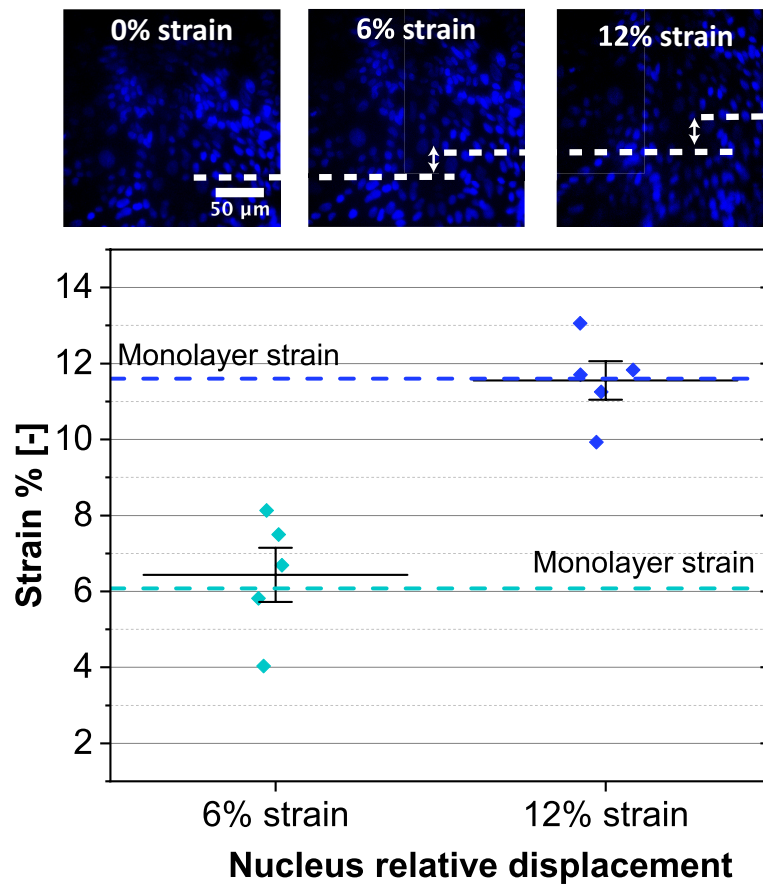
Figure 5.7 – Live cell fluorescence imaging of the nuclei during the actuation allows to track their displacement. We measure the nuclei relative displacement at 6% and 12% membrane strain and observe that the nuclei (represented with the dots) undergo the same strain imposed by the membrane (dotted line).

The fluorescence imaging was performed using inverted fluorescence microscopy on the whole device and using a 10x objective. During the deformation there was no need in adjusting the focus, indicating the planar deformation of the membrane. It was not possible to perform measurement at higher magnification than 10x with the current configuration because of the substantial distance between the membrane and the objective. Long working distance objectives may be used to overcome this problem or the design should be adapted to allow the objective to come closer to the cell layer. For example, the device could have a thinner bottom layer or upright microscope may be used to image the cells from above in immersion mode.

This experiment demonstrate the compatibility of the device with fluorescent live cell imaging and gives a further confirmation of the good adhesion between the whole cells and the PDMS membrane.

5.5   Adherent cell layer Young's modulus measurements

Measurements were performed on both epithelial cells and osteoblasts cells (the latter introduced in Section 3.5.2). To measure cell layer Young's modulus, the cell were cultured inside the device using the patterning protocol as explained in Section 5.3.2, the monolayer was cyclically stretched up to 5% strain at 0.01 Hz and pictures were taken at 10 frames/s during the deformation.

The pictures were then analysed to measure the strains of the individual regions over time. Figure 5.8 illustrate an example of pictures captured at 0% and 10% strain and in yellow the borders that are tracked by the pattern recognition algorithm. This allows to obtain a measurement of the whole membrane strain and the individual regions' strains over time.

The measured strain for the individual regions is considerably different because of the cell presence stiffening the membrane. As shown in Figure 5.9, for a total applied deformation of around 4% on the membrane, the bare region deforms of almost 6% while the cell region deforms of 2.5%. The experimental strains measured on the individual regions at constant pressure together with the already known geometrical dimensions of the sample and the Young's modulus of the suspended membrane, allow to measure the Young's modulus of the cell layer using Equation 4.3.

As explained in Section 5.6, around 15 s are needed for the strain to rise to its maximum level. I therefore consider only the strain values after 15 s the pressure is changed for the Young's modulus measurements. The final Young's modulus is obtained as the average over the strain during three pressure cycles. The result obtained for the MDCK cell monolayer averaged over 10 samples is (24.5±7.5)kPa. This is in accordance with previously published studies using the same cells and performing measurements on monolayers [8, 122]. The same procedure was also performed on osteoblast cell layer and the resulting Young's modulus is (72.9±10.3)kPa over 5 samples. This result is in accordance with the measurements obtained using the custom pull-test set-up presented in Section 3.5.2. However these measurement could not be

compared with already published results as there is no published work on osteoblast cell layer measurements.
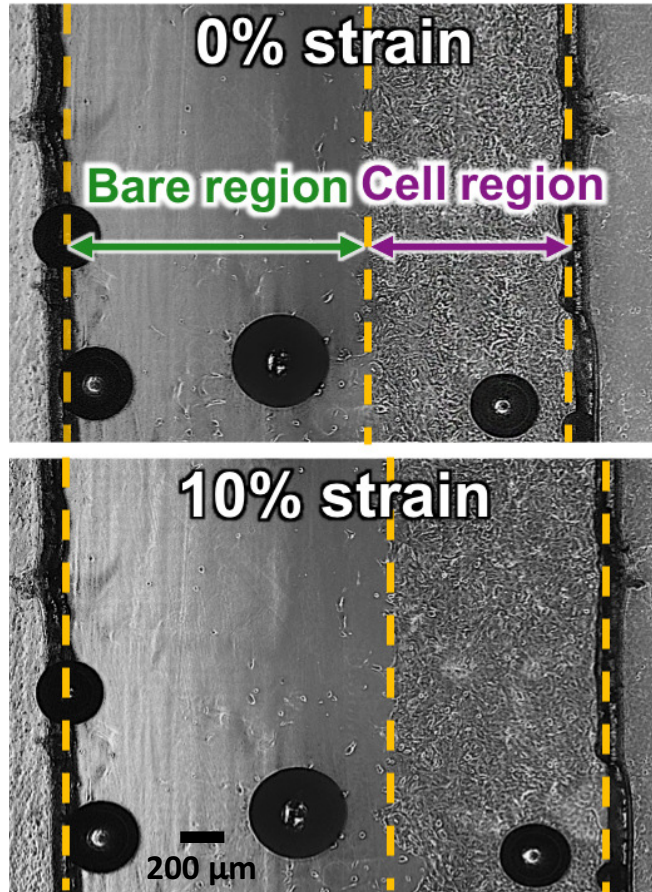
Figure 5.8 – Example of the images taken during the experiment, in this case comparing the 0% and 10% membrane strain. The three borders corresponding to the membrane edges and the border line between the cell and bare regions (illustrated as the yellow dotted lines) are tracked by a pattern recognition algorithm. The batch analysis of all the pictures acquired during the experiment allows to obtain the strain in the individual regions over time.

All together these results indicate a higher Young's modulus when cells are measured in a monolayer configuration than when they are measured as single cells. The Young's modulus of the cell monolayer was 15 and 30 times higher for $SaOS_2$ and MDCK respectively than the elasticity of single cells measured with AFM [159, 160]. This can be explained by the fact that AFM measures a local point on a single cell in the transversal direction while with our method we consider the global response of cells as a population and in the in-plane direction. Our results indicate therefore the big effect of anisotropy in cell mechanics as well as the cruciality of cell-cell contacts in the overall mechanical properties.
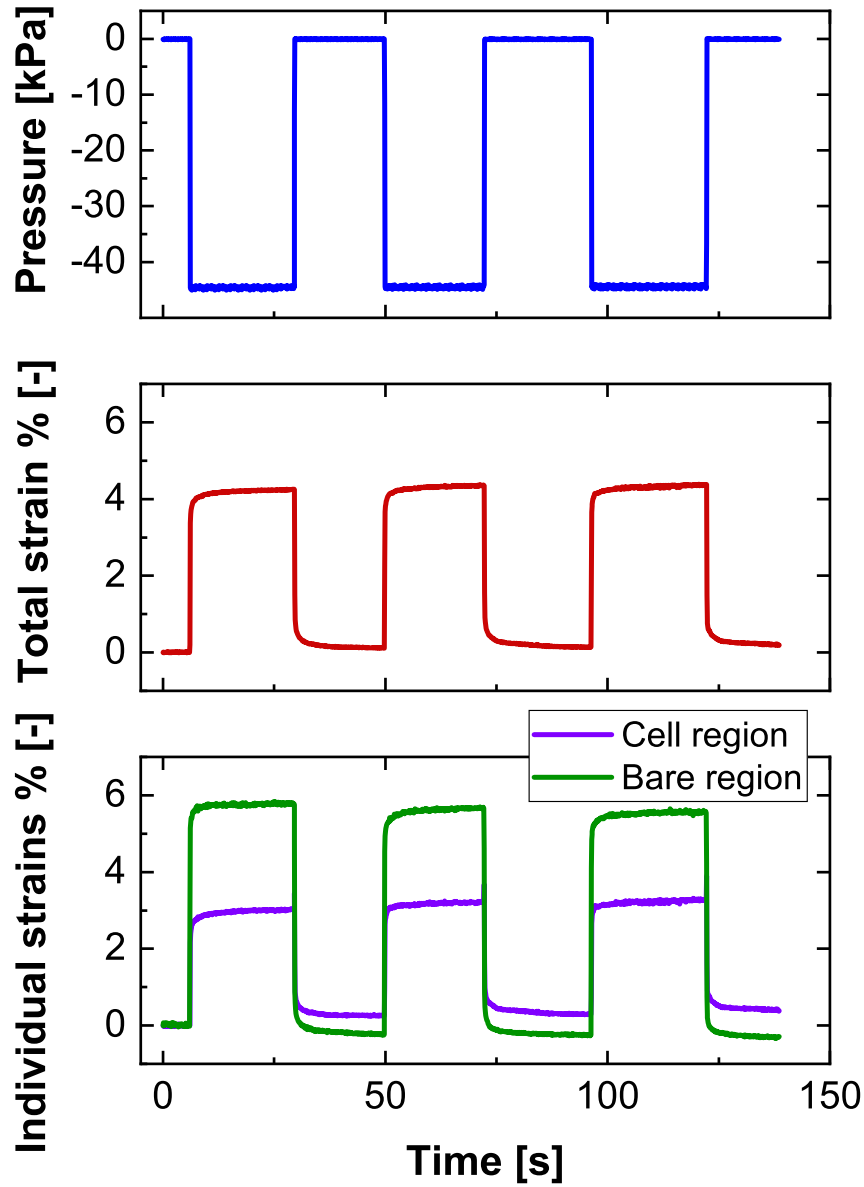
Figure 5.9 – Typical measurement graphs are the pressure applied, the total strain of the membrane and the corresponding individual strains of the two regions over time. The stiffening effect of the cells results in half of the strain within the cell region in respect to the bare region as shown in the bottom graph. The Young's modulus of the cell layer is then calculated from the ratio between the two regions' strains.

5.6 Measuring the viscoelastic properties of cell monolayer

As explained in the previous paragraph, during the Young's modulus measurements the membrane deformation is kept constant for 30 seconds to allow the strain to reach its maximum value for that applied pressure. As both the PDMS and the cells are viscoelastic materials, in fact, the response over time is not immediate as it would be for a purely elastic material. In order to investigate the viscoelastic response when cells are present on the membrane I performed creep measurements, where the strain is measured over the 30 minutes at constant pressure.
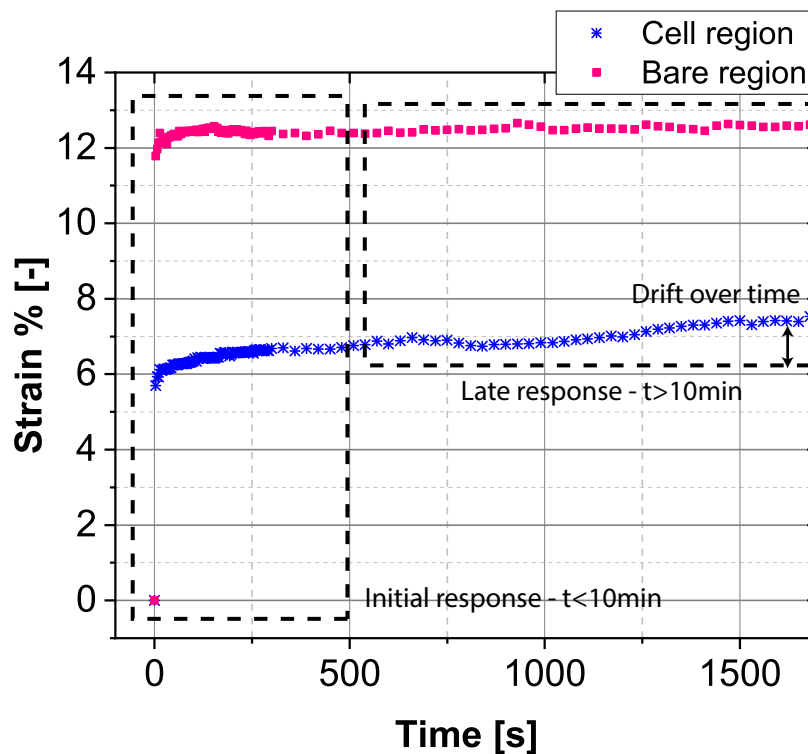
Figure 5.10 – Typical graph reporting the creep response of cell and bare regions over 30 minutes. After an initial response where the strain stabilizes, the cell region exhibits a drift over time which can be explained by active rearrangements of single cells and within the cell monolayer [161].

Figure 5.10 shows a typical trend of the creep measurements, where after around 10 minutes at constant strain, the cell region exhibits a drift with increasing strain over time. This behaviour is similar to previously observed behaviour of single cells under constant stress which results in a strain relaxation over time because of the cell re-adaptation [161]. In order not to take into account active modification of the cell layer, I therefore investigate only the first part of the curve where the strain in both regions rises until reaching a stable value. By observing the normalized response of the cell and bare regions over the first 30 s (Figure 5.11), it is possible to distinguish two main regions: a rising region characterized by a certain rising time

to reach the maximum strain value and a stable region. The Young's modulus measurements reported in the previous section are performed using strain value within the stable region, and therefore considering the sample as fully elastic. However, the rising time of the curve can give information on the viscoelastic properties of the material under study.
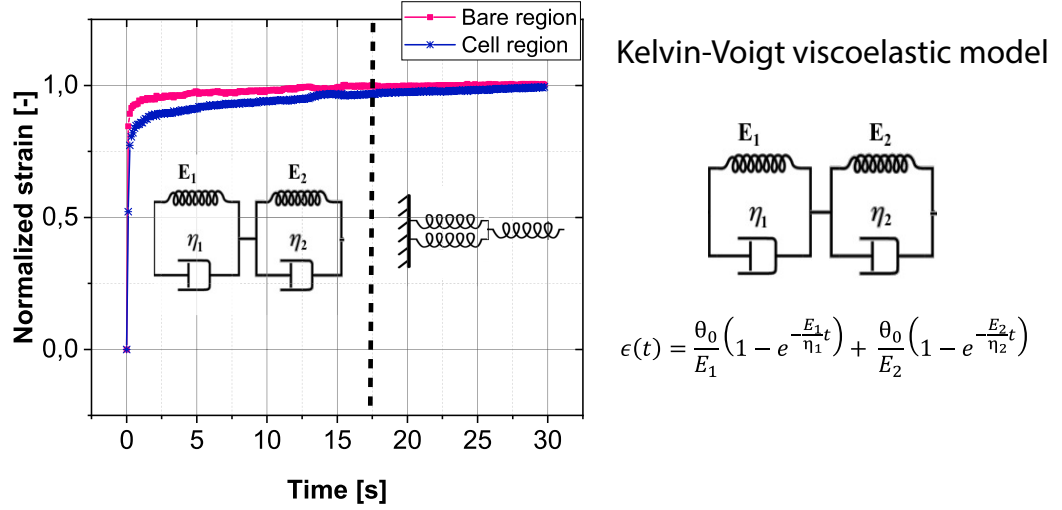
Figure 5.11 – Normalized strain over time over 30 seconds. The normalized strain response over the first 30 seconds shows a different trend between the two regions because of the higher viscosity of the cells. A double Kelvin-Voigt model with two time-constants is used to fit the creep curves.

These curves can be fitted with a Kelvin-Voigt model that is typically used for viscoelastic material creep response modelling [4]. To fit at best our curves, I chose to use this model with two time-constants. By fitting the normalized creep curves with the double exponential law predicted by the model, I could measure the time constants of both regions. The results, summarized in Table 5.1, show a clear difference between the bare and cell regions in terms of viscoelasticity. The cell region has both time constants higher than the bare region, in particular τ_1 is around three times higher and τ_2 two time higher. Cell mechanics is therefore measurable on our device also in terms of their higher viscoelastic properties in respect to the substrate.

The creep response measurements show the possibility to extract information on the viscoelastic properties of cells in addition to the elastic modulus. However further investigation of this feature should be done in the future to be able to extract quantitative information on cell rheological properties. It is in fact not straightforward to relate and validate the correspondence between cellular components and elements of the Kelvin-Voigt model. Furthermore, the viscoelastic properties of the membrane have not been quantified within this study. Therefore, cell rheological properties cannot be measured at this stage. However, the evidence that cell behaviour can be differentiate from the bare membrane, open the possibility for rheological measurements in the future.

Bare region	τ_1	(3.18 ± 1.47)s
	τ_2	(0.079 ± 0.021)s
Cell region	τ_1	(10.09 ± 1.42)s
	τ_2	(0.14 ± 0.07)s

Table 5.1 – Time constants values extracted from a Kelvin-Voigt fitting of the curves (average over 5 curves) show a clear difference between cell and bare regions, indicating the possibility to extract information on the viscoelastic properties of cell in addition to the fully elastic ones.

5.7 Conclusion

In summary, I demonstrated in this chapter the first measurements of adherent cell monolayer mechanics performed on-chip. Measurements were performed on two cell lines, MDCK and SaOS$_2$ and results showed the same trend as previously published measurements. I demonstrated that cells adhere on the suspended membrane by imaging their focal adhesions and from the linear correlation of single cell and whole monolayer deformation. Also, I demonstrated the possibility to perform live fluorescence tracking of the cells at 10x magnification during the stretching and the capability in measuring the rheological response of cells through creep experiments. The measured cell layers Young's moduli are around one order of magnitude higher than the values measured on single cells. This result indicates the significant effect of cell mechanical anisotropy as well as cellular configuration to their mechanical response. Cell mechanical response seems to be anisotropic: the response to in-plane deformations (as in the measurements I performed) is substantially different from out-of-plane ones (such as using AFM). Also, the fact that cells organize differently within a monolayer than in single cells (different cytoskeleton arrangement and cell-cell mechanical coupling) plays a role in their mechanical response.

The significant difference between single cell and cell layer Young's moduli highlights the importance in performing measurements on cell monolayers as they better represent the in-vivo environment leading to more relevant results.

6 Measurements of cell monolayer mechanics under external stimuli

6.1 Summary

Cell elasticity is known to change at different stages of several diseases [162]. Being able to accurately determine elasticity is therefore of great interest because of the applications in diagnosis and drug screening. In this chapter, I summarize the experimental results obtained measuring cell elasticity over time under external stimulations.

Three types of external stimuli have been imposed to the cell culture: chemical treatment and physical changes of the environment, more in specific additional mechanical loading and temperature modifications. The experiments were performed on MDCK (Madin-Darby Canine Kidney) epithelial cells and several control tests were performed as well to validate the obtained results. Regarding the chemical modifications, I present results of both stiffening and softening the cell layer using known chemicals for validation purposes, however the developed device is envisioned for determining the influence of chemicals with unknown effect on cells. Regarding the physical stimulation of cells, I report an increase in Young's modulus due to cyclic stretching at 0.25 Hz for 1 hour. A stiffening effect was also observed when lowering the temperature to 33°C.

In the next sections, I describe each experiment detailing the protocol used to stimulate the cells, the validation through control experiments and the measured changes in cell layer elastic modulus over time. The results presented in this chapter altogether demonstrate the capability of measuring changes in cell mechanics over time and therefore its potential for determining the effect of diverse physical and chemical stimuli on cell mechanics.

6.2 Chemical modification of the cell layer

In this section, I present the results obtained by chemically modifying the cell layer using chemicals of known effect. The interest in these type of measurements lies in the possibility to determine the contributions of single proteins to the monolayer mechanics. The chemicals

can in fact be chosen for their targeting a specific protein within the cells, thus providing information on that protein contribution to cell elasticity. I chose to use glutaraldehyde which by crosslinking actin filaments makes cell stiffer and EDTA (Ethylenediaminetetraacetic acid) which by disrupting the tight junction proteins (ZO-1 proteins) removes the mechanical bonding among cells. The experimental procedure consists in comparing the Young's modulus before and after treatment on the same device. Control experiments (Figure 6.1) show that the chemicals themselves do not affect the membrane mechanical properties.
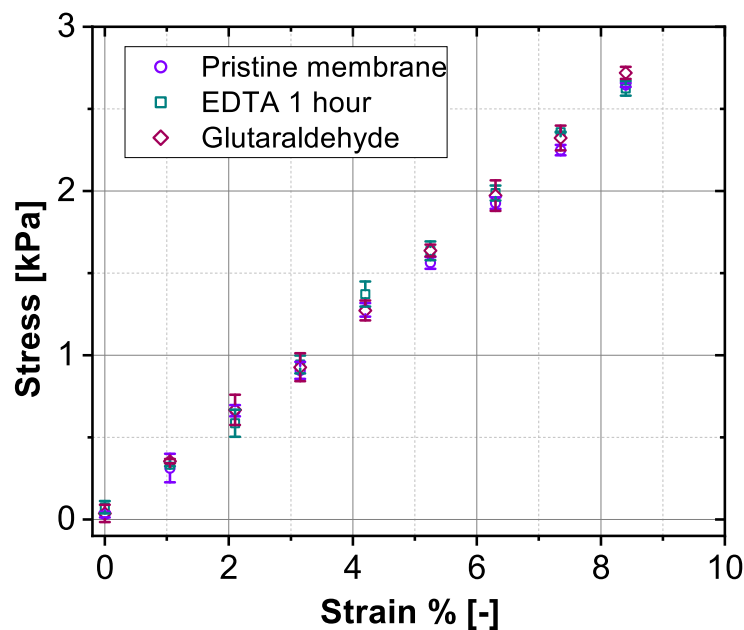
Figure 6.1 – Stress versus strain curves comparing the response of pristine PDMS membrane and after EDTA and glutaraldehyde treatments (3 samples each). These two chemicals do not affect the mechanical properties of the PDMS membrane.

6.2.1 Stiffening of the cell layer

I chose glutaraldehyde as chemical to stiffen cells. Thanks its high reactivity to proteins, glutaraldheyde is used in biology and biochemestry as a fixative and preservative for long-term storage of biological samples. As a fixative, glutaraldheyde crosslinks actin filaments within cells thus making them stiffer and allowing to preserve them without altering their shape and conformation [163]. A confluent cell layer was measured after 5 hours cell culture. The cells were then treated with 4% glutaraldehyde for 3 minutes and finally washed in PBS. A measurement was performed again to determine the effect of the treatment. Cells treated with glutaraldehyde showed an increase in Young's modulus of more than 10 times higher with a final Young's modulus of (249.58±31.02)kPa in respect to their value before the treatment (24.5±7.5)kPa (Figure 6.2a).

(a)   (b)
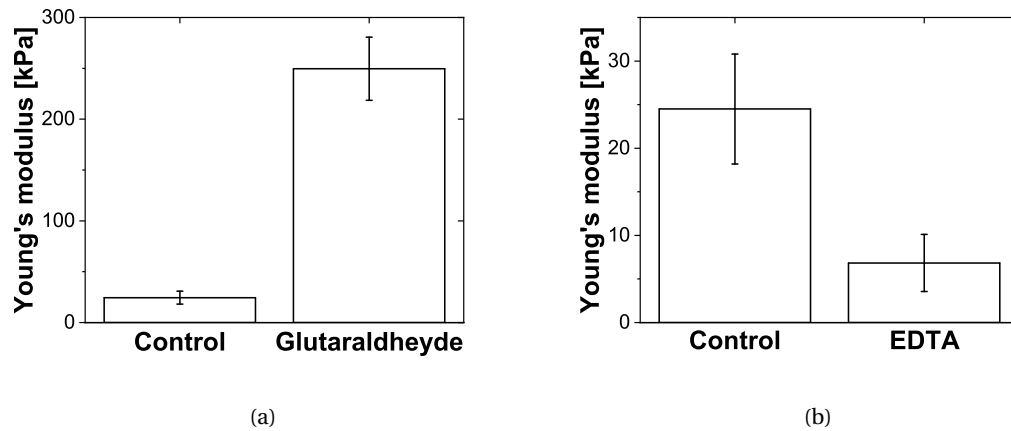
Figure 6.2 – Measured Young's modulus when (a) stiffening the cell layer with glutaraldehyde (values obtained over 3 samples) and (b) softening the cell layer by EDTA incubation (values obtained over 3 samples).

6.2.2   Softening of the cell layer

I then investigate the contribution of cellular junctions to the overall mechanics by treating the cell monolayer with EDTA. EDTA is used in biochemistry and molecular biology as a ion depletion agent. Through this action, EDTA deactivates metal-dependent enzymes. In particular, in cell culture EDTA binds to the calcium present in the cell culture medium which prevents the joining of cell-cell connection proteins. Therefore, cells cultured in medium containing EDTA do not exhibit the mechanical coupling among cells.

The first step consisted in choosing the treatment protocol for efficient disruption of cellular tight junctions. For this, EDTA at 3 mM concentration was incubated on cells for different times. The choice of the EDTA treatment incubation time was made by comparing confocal images of one protein (ZO-1) presents in cell tight junctions at 0, 30 minutes and 1 hour incubation (Figure 6.3). Longer incubation times have been discarded to avoid harming the cells. After 1 hour time incubation the junctions are almost completely disrupted in comparison to a control sample, however the cells still adhere to the substrate. The modification of the tight junctions led to a significant decrease of the measured Young's modulus (Figure 6.2b) from an initial value of (24.5 ± 7.5)kPa to (6.835 ± 3.27)kPa. This 70% decrease in Young's modulus clearly indicates the importance of tight junctions for mechanically stabilizing the whole monolayer.

The proposed device allows therefore to measure both an increase or decrease in cell elasticity due to chemical modification of known protein in the cell layer. The results obtained with EDTA and softening of the monolayer because of cell junction rupture, prove the importance of cell-cell mechanical connections to the stability of cell layers. This further points to the relevance of measuring cells within a population configuration instead than single cells.
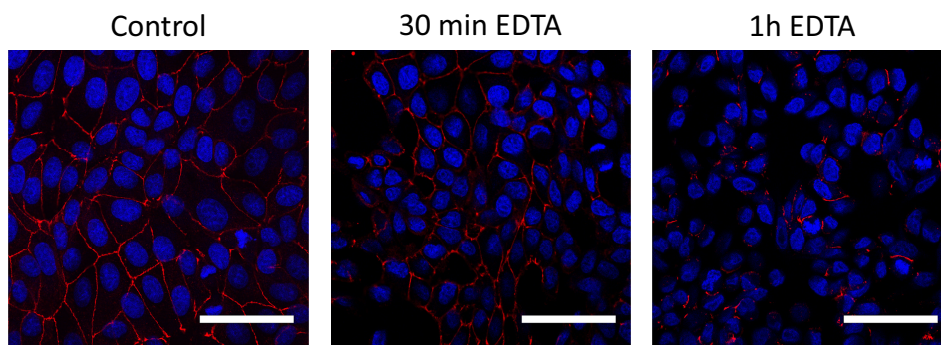
Figure 6.3 – Confocal images of MDCK cultured on a suspended PDMS membrane at different EDTA incubation times (DAPI in blue and ZO-1 in red). In the control figure the tight junctions (ZO-1 protein) are well developed and are uniformly present, after 30 minutes EDTA incubation, cellular tight junctions start to be damaged and at 1 hour incubation time they are almost completely disrupted. (scale bar is 50 μm)

6.3 Response to dynamic loading

It is known that continuous stretching of cells and tissue has an influence on their morphology, physiology and mechanics [164]. The mechanical properties of smooth muscle cells are altered in response to elevated blood pressure in order to maintain adequate blood circulation [165]. Also, bone cells proliferation rate and ECM secretion increase when subjected to mechanical loading [166]. I measured therefore the effect of cyclically stretching MDCK cells on the device over one hour to determine the effect of dynamic loading on their mechanical properties.

6.3.1 Dynamic loading protocol

The total deformation and frequency necessary to actively modify the cells are highly dependent on the cell type. From literature reported values, I choose to keep the deformation constant to 5% as during a measurement and increase the stretching frequency to 0.25 Hz [167]. The cyclic stretching protocol consists in stretching the cells at higher frequency (0.25 Hz) than during a normal measurement (0.02 Hz) and for 1 hour. Measurement cycles at lower frequency are performed at time 0 and then every 15 minutes. After one hour of mechanical loading, cells are kept at rest without any deformation and finally measured after 1 hour resting time.

The loading protocol is schematically illustrated in Figure 6.2b. The pressure varied to obtain around 5% deformation of the membrane. A measurement consists on three cycles at 0.02 Hz, while the stretching applied for the rest of the time is a cyclic deformation at 0.25 Hz frequency. The measurement cycles are performed at time 0, and then after 15, 30, 45 and 60 minutes after the mechanical loading. Also, the sample is measured again after 1 hour rest with no mechanical loading.
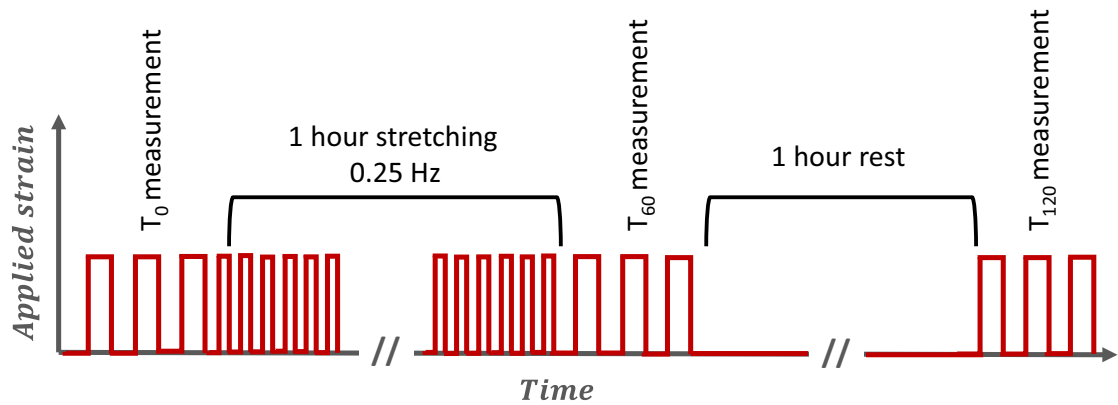
Figure 6.4 – Schematic illustrating the stretching profile during the mechanical stimulation of the cell layer. The mechanical stimulation consists in cyclic deformation up to 5% strain at a frequency of 0.25 Hz for one hour. Measurement cycles at lower frequency are performed before the measurement, during the stimulation at 15, 30 and 60 minutes and after one hour rest.
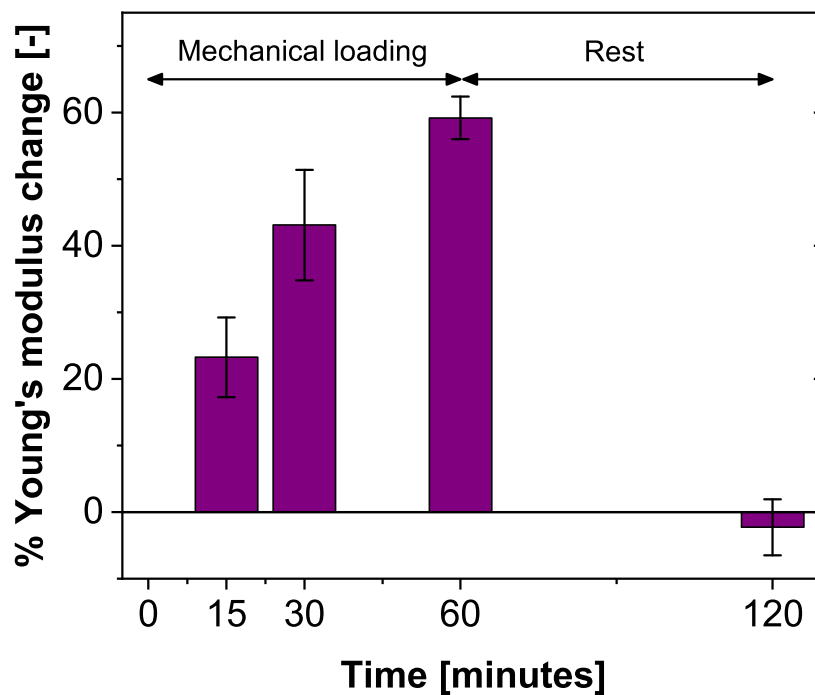
Figure 6.5 – The graph illustrates the results obtained over 4 samples when stretching for one hour followed by one hour without mechanical stimulation. The obtained results show an increase in Young's modulus of the cells reaching a 60% increase after one hour stretching. This was followed by a recover of the initial properties after one hour without stimulation.

6.3.2   Cell layer stiffening induced by dynamic loading

The results obtained by measuring the sample every 15 minutes during the mechanical actuation and then after 1 hour rest are grouped in Figure 6.5. The results shown are an average over 4 samples and indicate a clear increase in Young's modulus during the mechanical stimulation as well as the returning to the initial Young's modulus value after the resting period. An average increase of around 60% in Young's modulus is measured after one hour dynamic stimulation. The restoring of Young's modulus to the initial value after 1 hour resting time shows the reversibility of this experiment and indicates that the stretching is actively modifying the cells for a limited amount of time.

Overall, the presented results are in line with numerous previous studies demonstrating that cyclic stretch induce a Young's modulus increase [164, 167, 168, 169]. However, it is not straighforward to compare the exact change in elastic modulus with literature results because of the high dependence of these measurements on the cell type and stimulation profile used. Rapid increase in Young's modulus value (within 5 min) was observed in vascular smooth muscle cells subjected to similar stretching profile as in my experiment (10% stretching at 0.25 Hz) [167]. Furthermore, the stiffening effect has been correlated by immunofluorescence imaging to an increased number of focal adhesion sites and conformational changes in filamentous actin compared to the unstretched control [168, 169].

6.3.3   Control experiment for the dynamic loading

I performed two experimental controls to validate that the mechanical stimulation is not affecting the device itself leading to false changes in measured elasticity. These controls tests are necessary to ensure that the obtained results arise uniquely from a change in cells Young's modulus induced by the mechanical stimulation. The two control experiments had the following objectives:

- Validating that the Young's modulus of PDMS samples measured in the place of the cells is constant when subjected to the same cycling actuation over 1 hour. This will allow to conclude that the cyclic stretch does not affect the device itself or the measurement principle.

- Prove that over 2 hour cells that are not subjected to mechanical stimulation do not exhibit a similar increase in Young's modulus. This control will allow to conclude that the change in Young's modulus is due to the mechanical stimulation alone.

Figure 6.6a reports the results obtained on simple PDMS membranes measured in the device instead of the cells following the same mechanical stimulation protocol. The graph illustrates the change in Young's modulus after 60 minutes mechanical loading and after another 60 minutes resting. The reported values are averaged over 3 samples, and report a difference within ±5% of the initial value. These results thus confirm that the mechanical stimulation

(a)

(b)
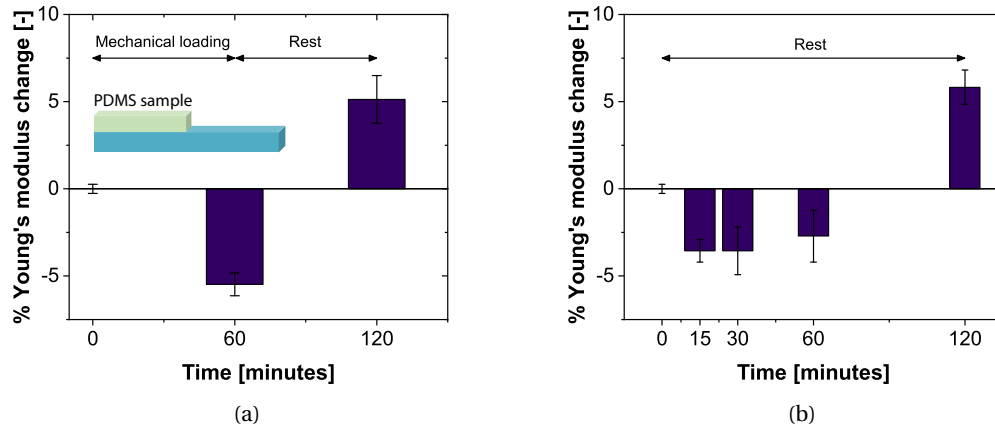
Figure 6.6 – Graphs illustrating the control experiments results: (a) shows that when the dynamic loading is applied on a calibrated membrane instead of the cells, no change in its mechanical properties is observed, while (b) confirms that the increase in elasticity is not happening when cells are not mechanically stimulated. These two controls prove that the measured modification in elastic modulus are indeed coming from cellular active modifications due to the cyclic stretching.

does not affect the device itself or the measurement procedure and that the difference in the results comes indeed from the cells.

The results of the second control experiment are illustrated in Figure 6.6b and show that cell Young's modulus over two hours remains between ±5% of the initial value when no mechanical stimulation is performed on the cell culture. This confirms therefore that cells do not exhibit significant changes in their elasticities without the mechanical stimulation.

Both control experiments clearly indicate that the change in Young's modulus is entirely resulting from mechanical stimulation induced cellular modifications.

6.4 Response to temperature changes

Changes in temperature occur everyday throughout the body. They can be a consequence of cellular metabolism, dissipation after cyclic mechanical loading and disease states to cite few examples. In addition, within living cells, several phenomena such as cross-linker binding rates, molecular motor activity and actin filaments polymerization are known to be temperature dependent [170]. Thus, temperature changes directly affect cell activities, their architecture and mechanical properties. However, the relation between cell mechanics and temperature is still largely unknown. And this is mainly due to the lack of measurement platforms compatible with temperature modifications. In the next section I present the results obtained when modifying the culture temperature cyclically between 37°C and 33°C. This

range was chosen within the physiological temperatures that cell can feel within the body [171].

6.4.1 Temperature changes protocol

In order to cyclically modify the temperature of the cultured cells, I perform measurements outside the incubator and placing the petri-dish with the device onto a heater.

(a)

(b)
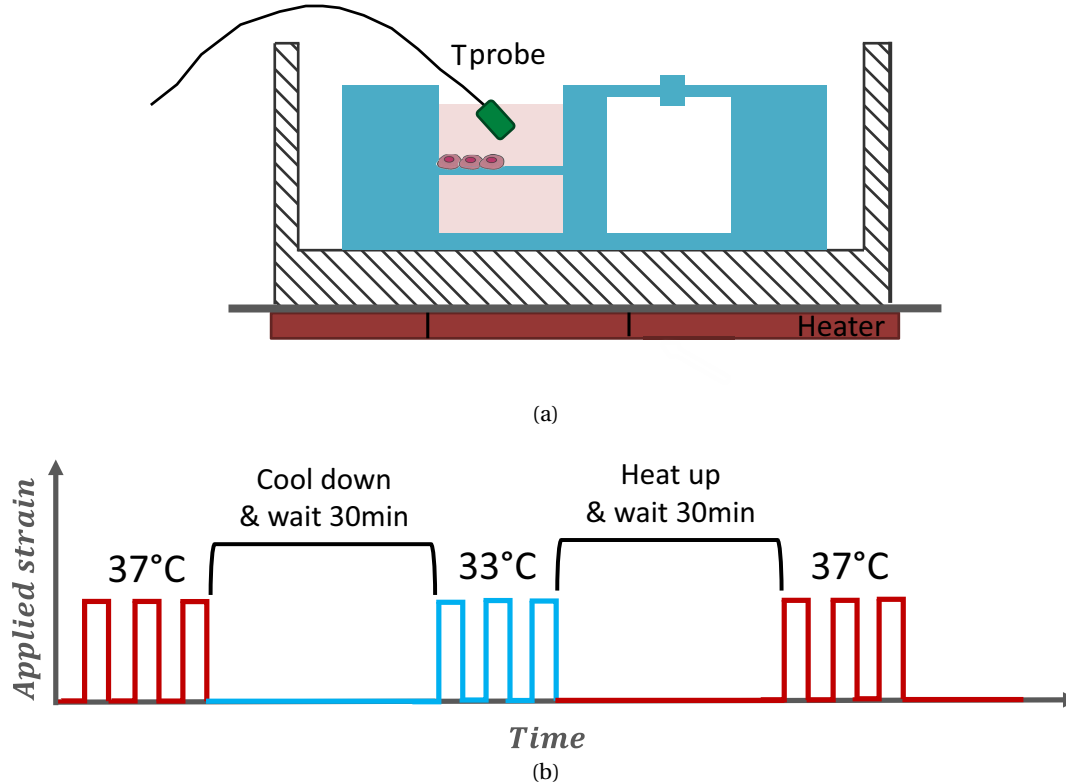
Figure 6.7 – Schematics representing the experimental set-up and protocol used to study the effect of temperature on cell mechanical properties: (a) The Petri-dish containing the device is placed on a heater and a temperature sensor is insert inside the medium surrounding the cells to have a real-time measurement of the temperature around the cells, (b) the temperature is cycled between 33°C and 37°C, the sample is let 30 minutes at each temperature before the measurement to let the cells adjust to the new conditions.

The resistive heater was custom-made with a hole in the center allowing continuous optical monitoring of the cells. Furthermore, a temperature probe (thermistor based) was placed in contact with the medium inside the device to have a direct measurement of the temperature around the cells as shown in Figure 6.7a. The protocol, schematically represented in Figure 6.7b is the following: a first measurement consisting of 3 stretching cycles up to 5% strain and at 0.02 Hz is performed at 37°C, the sample is then cooled down to 33°C let 30 minutes at constant temperature before performing another measurement. Few temperature cycles are performed to estimate the repeatability of the measurements.

6.4.2 Cell layer mechanical properties dependence to temperature

The temperature is cycled between 37°C and 33°C and measured in real time thanks to the temperature sensor. The temperature is kept constant for 30 minutes at each temperature to ensure enough time for cell adaptation to the new conditions. Mechanical properties measurements are effectuated at time 0 and then after 15 minutes.
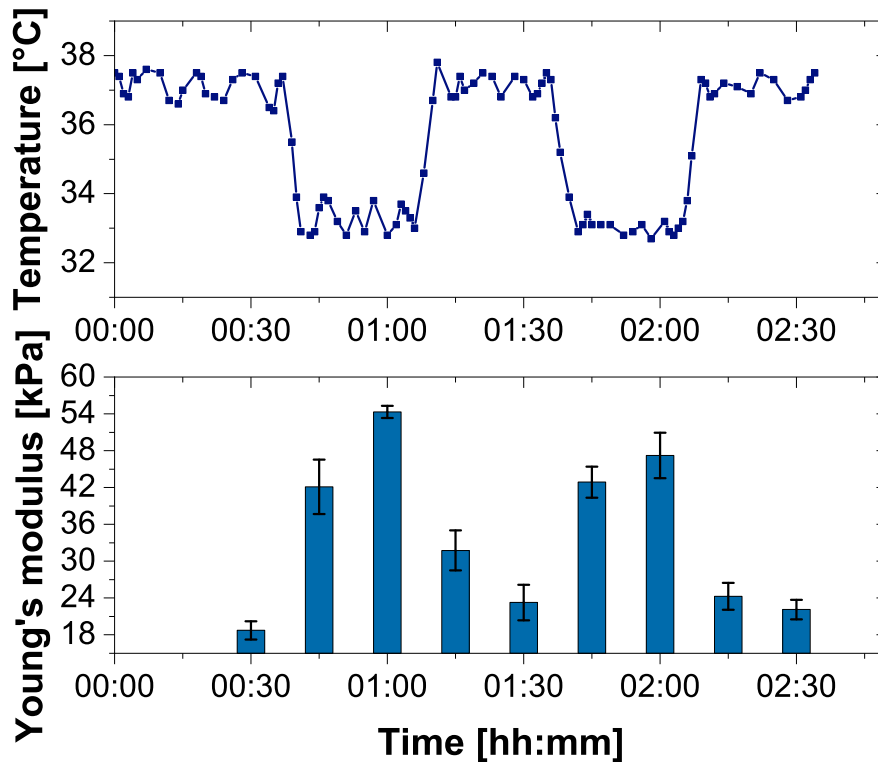
Figure 6.8 – Graphs representing the results of temperature modification on cell mechanical properties. The temperature is cycled between 33°C and 37°C and measured thanks to a temperature sensor. The cell layer Young's modulus is measured after 15 and 30 minutes at each temperature. The obtained results show that decreasing the temperature results in stiffening the cells and that this effect is reversible when the temperature is restored to the initial value.

The resulting change in cell elasticity is illustrated in Figure 6.8. The Young's modulus is initially around 18 kPa at 37°C and increase up to 54 kPa after 30 minutes at 33°C. When the temperature goes back to 37°C, also the elastic properties return to their initial values and the same happens for the following cycles. These results show therefore that Young's modulus increases with decreasing temperature and this is a reversible effect. Literature in the field is quite controversial as some papers report the increase of Young's modulus with decreasing temperature [172, 173] while others [174] report a decrease in Young's modulus at lower temperature. This difference is most probably due to the different measurement approach, different configurations for the cells (adhering to a surface or suspended) and

also because of the different cell types. The fundamental reasons for these changes are not presented here as they are still under study.

In addition, I compared the strain time constants when a pressure step is applied for the two temperatures. The curves showing the cell region strain versus time are reported in Figure 6.9. The graphs indicate an increase in the viscoelasticity of cell at lower temperature because of the longer time needed to reach the maximum membrane strain after a pressure step.
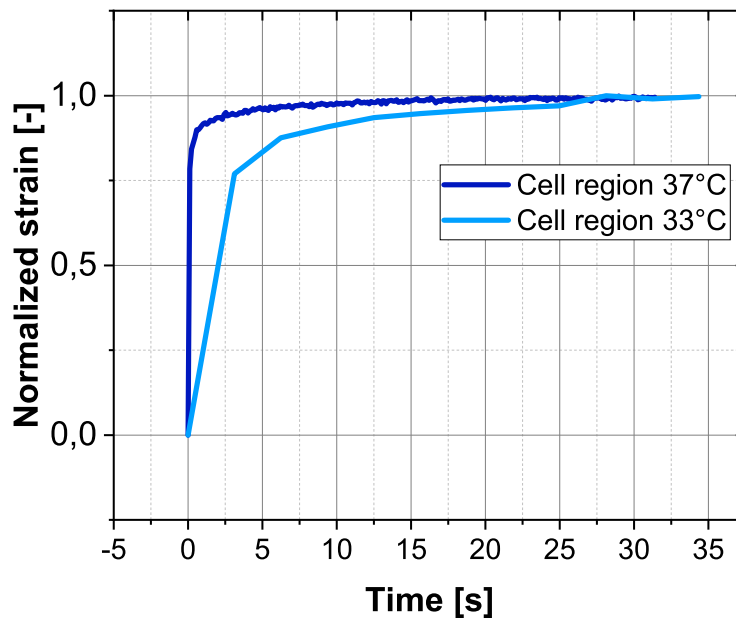
Figure 6.9 – Graph representing the the cell region strain step response over 30 seconds at 37°C and 33°C. Decreasing the temperature result in an increase in the time needed for the strain to reach its maximum value. This can be related to an increase of cellular viscosity.

		37°C	33°C
Bare region	τ_1	(3.18±1.47)s	(2.51±0.165)s
	τ_2	(0.079±0.021)s	(0.28±0.15)s
Cell region	τ_1	(10.09±1.42)s	(19.11±2.05)s
	τ_2	(0.14±0.07)s	(1.36±0.08)s

Table 6.1 – The table summarizes the time constants for both the cell and bare regions at 37°C and 33°C. These values were obtained from the Kelvin-Voigt double exponetial fit of the strain versus time curves. While the values remain comparable for the bare region, the cell region exhibits an increase of both time constants when decreasing the temperature.

The measured rising times obtained from a Kelvin-Voigt fit of the curves (see Section 5.6) are summarized in Table 6.1. While both time constants of the bare region remain within the error

bar difference, the cell region time constants both significantly increase when decreasing the temperature (one almost double, the other has almost 10 times fold increase). The presented results suggest therefore that temperature has a direct influence on the rheological properties of cells as well as their Young's modulus. Similar trend in the strain creep response was shown in literature [175].

6.4.3 Calibration sample measurements

In this case as well, I performed control experiments to confirm that the measured Young's modulus is indeed a consequence of cell modification because of the temperature change and that temperature change is not having an effect on the measurement set-up.
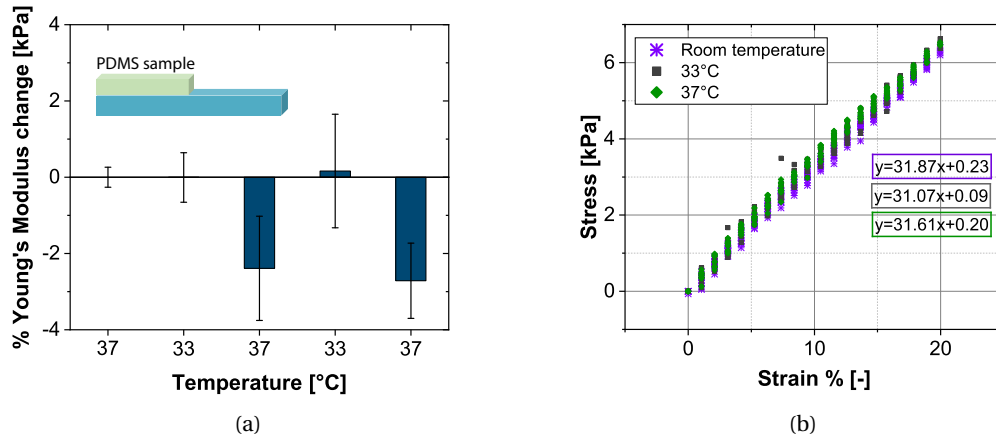
Figure 6.10 – Control experiment results performed to verify the validity of temperature-induced cell modifications. When calibrated samples are used instead of the cells, no significant Young's modulus change is measured between the two temperatures 33°C and 37°C (a). Also, MED4086 has relatively stable mechanical properties within that range of temperature as shown by their stress versus strain curves (b).

PDMS samples were placed on the device instead of the cells and their elastic modulus measured over time while varying the temperature. No substantial difference in the mechanical properties was observed as shown in Figure 6.10a. With a change in Young's modulus of 2%, these results allow to conclude that the temperature changes do not affect the device or the measurement principle. Also, the mechanical properties of the membrane were measured at both temperatures. The resulting stress versus strain graph of suspended membrane in liquid made of PDMS formulation MED4086 and at different temperatures are shown in Figure 6.10b. The slopes at room temperature, 33°C and 37°C are essentially the same, indicating the constant mechanical properties over that temperature range.

Both control experiments show that within the chosen range of temperatures, the membrane and the device are not considerably affected regarding their mechanical response. This

indicate that the Young's modulus changes are due to cellular modifications induced by the temperature difference.

6.5   Conclusion

This chapter summarizes the results obtained by measuring cell Young's modulus changes externally induced by chemical or physical stimulations. The developed device is successfully applied for measuring elasticity changes in real-time.

I showed it is possible to measure changes in cell mechanical properties due to chemical modification of the cell layer. The reported experiments consist in treating the cells with chemicals with known effect on cell mechanical properties such as softening through EDTA and stiffening by glutaraldheyde fixation. The successful measurements of both cell stiffening and softening validates the capability of measuring mechanical properties modifications due to drug incubation. In particular, the 70% decrease in Young's modulus after EDTA treatment, suggests the significant contribution of cell-cell junctions to the overall mechanics of the cell monolayer. This opens several possibilities for testing the effect of unknown chemicals on cells or for determining the contribution of specific cellular proteins to the overall mechanics.

The application of physical stimuli, in this case cyclic stretching and temperature fluctuations, and the associated change in mechanical properties was reported. In both cases, the obtained results show an increase in the elastic modulus that is reversible when the initial conditions are restored. I report a 60% increase in Young's modulus after 1 hour stretching at 0.25 Hz followed by a recovering of the initial value after 1 hour without mechanical stimulation. This result is in agreement with previous works demonstrating an increase in elasticity induced by mechanical stimulation and was correlated to an increase in cell focal adhesion sites and actin reorganization.
Regarding the temperature stimulation, I report an increase in Young's modulus of around 3 times when the temperature is decreased to 33°C. This also happens along with an increase of the time constant for the strain to reach its maximum value when a deformation is imposed, indicating a change in the rheological properties of cells as well. The results obtained from the mechanical and temperature stimulations have been validated through control experiments and are in line with previously published results even if they cannot be quantitatively compared because of the difference in cell used.

All together the results presented in this chapter, show the possibilities and potential of the developed device for measuring changes in cell mechanics in real-time. This has several applications not only in understanding the fundamental processes in mechanotransduction, but also in more applied studies for determining the influence of drugs or other type of stimulations on the cells.

7 Conclusion

7.1 Summary

My thesis contributes to the field of micro-systems for cell mechanobiology by providing a simple and effective method to interface tensile mechanical testing with cell culture within a miniaturized device. This work, also demonstrates the relevance of measuring the mechanical response on cell monolayer instead of individual cell because of the different morphology, cytoskeleton organization which results in measurements that are more representative of the in-vivo environment.

The key innovation consists in the combined use of culture cells substrates with elasticity in the same order of magnitude as the cells and the use of differential strain read-out between bare and cell covered regions of the membrane. Through optical differential strain measurements, it is possible to avoid complex and bulky force measurement equipments and make the whole device much more compact. In order to meet the specific requirements for combining adherent cells with Young's modulus measurements, I optimized the substrate geometry and mechanical properties for choosing the best combination allowing high sensitivity. The final design is the best trade-off between fabrication feasibility, cell proliferation compatibility and measurement sensitivity. I also developed specific fabrication process and cell protocols with high performance reproducibility. Also, the use of optical read-out and pneumatic actuation does not involve any contact directly with the biological sample or the cell culture medium, that is an essential aspect to avoid contamination. The final device is compatible with measurements on adherent cells in their physiological environment and with standard biology equipments and protocols. In general, the fabrication of the device and the measurement principle itself are quite simple but only thanks to the overall proper design and material choice this measurement is feasible.

Main results

In this thesis, I successfully designed, developed and experimentally tested a novel device for Young's modulus tensile measurements of cell monolayers. For the first time, a miniaturized

device allows to combine in-plane cell stretching capabilities with the possibility to measure cell mechanics within cell physiological environment.

The core of our technology is the use of differential strain measurements between a region covered with cells and a bare region of the membrane. This allows to measure the mechanical properties of the adherent cell layers by subtracting the effect of the membrane. Furthermore, using a differential approach makes the system independent of many variables (surface covered by the cells, pressure variations) that would otherwise significantly affect its precision.

The substrate hosting the cells was designed to fulfil the sensitivity requirements and thus allowing to decouple cell mechanical response from the substrate's one. The successful design of the membrane hosting the cells has been demonstrated by proof of concept measurements using a customized pull test set-up. These involved measurements on calibrated samples and then on cells which validated the measurement approach.

Following the proof of concept of the measurement procedure, the platform has been miniaturized into a fluidic device. The device is actuated through pneumatic actuation and relies on optical strain measurements, thus being scalable and fully compatibility with sterile measurements.
I developed the fabrication process for this device taking particular care for its being compatible with conventional biological cell culture equipments and protocols, such as ethanol sterilization, protein functionalization of the surface, incubation at 37°C, culture medium immersion, and cell immunostaining. Also, the system is compatible with imaging using inverted microscopes, and cells could be imaged while the deformation was occurring (up to 20x magnification).
This compact cell stretcher allows to achieve up to 15% uniaxial tensile strain with minimal inward lateral compression thanks to the high aspect ratio of the membrane used a substrate. In addition, the deformation is highly planar, which can be observed by the fact that the membrane and the cells remains in the focal plane when imaging in real-time during the deformation.

Cells are cultured using standard techniques on suspended membranes within the device. Thanks to a pre-stretch of the membrane, which avoids membrane sagging, cells can be cultured on the membranes for up to one week. In order to perform differential strain readout, I developed a cell patterning protocol allowing to define a cell and a bare regions on the membrane. The protocol is easily reproducible and allows a stability of cell patterning over 2 days.
During the stretching, cells adhere on the membrane and deform together with it as indicated by the linear correlation between single cell and whole monolayer deformation.

The developed device has been used for measuring the Young's modulus of two cell types. Populations of around ~100 10^5 cells of Sarcoma Osteogenic cells (SaOS$_2$) and Madin-Darby Canine Kidney cells (MDCK) have been measured at 5% tensile strain and 0.025 Hz. The results show that cell monolayer Young's modulus for both cell types is around one order of

magnitude higher than in single cells (based on out-of-plane deformations such as in atomic force microscopy). This result indicates the significant effect of cell anisotropy and thus the importance of performing in-plane tensile measurements on cell populations.

Finally, I designed experiments where cells were subjected to additional external chemical or physical stimulation to asses their effect on cell mechanical properties and demonstrate the device capabilities to measure Young's modulus changes over time.
I performed experiments using chemical of known effect on cells for validation purposes. The successful measurements of both cell stiffening and softening validates the capability of measuring mechanical properties modifications due to drug incubation. In particular, the 70% decrease in Young's modulus after EDTA treatment, suggests the significant contribution of cell-cell junctions to the overall mechanics of the cell monolayer.
The device can thus be envisioned for determining the influence of chemicals with unknown effect on cells mechanics and for determining the contribution of specific cellular proteins to the overall mechanics.
Regarding the physical stimulation, I report an increase in cell monolayer Young's modulus after both mechanical (1 hour cyclic deformation at 0.25 Hz lead to 60% increase in Young's modulus) and temperature (measurements at 33°C, leading to an increase in Young's modulus of 3 times) stimulations. Both experiments were reversible, and cell mechanical properties returned to their initial value after restoring the initial conditions. Control experiments were performed for every test and demonstrate that the change in Young's modulus is to be attributed indeed to changes within the cells.

This developed device can be easily adapted to perform measurement with all types of adherent cells. Depending on the expected elasticity of cells to be measured, the membrane design can be optimized by tuning either its Young's modulus or the thickness to achieve the necessary sensitivity. The overall performance of the device as a cell stretcher was comparable to other existing platforms in terms of strains, but with the remarkable improvement of allowing tensile mechanical measurements at the same time.
All together the obtained results validate the capability of measuring cell population Young's modulus over time, and thus indicate the potential use of the developed device for determining changes in mechanical properties. This has several applications not only in understanding the fundamental processes in mechanotransduction, but also in more applied studies for determining the influence of drugs or other type of stimulations on the cells.

Impact statement

The work that I accomplished during my thesis provides the first demonstration that mechanical tensile measurements can be interfaced with cell monolayers. The presented device has been optimized for performing measurements over time when cells are within their physiological environment. Measurements of cells mechanical properties and under additional external stimuli such as drugs or physical stimulations validate the use of the device for biological applications. This is an important step towards long time cell measurements and better

representation of the in-vivo environment, thus opening the doors for further advancements in mechanobiology.

7.2 Future work

In this section, I propose three research topics which would broaden the application and the impact of the device developed within this thesis. With the demonstrated successful use of the device, the next steps consist into exploiting its capabilities through experiments on real-world biological applications. The current state of the device is already well developed for its scope and to meet the requirements needed for most biological experiments. However, I propose some additional improvements that could be useful and allow a broader applicability. In particular, to increase the relevance of the measurements, it is highly desirable to achieve measurements parallelization and possibly use electrical instead of optical read-out.

7.2.1 High throughput implementation

Measurement parallelization

As statistical studies are essential for advancements in cell biology, it is highly desirable to parallelize the measurements allowing high throughput experiments. The miniaturized device for measuring cell monolayer tensile mechanical properties presented in this thesis is designed for single experiments. However, it can be easily integrated into arrays for parametric or statistical studies. This is mainly an engineering work consisting in adapting the measurement principle to multiple measurements at a time, with main challenges in fabrication and assembly processes.

Two main approaches can be considered in the future: the development of engineered Petri-dishes hosting the measurement membranes and the pressure connections, or the integration of several membranes within the same fluidic device. The first approach (Figure 7.1a) consists in customized Petri-dishes having the low pressure connections and disposable inserts with the membrane could be placed inside the wells. This approach would allow to have several individual measurements and it is highly versatile regarding the number of measurements done in parallel. It has the advantage of relying on components that are fully compatible with standard biological equipment. The second approach (Figure 7.1b) is interesting because of the possibility to measure cells in the exact same conditions and thus minimize the experimental variability. In both approaches one low pressure source can be used if the same deformation profile is desired in all cell cultures, or different stretching conditions can be applied to the cells by controlling the individual negative pressures. Also for both approaches, the measurement should be automated using microscopes with a motorized stage for the read-out.

(a)

Pressure connection

(b)
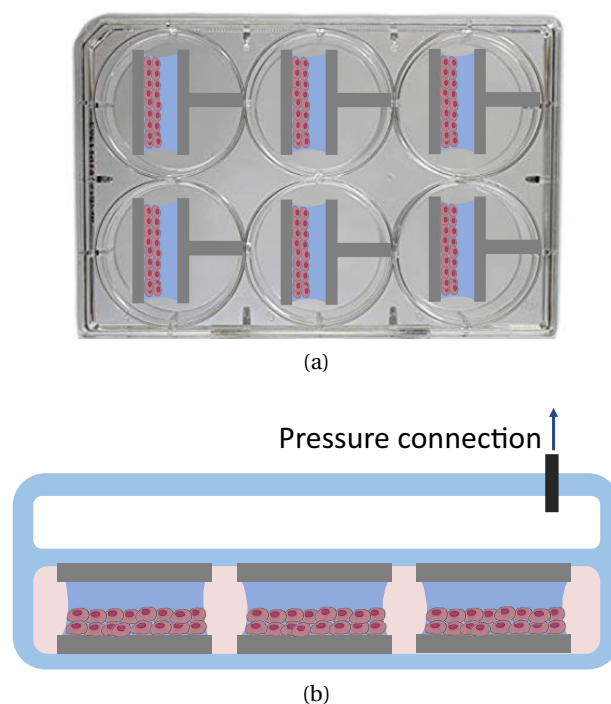
Figure 7.1 – Schematics representing two possible configurations for high throughput measurement arrays: (a) engineered multi-well Petri-dishes, (b) Cross-section representing the integration of multiple membranes into the same fluidic device.

Electrical read-out

Optical imaging of the sample is an essential requirement in biology. The choice of using optics as a read-out method was done in this thesis because of the minimal effect of cell culture environment on optical read-out. However, having an electrical-read-out, even if very challenging, would be an enormous step forward for higher measurement automation. For this reason, it is interesting to develop resistive or capacitive strain sensors that could be integrated within the membrane for cell culture. This would allow to eliminate the need of acquiring pictures during the strain and thus simplifies the measurement procedure.

The first challenge consists in developing strain sensors that are compatible with the thickness and Young's modulus sensitivity requirements of the substrate. Adding strain sensors on top of the membrane inevitably turns into an increase of the membrane stiffness, thus reducing its sensitivity. The strain sensors should be therefore soft enough to have a minimal impact on the mechanical response of the membrane. The second challenge consists in obtaining stable and reproducible measurements in liquid. The implementation of strain sensors compatible with in-liquid measurements is quite challenging because of the presence of ions within the cell growth medium as well as the high dependence of electrical response to temperature and humidity. In order to solve this, the strain sensors could be encapsulated in a non permeable material to avoid the ions to reach the conductive path. Again this may increase the overall

stiffness of the membrane leading to a trade-off between the measurement sensitivity and stability.

7.2.2 Biological cell experiments

Disease and healthy cells differentiation

From a biological point of view it would be of great interest to test the developed device for differentiating diseased and healthy cells through Young's modulus measurements. For this, collaborative work with partners with deep knowledge of a specific disease should be chosen and higher throughput platforms should be implemented to facilitate a statistical analysis. Biological testing could be performed by comparing cell mechanical response obtained from the same device before and after a drug treatment (known to induce or to cure a specific disease). These type of experiments would allow to decrease the experimental variability because measurements are performed on the same device. Another interesting experiment would be to culture healthy and diseased cells on different devices. This approach would give more relevant results, but requires a high number of devices and experiments.

The biological validation that healthy and diseased cells are differentiable through their mechanical properties would open the door for the use of the developed device in collaboration with hospitals as a diagnostic platform.

7.3 Concluding remark

Mechanobiology has progressed tremendously in the last decades. Several experimental and modelling-based advances have resulted in a better understanding of cell mechanics. Although the complexity of living cells, an increasing amount of information is nowadays available, several studies start to merge together and form a bigger picture of mechanotransduction processes. The technologies in the field have now started to be commercially available and rise the interest from biotechnology and pharmaceutical companies. This is therefore an exciting time in mechanobiology research for its unique potential in leading to better understand diseases mechanisms, their development as well as possible treatments.

Annex: FTIR spectroscopy for cell proliferation measurements

During the last year of this thesis I had the opportunity to lead an internal project within the group at CSEM. The main purpose of this project was to strengthen the working relationship within our group by working on an project involving our main expertises (optics, mechanical design and biology). The process to decide the technical content of this project consisted in having every member proposing an idea and then voting among these propositions. The proposition I made was selected and I have then been in charge of organising the work of this project. The work presented here has been performed by all the group members.

The technical objective of this project was to measure living cell proliferation using Fourier transform infra-red spectroscopy (FTIR) and validate the obtained results through comparison with a standard technique.
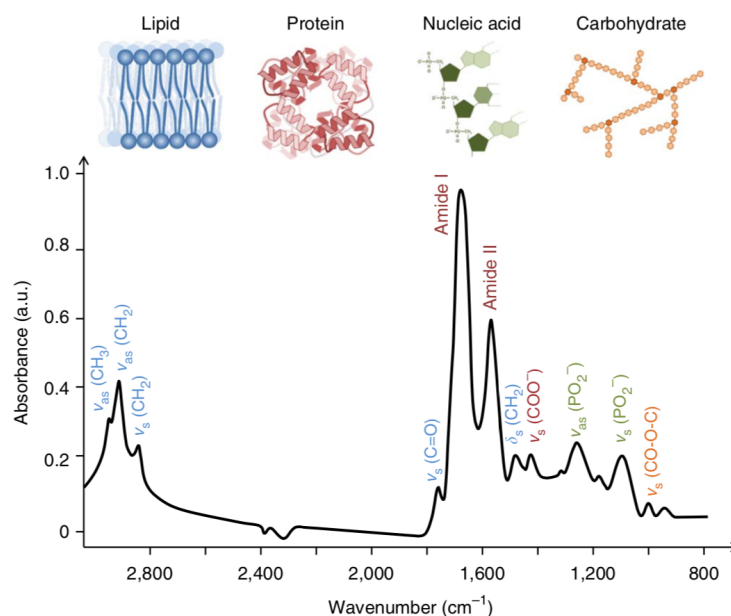
Figure 7.2 – Typical biological sample spectrum showing biomolecular peaks and the components to which they correspond (from [176]).

FTIR is a technique rapidly gaining interest for the analysis of biological samples. It has several

advantages over traditional analysis such as fluorescence based ones. It allows in fact rapid chemical identification without being destructive and allowing the investigation of sample dynamics [176].

This measurement is therefore very interesting for cell investigations, with the potential to distinguish between different type of cells as well as for detecting anomalies. FTIR relies on measuring the infra-red vibrational modes by analysing the interaction of the sample with light. These vibrational modes are strictly correlated to the molecular bonds within a sample and thus results in giving a quantified chemical fingerprint of the structure of the specimen as shown in Figure 7.2.

The interesting range for biological tissues lies within the mid-infrared range of 3 μm - 12.5 μm where it is possible to examine the structure and chemical composition of molecules such as phospholipids, proteins, nucleic acids and their interactions [177].
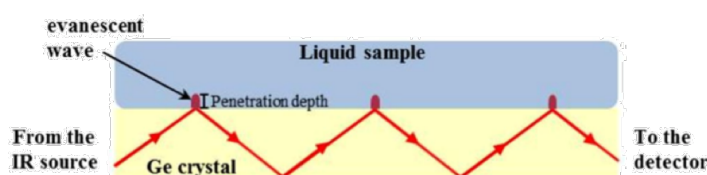
(a)
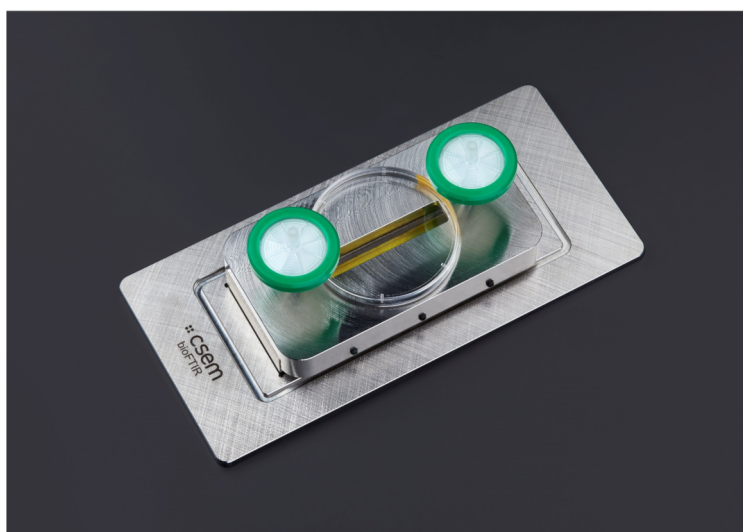
(b)

Figure 7.3 – ATR element for spectroscopy on liquid samples: (a) illustration fo the working mechanisms of ATR with a sample (from [177]), (b) Customized chamber built in this project, which makes the ATR element compatible with cell culture procedures.

Three major modes are commonly used for the analysis: transmission, transflection and attenuated total reflection (ATR). ATR has the main advantage to allow measurements in presence of water, thus analysing samples without modifying them through drying processes. Water shows in fact a very strong absorption over a broad range in the mid-IR which may

masks the absorption of other components of the tissue. ATR measurement principle relies on total internal reflection (Figure 7.3a). An IR beam enters the ATR element which acts as a wave-guide by reflecting the beam several times through its length. When a sample is in close contact to the crystal surface, the evanescent wave formed at the surface will lose energy at frequencies corresponding to the sample's absorbance.

In this project, we built a chamber for interfacing the ATR element with biological standard cell culture process and performing the cell proliferation measurements. The customized chamber shown in Figure 7.3b is made in biomedical grade stainless steel and is fixed onto the ATR element by means of lateral screws. This creates a chamber on top of the ATR element allowing the addition of liquid, also it allows to keep the sample sterility during the measurement. Sterile gas exchange is provided thanks to filters allowing air to enter the chamber.

(a)

(b)
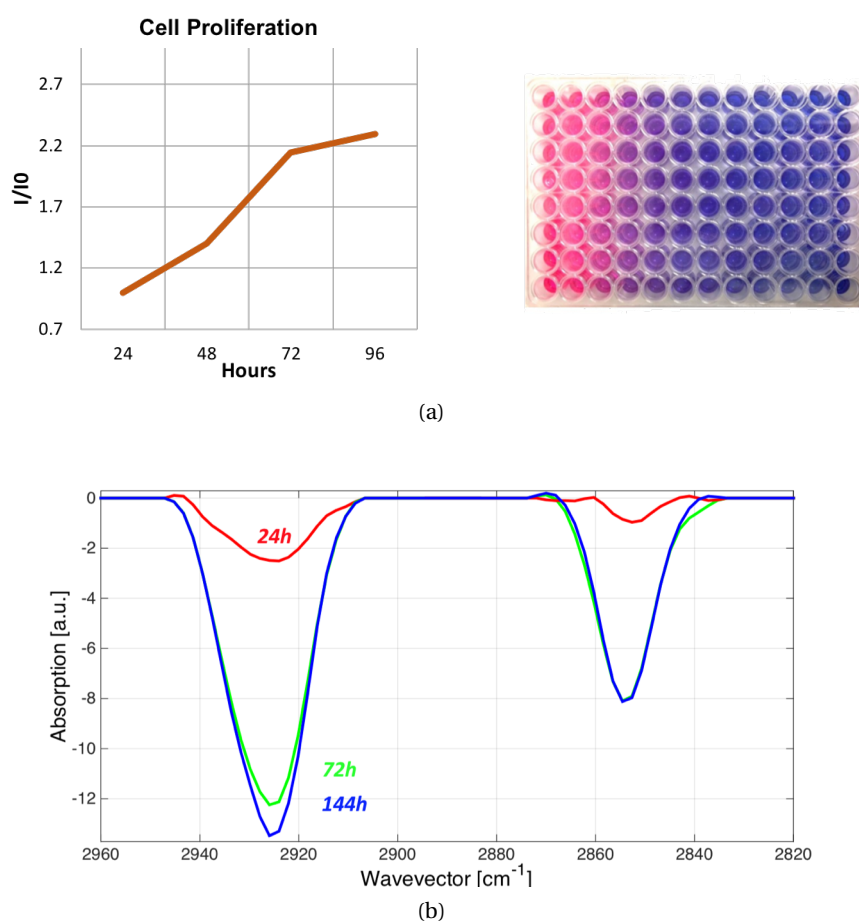
Figure 7.4 – Cell proliferation quantification through standard fluorescent Alamar Blue assay and FTIR: (a) The Alamar absorbance intensity increase with higher number of cells and a similar behaviour is showed by the FTIR results (b) where two peaks increase of intensity over time indicating an absorption increase from the sample. The increasing rate is similar between the two methods: characterized by a fast initial change followed by a saturation.

Human melanoma cells (WM239) are cultured on top of the ATR element within the chamber

and FTIR measurements are performed over few days to monitor their proliferation. In order to validate the FTIR measurement results, we compared FTIR measurement of cell proliferation over 4 days with a commercially available fluorescence method, Alamar Blue assay.

The Alamar Blue results obtained on melanoma cells over 4 days are showed in Figure 7.4a and show the intensity increasing fast up to the first three days and then slowing down because of the cell saturation on the surface.

The analysis of the FTIR measurement show the increase of two peaks height, indicating a higher absorption from the sample (Figure 7.4b). These peaks are in the IR region corresponding to lipid compounds suggesting that the measured signal is coming from the cell membrane, mainly made of lipid. These measurements show a response over few days which is very similar to the Alamar Blue assay one, an initial rapid increase of absorption followed by a saturation. The agreement with standard fluorescent assay indicates the validity of the FTIR measurements.

Within this project, we achieved the successful measurement of cell growth over few days performed with FTIR. These first results were in agreement with standard fluorescent-based assay. Further experiments are planned for the future, in particular to test the possibility to distinguish between two melanoma cells at different cancer stage.

Bibliography

[1] E. Moeendarbary and A. R. Harris, "Cell mechanics: principles, practices, and prospects," *Wiley Interdiscip Rev Syst Biol Med*, vol. 6, no. 5, pp. 371–88, 2014.

[2] J. Wang, D. Lu, D. Mao, and M. Long, "Mechanomics: an emerging field between biology and biomechanics," *Protein Cell*, vol. 5, no. 7, pp. 518–31, 2014.

[3] V. M. Weaver, "Cell and tissue mechanics: the new cell biology frontier," *Mol Biol Cell*, vol. 28, no. 14, pp. 1815–1818, 2017.

[4] F.-S. Quan and K. S. Kim, "Medical applications of the intrinsic mechanical properties of single cells," *Acta biochimica et biophysica Sinica*, vol. 48, no. 10, pp. 865–871, 2016.

[5] A. Poulin, C. S. Demir, S. Rosset, T. V. Petrova, and H. Shea, "Dielectric elastomer actuator for mechanical loading of 2d cell cultures," *Lab on a Chip*, vol. 16, no. 19, pp. 3788–3794, 2016.

[6] J. R. Lange, J. Steinwachs, T. Kolb, L. A. Lautscham, I. Harder, G. Whyte, and B. Fabry, "Microconstriction arrays for high-throughput quantitative measurements of cell mechanical properties," *Biophysical journal*, vol. 109, no. 1, pp. 26–34, 2015.

[7] J. Zlatanova and S. H. Leuba, "Magnetic tweezers: a sensitive tool to study dna and chromatin at the single-molecule level," *Biochemistry and cell biology*, vol. 81, no. 3, pp. 151–159, 2003.

[8] A. R. Harris, L. Peter, J. Bellis, B. Baum, A. J. Kabla, and G. T. Charras, "Characterizing the mechanics of cultured cell monolayers," *Proceedings of the National Academy of Sciences*, vol. 109, no. 41, pp. 16449–16454, 2012.

[9] D. Thompson, "'arcy w. on growth and form," *Cambridge: Univ. Press,*, 1917.

[10] T. Iskratsch, H. Wolfenson, and M. P. Sheetz, "Appreciating force and shape—the rise of mechanotransduction in cell biology," *Nature Reviews Molecular Cell Biology*, vol. 15, no. 12, p. 825, 2014.

[11] U. S. Schwarz, "Mechanobiology by the numbers: a close relationship between biology and physics," *NATURE REVIEWS| MOLECULAR CELL BIOLOGY*, vol. 18, p. 711, 2017.

Bibliography

[12] O. Du Roure, A. Saez, A. Buguin, R. H. Austin, P. Chavrier, P. Siberzan, and B. Ladoux, "Force mapping in epithelial cell migration," *Proceedings of the National Academy of Sciences*, vol. 102, no. 7, pp. 2390–2395, 2005.

[13] O. Araromi, A. Poulin, S. Rosset, M. Imboden, M. Favre, M. Giazzon, C. Martin-Olmos, F. Sorba, M. Liley, and H. Shea, "Optimization of thin-film highly-compliant elastomer sensors for contractility measurement of muscle cells," *Extreme Mechanics Letters*, vol. 9, pp. 1–10, 2016.

[14] S.-Y. Tee, J. Fu, C. S. Chen, and P. A. Janmey, "Cell shape and substrate rigidity both regulate cell stiffness," *Biophysical journal*, vol. 100, no. 5, pp. L25–L27, 2011.

[15] A. R. Harris and G. Charras, "Experimental validation of atomic force microscopy-based cell elasticity measurements," *Nanotechnology*, vol. 22, no. 34, p. 345102, 2011.

[16] A. W. Johnson and B. Harley, *Mechanobiology of cell-cell and cell-matrix interactions*. Springer Science & Business Media, 2011.

[17] J. M. Phillip, I. Aifuwa, J. Walston, and D. Wirtz, "The mechanobiology of aging," *Annual review of biomedical engineering*, vol. 17, pp. 113–141, 2015.

[18] D. R. Carter, G. S. Beaupré, N. J. Giori, and J. A. Helms, "Mechanobiology of skeletal regeneration.," *Clinical Orthopaedics and Related Research (1976-2007)*, vol. 355, pp. S41–S55, 1998.

[19] D. E. Discher, P. Janmey, and Y. L. Wang, "Tissue cells feel and respond to the stiffness of their substrate," *Science*, vol. 310, no. 5751, pp. 1139–43, 2005.

[20] A. J. Engler, S. Sen, H. L. Sweeney, and D. E. Discher, "Matrix elasticity directs stem cell lineage specification," *Cell*, vol. 126, no. 4, pp. 677–689, 2006.

[21] S. Giulitti, A. Zambon, F. Michielin, and N. Elvassore, "Mechanotransduction through substrates engineering and microfluidic devices," *Current Opinion in Chemical Engineering*, vol. 11, pp. 67–76, 2016.

[22] C. H. Turner and F. M. Pavalko, "Mechanotransduction and functional response of the skeleton to physical stress: the mechanisms and mechanics of bone adaptation," *Journal of orthopaedic science*, vol. 3, no. 6, pp. 346–355, 1998.

[23] M. Mullender, A. El Haj, Y. Yang, M. Van Duin, E. Burger, and J. Klein-Nulend, "Mechanotransduction of bone cellsin vitro: mechanobiology of bone tissue," *Medical and Biological Engineering and Computing*, vol. 42, no. 1, pp. 14–21, 2004.

[24] B. Williams, "Mechanical influences on vascular smooth muscle cell function," *Journal of hypertension*, vol. 16, no. 12, pp. 1921–1929, 1998.

[25] A. J. Putnam, "Mechanobiological control of cell fate for applications in cardiovascular regenerative medicine," in *Molecular and Cellular Mechanobiology*, pp. 219–253, Springer, 2016.

[26] K. Takahashi, Y. Kakimoto, K. Toda, and K. Naruse, "Mechanobiology in cardiac physiology and diseases," *Journal of cellular and molecular medicine*, vol. 17, no. 2, pp. 225–232, 2013.

[27] R. Peyronnet, J. M. Nerbonne, and P. Kohl, "Cardiac mechano-gated ion channels and arrhythmias," *Circulation research*, vol. 118, no. 2, pp. 311–329, 2016.

[28] B. Liu, S. McNally, J. I. Kilpatrick, S. P. Jarvis, and C. J. O'Brien, "Aging and ocular tissue stiffness in glaucoma," *Survey of ophthalmology*, 2017.

[29] D. J. Tschumperlin, F. Boudreault, and F. Liu, "Recent advances and new opportunities in lung mechanobiology," *Journal of biomechanics*, vol. 43, no. 1, pp. 99–107, 2010.

[30] J. M. Barnes, L. Przybyla, and V. M. Weaver, "Tissue mechanics regulate brain development, homeostasis and disease," *J Cell Sci*, vol. 130, no. 1, pp. 71–82, 2017.

[31] N. Khalilgharibi, J. Fouchard, P. Recho, G. Charras, and A. Kabla, "The dynamic mechanical properties of cellularised aggregates," *Current opinion in cell biology*, vol. 42, pp. 113–120, 2016.

[32] G. Bao and S. Suresh, "Cell and molecular mechanics of biological materials," *Nature materials*, vol. 2, no. 11, p. 715, 2003.

[33] M. L. Rodriguez, P. J. McGarry, and N. J. Sniadecki, "Review on cell mechanics: Experimental and modeling approaches," *Applied Mechanics Reviews*, vol. 65, no. 6, pp. 060801–060801, 2013.

[34] "The cytoskeleton online." http://www.macmillanhighered.com/BrainHoney/Resource/6716/digital_first_content/trunk/test/morris2e/morris2e_ch10_5.html. Accessed: 2018-08-28.

[35] D. A. Fletcher and R. D. Mullins, "Cell mechanics and the cytoskeleton," *Nature*, vol. 463, no. 7280, pp. 485–92, 2010.

[36] B. Ladoux and R. M. Mege, "Mechanobiology of collective cell behaviours," *Nat Rev Mol Cell Biol*, vol. 18, no. 12, pp. 743–757, 2017.

[37] H. Kubitschke, E. W. Morawetz, J. A. Käs, and J. Schnauß, *Physical Properties of Single Cells and Collective Behavior.* 2018.

[38] P. Friedl and D. Gilmour, "Collective cell migration in morphogenesis, regeneration and cancer," *Nature reviews Molecular cell biology*, vol. 10, no. 7, p. 445, 2009.

Bibliography

[39] A. G. Banerjee, S. Chowdhury, S. K. Gupta, and W. Losert, "Survey on indirect optical manipulation of cells, nucleic acids, and motor proteins," *Journal of Biomedical Optics*, vol. 16, no. 5, p. 051302, 2011.

[40] J.-F. Allemand, D. Bensimon, and V. Croquette, "Stretching dna and rna to probe their interactions with proteins," *Current opinion in structural biology*, vol. 13, no. 3, pp. 266–274, 2003.

[41] F. K. Glenister, R. L. Coppel, A. F. Cowman, N. Mohandas, and B. M. Cooke, "Contribution of parasite proteins to altered mechanical properties of malaria-infected red blood cells," *Blood*, vol. 99, no. 3, pp. 1060–1063, 2002.

[42] H. Zhang and K.-K. Liu, "Optical tweezers for single cells," *Journal of The Royal Society Interface*, vol. 5, no. 24, pp. 671–690, 2008.

[43] M. Dao, C. T. Lim, and S. Suresh, "Mechanics of the human red blood cell deformed by optical tweezers," *Journal of the Mechanics and Physics of Solids*, vol. 51, no. 11-12, pp. 2259–2280, 2003.

[44] W. R. Trickey, F. P. Baaijens, T. A. Laursen, L. G. Alexopoulos, and F. Guilak, "Determination of the poisson's ratio of the cell: recovery properties of chondrocytes after release from complete micropipette aspiration," *Journal of biomechanics*, vol. 39, no. 1, pp. 78–87, 2006.

[45] A. R. Harris, A. Daeden, and G. T. Charras, "Formation of adherens junctions leads to the emergence of a tissue-level tension in epithelial monolayers," *J Cell Sci*, pp. jcs–142349, 2014.

[46] A. M. Handorf, Y. Zhou, M. A. Halanski, and W.-J. Li, "Tissue stiffness dictates development, homeostasis, and disease progression," *Organogenesis*, vol. 11, no. 1, pp. 1–15, 2015.

[47] C. M. Nelson and J. P. Gleghorn, "Sculpting organs: mechanical regulation of tissue development," *Annual review of biomedical engineering*, vol. 14, pp. 129–154, 2012.

[48] R. Akhtar, M. J. Sherratt, J. K. Cruickshank, and B. Derby, "Characterizing the elastic properties of tissues," *Materials Today*, vol. 14, no. 3, pp. 96–105, 2011.

[49] Y.-B. Lu, K. Franze, G. Seifert, C. Steinhäuser, F. Kirchhoff, H. Wolburg, J. Guck, P. Janmey, E.-Q. Wei, J. Käs, *et al.*, "Viscoelastic properties of individual glial cells and neurons in the cns," *Proceedings of the National Academy of Sciences*, vol. 103, no. 47, pp. 17759–17764, 2006.

[50] M. Radmacher, M. Fritz, C. M. Kacher, J. P. Cleveland, and P. K. Hansma, "Measuring the viscoelastic properties of human platelets with the atomic force microscope," 1996.

[51] E. Evans, N. Mohandas, and A. Leung, "Static and dynamic rigidities of normal and sickle erythrocytes. major influence of cell hemoglobin concentration.," *The Journal of clinical investigation*, vol. 73, no. 2, pp. 477–488, 1984.

[52] D. A. Moulding, E. Moeendarbary, L. Valon, J. Record, G. T. Charras, and A. J. Thrasher, "Excess f-actin mechanically impedes mitosis leading to cytokinesis failure in x-linked neutropenia by exceeding aurora b kinase error correction capacity," *Blood*, pp. blood–2012, 2012.

[53] P. A. Coulombe, M. L. Kerns, and E. Fuchs, "Epidermolysis bullosa simplex: a paradigm for disorders of tissue fragility," *The Journal of clinical investigation*, vol. 119, no. 7, pp. 1784–1793, 2009.

[54] S. Getsios, A. C. Huen, and K. J. Green, "Working out the strength and flexibility of desmosomes," *Nature reviews Molecular cell biology*, vol. 5, no. 4, p. 271, 2004.

[55] E. Levine, C. H. Lee, C. Kintner, and B. M. Gumbiner, "Selective disruption of e-cadherin function in early xenopus embryos by a dominant negative mutant," *Development*, vol. 120, no. 4, pp. 901–909, 1994.

[56] A. A. Anlaş and C. M. Nelson, "Tissue mechanics regulates form, function, and dysfunction," *Current opinion in cell biology*, vol. 54, pp. 98–105, 2018.

[57] Y. Sharma, L. Atia, C. S. Rhodes, S. J. DeCamp, J. Mitchel, and J. J. Fredberg, "Scaling physiologic function from cell to tissue in asthma, cancer, and development," *Annals of the American Thoracic Society*, vol. 15, no. Supplement 1, pp. S35–S37, 2018.

[58] A. K. Schroer and W. D. Merryman, "Mechanobiology of myofibroblast adhesion in fibrotic cardiac disease," *J Cell Sci*, pp. jcs–162891, 2015.

[59] F. M. Maynard, M. B. Bracken, G. Creasey, J. F. Ditunno, W. H. Donovan, T. B. Ducker, S. L. Garber, R. J. Marino, S. L. Stover, C. H. Tator, *et al.*, "International standards for neurological and functional classification of spinal cord injury," *Spinal cord*, vol. 35, no. 5, pp. 266–274, 1997.

[60] T. R. Cox and J. T. Erler, "Remodeling and homeostasis of the extracellular matrix: implications for fibrotic diseases and cancer," *Disease models & mechanisms*, pp. dmm–004077, 2011.

[61] L. K. Wood, E. Kayupov, J. P. Gumucio, C. L. Mendias, D. R. Claflin, and S. V. Brooks, "Intrinsic stiffness of extracellular matrix increases with age in skeletal muscles of mice," *Journal of applied physiology*, vol. 117, no. 4, pp. 363–369, 2014.

[62] D. M. Skovronsky, V. M.-Y. Lee, and J. Q. Trojanowski, "Neurodegenerative diseases: new concepts of pathogenesis and their therapeutic implications," *Annu. Rev. Pathol. Mech. Dis.*, vol. 1, pp. 151–170, 2006.

Bibliography

[63] M. Stolz, R. Gottardi, R. Raiteri, S. Miot, I. Martin, R. Imer, U. Staufer, A. Raducanu, M. Düggelin, W. Baschong, *et al.*, "Early detection of aging cartilage and osteoarthritis in mice and patient samples using atomic force microscopy," *Nature nanotechnology*, vol. 4, no. 3, p. 186, 2009.

[64] G. Weder, M. C. Hendriks-Balk, R. Smajda, D. Rimoldi, M. Liley, H. Heinzelmann, A. Meister, and A. Mariotti, "Increased plasticity of the stiffness of melanoma cells correlates with their acquisition of metastatic properties," *Nanomedicine: Nanotechnology, Biology and Medicine*, vol. 10, no. 1, pp. 141–148, 2014.

[65] M. Makale, "Cellular mechanobiology and cancer metastasis," *Birth Defects Research Part C: Embryo Today: Reviews*, vol. 81, no. 4, pp. 329–343, 2007.

[66] S. P. Carey, T. M. D'Alfonso, S. J. Shin, and C. A. Reinhart-King, "Mechanobiology of tumor invasion: engineering meets oncology," *Critical reviews in oncology/hematology*, vol. 83, no. 2, pp. 170–183, 2012.

[67] "JPK - CellHesion200 online." https://www.jpk.com/products/cell-tissue-mechanics-and-adhesion/cellhesion-200. Accessed: 2018-08-29.

[68] "Lumiks - Acoustic Force Spectroscopy online." https://lumicks.com/afs-acoustic-force-spectroscopy/. Accessed: 2018-08-29.

[69] "ZellMechanik online." https://www.zellmechanik.com/Products/AcCellerator.html. Accessed: 2018-08-29.

[70] "ParkSystems online." https://www.parksystems.com/index.php/jp/2018-07-05-09-27-23/474-bio-cell-analysis-with-the-launch-of-park-nx-bio. Accessed: 2018-08-29.

[71] T. Ohashi, M. Hagiwara, D. Bader, and M. Knight, "Intracellular mechanics and mechanotransduction associated with chondrocyte deformation during pipette aspiration," *Biorheology*, vol. 43, no. 3, 4, pp. 201–214, 2006.

[72] P. Honarmandi, H. Lee, M. J. Lang, and R. D. Kamm, "A microfluidic system with optical laser tweezers to study mechanotransduction and focal adhesion recruitment," *Lab on a chip*, vol. 11, no. 4, pp. 684–694, 2011.

[73] R. M. Hochmuth, "Micropipette aspiration of living cells," *Journal of biomechanics*, vol. 33, no. 1, pp. 15–22, 2000.

[74] S. Henon, G. Lenormand, A. Richert, and F. Gallet, "A new determination of the shear modulus of the human erythrocyte membrane using optical tweezers," *Biophysical journal*, vol. 76, no. 2, pp. 1145–1151, 1999.

[75] L. Wolff, P. Fernández, and K. Kroy, "Resolving the stiffening-softening paradox in cell mechanics," *PloS one*, vol. 7, no. 7, p. e40063, 2012.

[76] R. D. Goldman, S. Khuon, Y. H. Chou, P. Opal, and P. M. Steinert, "The function of intermediate filaments in cell shape and cytoskeletal integrity.," *The Journal of cell biology*, vol. 134, no. 4, pp. 971–983, 1996.

[77] X. Trepat, L. Deng, S. S. An, D. Navajas, D. J. Tschumperlin, W. T. Gerthoffer, J. P. Butler, and J. J. Fredberg, "Universal physical responses to stretch in the living cell," *Nature*, vol. 447, no. 7144, p. 592, 2007.

[78] R. Krishnan, C. Y. Park, Y.-C. Lin, J. Mead, R. T. Jaspers, X. Trepat, G. Lenormand, D. Tambe, A. V. Smolensky, A. H. Knoll, *et al.*, "Reinforcement versus fluidization in cytoskeletal mechanoresponsiveness," *PloS one*, vol. 4, no. 5, p. e5486, 2009.

[79] K. Wolf, M. Te Lindert, M. Krause, S. Alexander, J. Te Riet, A. L. Willis, R. M. Hoffman, C. G. Figdor, S. J. Weiss, and P. Friedl, "Physical limits of cell migration: control by ecm space and nuclear deformation and tuning by proteolysis and traction force," *J Cell Biol*, vol. 201, no. 7, pp. 1069–1084, 2013.

[80] C. Rotsch, K. Jacobson, and M. Radmacher, "Dimensional and mechanical dynamics of active and stable edges in motile fibroblasts investigated by using atomic force microscopy," *Proceedings of the National Academy of Sciences*, vol. 96, no. 3, pp. 921–926, 1999.

[81] D. Pesen and J. H. Hoh, "Micromechanical architecture of the endothelial cell cortex," *Biophysical journal*, vol. 88, no. 1, pp. 670–679, 2005.

[82] S. E. Cross, Y.-S. Jin, J. Rao, and J. K. Gimzewski, "Nanomechanical analysis of cells from cancer patients," *Nature nanotechnology*, vol. 2, no. 12, p. 780, 2007.

[83] M. Lekka, "Discrimination between normal and cancerous cells using afm," *Bionanoscience*, vol. 6, no. 1, pp. 65–80, 2016.

[84] K. Haase and A. E. Pelling, "Investigating cell mechanics with atomic force microscopy," *Journal of The Royal Society Interface*, vol. 12, no. 104, p. 20140970, 2015.

[85] A. M. Collinsworth, S. Zhang, W. E. Kraus, and G. A. Truskey, "Apparent elastic modulus and hysteresis of skeletal muscle cells throughout differentiation," *American Journal of Physiology-Cell Physiology*, vol. 283, no. 4, pp. C1219–C1227, 2002.

[86] W. A. Lam, M. J. Rosenbluth, and D. A. Fletcher, "Chemotherapy exposure increases leukemia cell stiffness," *Blood*, vol. 109, no. 8, pp. 3505–3508, 2007.

[87] M. J. Rosenbluth, W. A. Lam, and D. A. Fletcher, "Force microscopy of nonadherent cells: a comparison of leukemia cell deformability," *Biophysical journal*, vol. 90, no. 8, pp. 2994–3003, 2006.

[88] S. Féréol, R. Fodil, G. Pelle, B. Louis, and D. Isabey, "Cell mechanics of alveolar epithelial cells (aecs) and macrophages (ams)," *Respiratory physiology & neurobiology*, vol. 163, no. 1-3, pp. 3–16, 2008.

[89] V. Swaminathan, K. Mythreye, E. T. O'Brien, A. Berchuck, G. C. Blobe, and R. Superfine, "Mechanical stiffness grades metastatic potential in patient tumor cells and in cancer cell lines," *Cancer research*, pp. canres–0247, 2011.

[90] A. R. Bausch, W. Möller, and E. Sackmann, "Measurement of local viscoelasticity and forces in living cells by magnetic tweezers," *Biophysical journal*, vol. 76, no. 1, pp. 573–579, 1999.

[91] C.-H. Chiou, Y.-Y. Huang, M.-H. Chiang, H.-H. Lee, and G.-B. Lee, "New magnetic tweezers for investigation of the mechanical properties of single dna molecules," *Nanotechnology*, vol. 17, no. 5, p. 1217, 2006.

[92] A. S. Kris, R. D. Kamm, and A. L. Sieminski, "Vasp involvement in force-mediated adherens junction strengthening," *Biochemical and biophysical research communications*, vol. 375, no. 1, pp. 134–138, 2008.

[93] N. Walter, C. Selhuber, H. Kessler, and J. P. Spatz, "Cellular unbinding forces of initial adhesion processes on nanopatterned surfaces probed with magnetic tweezers," *Nano letters*, vol. 6, no. 3, pp. 398–402, 2006.

[94] B. D. Matthews, D. R. Overby, F. J. Alenghat, J. Karavitis, Y. Numaguchi, P. G. Allen, and D. E. Ingber, "Mechanical properties of individual focal adhesions probed with a magnetic microneedle," *Biochemical and biophysical research communications*, vol. 313, no. 3, pp. 758–764, 2004.

[95] G. Schmid-Schönbein, K.-L. Sung, H. Tözeren, R. Skalak, and S. Chien, "Passive mechanical properties of human leukocytes," *Biophysical Journal*, vol. 36, no. 1, pp. 243–256, 1981.

[96] K. Guevorkian and J.-L. Maître, "Micropipette aspiration: A unique tool for exploring cell and tissue mechanics in vivo," in *Methods in cell biology*, vol. 139, pp. 187–201, Elsevier, 2017.

[97] J. Dai and M. P. Sheetz, "Mechanical properties of neuronal growth cone membranes studied by tether formation with laser optical tweezers," *Biophysical journal*, vol. 68, no. 3, pp. 988–996, 1995.

[98] K. Ramser and D. Hanstorp, "Optical manipulation for single-cell studies," *Journal of biophotonics*, vol. 3, no. 4, pp. 187–206, 2010.

[99] M. Gyger, R. Stange, T. R. Kießling, A. Fritsch, K. B. Kostelnik, A. G. Beck-Sickinger, M. Zink, and J. A. Käs, "Active contractions in single suspended epithelial cells," *European Biophysics Journal*, vol. 43, no. 1, pp. 11–23, 2014.

[100] K. D. Nyberg, K. H. Hu, S. H. Kleinman, D. B. Khismatullin, M. J. Butte, and A. C. Rowat, "Quantitative deformability cytometry: rapid, calibrated measurements of cell mechanical properties," *Biophysical journal*, vol. 113, no. 7, pp. 1574–1584, 2017.

[101] A. Mietke, O. Otto, S. Girardo, P. Rosendahl, A. Taubenberger, S. Golfier, E. Ulbricht, S. Aland, J. Guck, and E. Fischer-Friedrich, "Extracting cell stiffness from real-time deformability cytometry: theory and experiment," *Biophysical journal*, vol. 109, no. 10, pp. 2023–2036, 2015.

[102] C.-C. Chang, K. Wang, Y. Zhang, D. Chen, B. Fan, C.-H. Hsieh, J. Wang, M.-H. Wu, and J. Chen, "Mechanical property characterization of hundreds of single nuclei based on microfluidic constriction channel," *Cytometry Part A*, 2018.

[103] J. Qu, W. Zhang, A. Jung, S. Silva-Da Cruz, and X. Liu, "Microscale compression and shear testing of soft materials using an mems microgripper with two-axis actuators and force sensors.," *IEEE Trans. Automation Science and Engineering*, vol. 14, no. 2, pp. 834–843, 2017.

[104] B. Barazani, S. Warnat, A. Fine, and T. Hubbard, "Mems squeezer for the measurement of single cell rupture force, stiffness change, and hysteresis," *Journal of Micromechanics and Microengineering*, vol. 27, no. 2, p. 025002, 2016.

[105] E. Sadeghipour, M. A. Garcia, W. J. Nelson, and B. L. Pruitt, "Mems enabled live cell mechanics and dynamics in shear loading," in *Solid-State Sensors, Actuators and Microsystems (TRANSDUCERS), 2017 19th International Conference on*, pp. 202–205, IEEE, 2017.

[106] D. B. Serrell, J. Law, A. J. Slifka, R. L. Mahajan, and D. S. Finch, "A uniaxial biomems device for imaging single cell response during quantitative force-displacement measurements," *Biomedical microdevices*, vol. 10, no. 6, p. 883, 2008.

[107] S. Kollimada, S. Balakrishnan, C. K. Malhi, S. R. Raju, M. Suma, S. Das, and G. Ananthasuresh, "A micro-mechanical device for in-situ stretching of single cells cultured on it," *Journal of Micro-Bio Robotics*, vol. 13, no. 1-4, pp. 27–37, 2017.

[108] H. Kamble, M. J. Barton, M. Jun, S. Park, and N.-T. Nguyen, "Cell stretching devices as research tools: engineering and biological considerations," *Lab on a Chip*, vol. 16, no. 17, pp. 3193–3203, 2016.

[109] D. Tremblay, S. Chagnon-Lessard, M. Mirzaei, A. E. Pelling, and M. Godin, "A microscale anisotropic biaxial cell stretching device for applications in mechanobiology," *Biotechnology letters*, vol. 36, no. 3, pp. 657–665, 2014.

[110] C. Simmons, J. Sim, P. Baechtold, A. Gonzalez, C. Chung, N. Borghi, and B. Pruitt, "Integrated strain array for cellular mechanobiology studies," *Journal of Micromechanics and Microengineering*, vol. 21, no. 5, p. 054016, 2011.

[111] K. Van Vliet, G. Bao, and S. Suresh, "The biomechanics toolbox: experimental approaches for living cells and biomolecules," *Acta materialia*, vol. 51, no. 19, pp. 5881–5905, 2003.

[112] C. Neidlinger-Wilke, H.-J. Wilke, and L. Claes, "Cyclic stretching of human osteoblasts affects proliferation and metabolism: a new experimental method and its application," *Journal of Orthopaedic Research*, vol. 12, no. 1, pp. 70–78, 1994.

[113] C. Neidlinger-Wilke, E. Grood, J.-C. Wang, R. Brand, and L. Claes, "Cell alignment is induced by cyclic changes in cell length: studies of cells grown in cyclically stretched substrates," *Journal of Orthopaedic Research*, vol. 19, no. 2, pp. 286–293, 2001.

[114] C. A. Davis, S. Zambrano, P. Anumolu, A. C. Allen, L. Sonoqui, and M. R. Moreno, "Device-based in vitro techniques for mechanical stimulation of vascular cells: a review," *Journal of biomechanical engineering*, vol. 137, no. 4, p. 040801, 2015.

[115] H. J. Kim, D. Huh, G. Hamilton, and D. E. Ingber, "Human gut-on-a-chip inhabited by microbial flora that experiences intestinal peristalsis-like motions and flow," *Lab on a Chip*, vol. 12, no. 12, pp. 2165–2174, 2012.

[116] A. Marsano, C. Conficconi, M. Lemme, P. Occhetta, E. Gaudiello, E. Votta, G. Cerino, A. Redaelli, and M. Rasponi, "Beating heart on a chip: a novel microfluidic platform to generate functional 3d cardiac microtissues," *Lab on a Chip*, vol. 16, no. 3, pp. 599–610, 2016.

[117] "Flexcell International Corporation online." http://www.flexcellint.com. Accessed: 2018-08-26.

[118] D. Huh, B. D. Matthews, A. Mammoto, M. Montoya-Zavala, H. Y. Hsin, and D. E. Ingber, "Reconstituting organ-level lung functions on a chip," *Science*, vol. 328, no. 5986, pp. 1662–1668, 2010.

[119] N. R. Chevalier, E. Gazguez, S. Dufour, and V. Fleury, "Measuring the micromechanical properties of embryonic tissues," *Methods*, vol. 94, pp. 120–128, 2016.

[120] G. Bartalena, Y. Loosli, T. Zambelli, and J. G. Snedeker, "Biomaterial surface modifications can dominate cell-substrate mechanics: the impact of pdms plasma treatment on a quantitative assay of cell stiffness," *Soft Matter*, vol. 8, no. 3, pp. 673–681, 2012.

[121] J. C. Selby and M. A. Shannon, "Apparatus for measuring the finite load-deformation behavior of a sheet of epithelial cells cultured on a mesoscopic freestanding elastomer membrane," *Review of Scientific Instruments*, vol. 78, no. 9, p. 094301, 2007.

[122] E. Kang, J. Ryoo, G. S. Jeong, Y. Y. Choi, S. M. Jeong, J. Ju, S. Chung, S. Takayama, and S.-H. Lee, "Large-scale, ultrapliable, and free-standing nanomembranes," *Advanced Materials*, vol. 25, no. 15, pp. 2167–2173, 2013.

[123] C. Gullekson, M. Walker, J. L. Harden, and A. E. Pelling, "Measuring mechanodynamics in an unsupported epithelial monolayer grown at an air–water interface," *Molecular biology of the cell*, vol. 28, no. 1, pp. 111–119, 2017.

[124] D. E. Backman, B. L. LeSavage, and J. Y. Wong, "Versatile and inexpensive hall-effect force sensor for mechanical characterization of soft biological materials," *Journal of biomechanics*, vol. 51, pp. 118–122, 2017.

[125] P. H. Wu, D. R. Aroush, A. Asnacios, W. C. Chen, M. E. Dokukin, B. L. Doss, P. Durand-Smet, A. Ekpenyong, J. Guck, N. V. Guz, P. A. Janmey, J. S. H. Lee, N. M. Moore, A. Ott, Y. C. Poh, R. Ros, M. Sander, I. Sokolov, J. R. Staunton, N. Wang, G. Whyte, and D. Wirtz, "A comparison of methods to assess cell mechanical properties," *Nat Methods*, 2018.

[126] C.-H. Lin, C.-K. Wang, Y.-A. Chen, C.-C. Peng, W.-H. Liao, and Y.-C. Tung, "Measurement of in-plane elasticity of live cell layers using a pressure sensor embedded microfluidic device," *Scientific reports*, vol. 6, p. 36425, 2016.

[127] H. Liu, L. A. MacQueen, J. F. Usprech, H. Maleki, K. L. Sider, M. G. Doyle, Y. Sun, and C. A. Simmons, "Microdevice arrays with strain sensors for 3d mechanical stimulation and monitoring of engineered tissues," *Biomaterials*, vol. 172, pp. 30–40, 2018.

[128] D. Lee, A. G. Erickson, T. You, A. T. Dudley, and S. Ryu, "Pneumatic microfluidic cell compression device for high-throughput study of chondrocyte mechanobiology," *Lab on a Chip*, 2018.

[129] L. MacQueen, O. Chebotarev, C. A. Simmons, and Y. Sun, "Miniaturized platform with on-chip strain sensors for compression testing of arrayed materials," *Lab Chip*, vol. 12, no. 20, pp. 4178–84, 2012.

[130] S. Holmberg, B. Enquist, and P. Thilderkvist, "Evaluation of sheet metal formability by tensile tests," *Journal of Materials Processing Technology*, vol. 145, no. 1, pp. 72–83, 2004.

[131] W. Chen, F. Lu, and M. Cheng, "Tension and compression tests of two polymers under quasi-static and dynamic loading," *Polymer testing*, vol. 21, no. 2, pp. 113–121, 2002.

[132] A. N. Annaidh, K. Bruyère, M. Destrade, M. D. Gilchrist, and M. Otténio, "Characterization of the anisotropic mechanical properties of excised human skin," *Journal of the mechanical behavior of biomedical materials*, vol. 5, no. 1, pp. 139–148, 2012.

[133] A. R. Harris, J. Bellis, N. Khalilgharibi, T. Wyatt, B. Baum, A. J. Kabla, and G. T. Charras, "Generating suspended cell monolayers for mechanobiological studies," *Nature protocols*, vol. 8, no. 12, p. 2516, 2013.

[134] X. Ji, A. El Haitami, F. Sorba, S. Rosset, G. T. Nguyen, C. Plesse, F. Vidal, H. R. Shea, and S. Cantin, "Stretchable composite monolayer electrodes for low voltage dielectric elastomer actuators," *Sensors and Actuators B: Chemical*, vol. 261, pp. 135–143, 2018.

[135] S. Schlatter, S. Rosset, and H. Shea, "Inkjet printing of carbon black electrodes for dielectric elastomer actuators," in *Electroactive Polymer Actuators and Devices (EAPAD) 2017*, vol. 10163, p. 1016311, International Society for Optics and Photonics, 2017.

Bibliography

[136] "Rule of mixture derivation online." https://www.doitpoms.ac.uk/tlplib/bones/derivation_mixture_rules.php. Accessed: 2019-03-18.

[137] I. M. Ward and D. W. Hadley, "An introduction to the mechanical properties of solid polymers," 1993.

[138] E. M. Ahmed, "Hydrogel: Preparation, characterization, and applications: A review," *Journal of advanced research*, vol. 6, no. 2, pp. 105–121, 2015.

[139] T. Billiet, M. Vandenhaute, J. Schelfhout, S. Van Vlierberghe, and P. Dubruel, "A review of trends and limitations in hydrogel-rapid prototyping for tissue engineering," *Biomaterials*, vol. 33, no. 26, pp. 6020–6041, 2012.

[140] C.-W. Tsao, "Polymer microfluidics: Simple, low-cost fabrication process bridging academic lab research to commercialized production," *Micromachines*, vol. 7, no. 12, p. 225, 2016.

[141] G. Kofod, "Dielectric elastomer actuators." PhD thesis, 2001.

[142] R. N. Palchesko, L. Zhang, Y. Sun, and A. W. Feinberg, "Development of polydimethylsiloxane substrates with tunable elastic modulus to study cell mechanobiology in muscle and nerve," *PloS one*, vol. 7, no. 12, p. e51499, 2012.

[143] K. J. Regehr, M. Domenech, J. T. Koepsel, K. C. Carver, S. J. Ellison-Zelski, W. L. Murphy, L. A. Schuler, E. T. Alarid, and D. J. Beebe, "Biological implications of polydimethylsiloxane-based microfluidic cell culture," *Lab on a Chip*, vol. 9, no. 15, pp. 2132–2139, 2009.

[144] J. Gao, D. Guo, S. Santhanam, and G. K. Fedder, "Material characterization and transfer of large-area ultra-thin polydimethylsiloxane membranes," *Journal of Microelectromechanical Systems*, vol. 24, no. 6, pp. 2170–2177, 2015.

[145] M. Liu, J. Sun, Y. Sun, C. Bock, and Q. Chen, "Thickness-dependent mechanical properties of polydimethylsiloxane membranes," *Journal of micromechanics and microengineering*, vol. 19, no. 3, p. 035028, 2009.

[146] G. T. Charras and M. A. Horton, "Single cell mechanotransduction and its modulation analyzed by atomic force microscope indentation," *Biophysical journal*, vol. 82, no. 6, pp. 2970–2981, 2002.

[147] M. D. Francesca Sorba, Herbert Shea and C. Martin-Olmos, "Determining the stiffness of cell monolayers with a pneumatically actuated microfluidic device," *Twenty Second International Conference on Miniaturized Systems for Chemistry and Life Sciences, conference proceedings*, 2018.

[148] H. Vandenburgh, J. Shansky, F. Benesch-Lee, K. Skelly, J. M. Spinazzola, Y. Saponjian, and B. S. Tseng, "Automated drug screening with contractile muscle tissue engineered from dystrophic myoblasts," *The FASEB Journal*, vol. 23, no. 10, pp. 3325–3334, 2009.

[149] L. Trichet, J. Le Digabel, R. J. Hawkins, S. R. K. Vedula, M. Gupta, C. Ribrault, P. Hersen, R. Voituriez, and B. Ladoux, "Evidence of a large-scale mechanosensing mechanism for cellular adaptation to substrate stiffness," *Proceedings of the National Academy of Sciences*, vol. 109, no. 18, pp. 6933–6938, 2012.

[150] S. A. Maskarinec, C. Franck, D. A. Tirrell, and G. Ravichandran, "Quantifying cellular traction forces in three dimensions," *Proceedings of the National Academy of Sciences*, vol. 106, no. 52, pp. 22108–22113, 2009.

[151] F. Sorba and C. Martin-Olmos, "High resolution polymer coated strain sensors for in-liquid operation," *Microelectronic Engineering*, vol. 191, pp. 38–41, 2018.

[152] S. Rosset, O. A. Araromi, S. Schlatter, and H. R. Shea, "Fabrication process of silicone-based dielectric elastomer actuators," *Journal of visualized experiments: JoVE*, no. 108, 2016.

[153] G. Rápalo, J. D. Herwig, R. Hewitt, K. R. Wilhelm, C. M. Waters, and E. Roan, "Live cell imaging during mechanical stretch," *Journal of visualized experiments: JoVE*, no. 102, 2015.

[154] C. Guillot and T. Lecuit, "Mechanics of epithelial tissue homeostasis and morphogenesis," *Science*, vol. 340, no. 6137, pp. 1185–1189, 2013.

[155] R. Montesano, G. Schaller, and L. Orci, "Induction of epithelial tubular morphogenesis in vitro by fibroblast-derived soluble factors," *Cell*, vol. 66, no. 4, pp. 697–711, 1991.

[156] "MDCKII culture protocol online." https://www.atcc.org/products/all/CCL-34.aspx. Accessed: 2018-11-22.

[157] S. M. Zehnder, M. Suaris, M. M. Bellaire, and T. E. Angelini, "Cell volume fluctuations in mdck monolayers," *Biophysical journal*, vol. 108, no. 2, pp. 247–250, 2015.

[158] A. Ettinger and T. Wittmann, "Fluorescence live cell imaging," in *Methods in cell biology*, vol. 123, pp. 77–94, Elsevier, 2014.

[159] H. Zoellner, N. Paknejad, K. Manova, and M. A. Moore, "A novel cell-stiffness-fingerprinting analysis by scanning atomic force microscopy: comparison of fibroblasts and diverse cancer cell lines," *Histochemistry and cell biology*, vol. 144, no. 6, pp. 533–542, 2015.

[160] B. R. Brückner, H. Nöding, and A. Janshoff, "Viscoelastic properties of confluent mdck ii cells obtained from force cycle experiments," *Biophysical journal*, vol. 112, no. 4, pp. 724–735, 2017.

[161] N. Desprat, A. Richert, J. Simeon, and A. Asnacios, "Creep function of a single living cell," *Biophysical journal*, vol. 88, no. 3, pp. 2224–2233, 2005.

[162] N. D. Evans, R. O. Oreffo, E. Healy, P. J. Thurner, and Y. H. Man, "Epithelial mechanobiology, skin wound healing, and the stem cell niche," *Journal of the mechanical behavior of biomedical materials*, vol. 28, pp. 397–409, 2013.

[163] D. A. Schreier, O. Forouzan, T. A. Hacker, J. Sheehan, and N. Chesler, "Increased red blood cell stiffness increases pulmonary vascular resistance and pulmonary arterial pressure," *Journal of biomechanical engineering*, vol. 138, no. 2, p. 021012, 2016.

[164] K. Takemoto, T. Mizutani, K. Tamura, K. Takeda, H. Haga, and K. Kawabata, "The number of cyclic stretch regulates cellular elasticity in c2c12 myoblasts," *Open Journal of Cell Biology*, vol. 2, no. 03, p. 0, 2012.

[165] I. Schofield, R. Malik, A. Izzard, C. Austin, and A. Heagerty, "Vascular structural and functional changes in type 2 diabetes mellitus: evidence for the roles of abnormal myogenic responsiveness and dyslipidemia," *Circulation*, vol. 106, no. 24, pp. 3037–3043, 2002.

[166] J. Harle, V. Salih, F. Mayia, J. C. Knowles, and I. Olsen, "Effects of ultrasound on the growth and function of bone and periodontal ligament cells in vitro," *Ultrasound in medicine & biology*, vol. 27, no. 4, pp. 579–586, 2001.

[167] S. Na, A. Trache, J. Trzeciakowski, Z. Sun, G. Meininger, and J. Humphrey, "Time-dependent changes in smooth muscle cell stiffness and focal adhesion area in response to cyclic equibiaxial stretch," *Annals of biomedical engineering*, vol. 36, no. 3, pp. 369–380, 2008.

[168] L. Sigaut, C. von Bilderling, M. Bianchi, J. E. Burdisso, L. Gastaldi, and L. I. Pietrasanta, "Live cell imaging reveals focal adhesions mechanoresponses in mammary epithelial cells under sustained equibiaxial stress," *Scientific reports*, vol. 8, no. 1, p. 9788, 2018.

[169] X. Trepat, F. Puig, N. Gavara, J. J. Fredberg, R. Farre, and D. Navajas, "Effect of stretch on structural integrity and micromechanics of human alveolar epithelial cell monolayers exposed to thrombin," *American Journal of Physiology-Lung Cellular and Molecular Physiology*, vol. 290, no. 6, pp. L1104–L1110, 2006.

[170] T. R. Kießling, R. Stange, J. A. Käs, and A. W. Fritsch, "Thermorheology of living cells—impact of temperature variations on cell mechanics," *New Journal of Physics*, vol. 15, no. 4, p. 045026, 2013.

[171] P. Abdel-Sayed, M. N. Moghadam, R. Salomir, D. Tchernin, and D. P. Pioletti, "Intrinsic viscoelasticity increases temperature in knee cartilage under physiological loading," *journal of the mechanical behavior of biomedical materials*, vol. 30, pp. 123–130, 2014.

[172] R. Sunyer, X. Trepat, J. Fredberg, R. Farre, and D. Navajas, "The temperature dependence of cell mechanics measured by atomic force microscopy," *Physical biology*, vol. 6, no. 2, p. 025009, 2009.

[173] M. Li, L. Liu, N. Xi, Y. Wang, X. Xiao, and W. Zhang, "Effects of temperature and cellular interactions on the mechanics and morphology of human cancer cells investigated by atomic force microscopy," *Science China Life Sciences*, vol. 58, no. 9, pp. 889–901, 2015.

[174] F. Rico, C. Chu, M. H. Abdulreda, Y. Qin, and V. T. Moy, "Temperature modulation of integrin-mediated cell adhesion," *Biophysical journal*, vol. 99, no. 5, pp. 1387–1396, 2010.

[175] C. Chan, G. Whyte, L. Boyde, G. Salbreux, and J. Guck, "Impact of heating on passive and active biomechanics of suspended cells," *Interface focus*, vol. 4, no. 2, p. 20130069, 2014.

[176] M. J. Baker, J. Trevisan, P. Bassan, R. Bhargava, H. J. Butler, K. M. Dorling, P. R. Fielden, S. W. Fogarty, N. J. Fullwood, K. A. Heys, *et al.*, "Using fourier transform ir spectroscopy to analyze biological materials," *Nature protocols*, vol. 9, no. 8, p. 1771, 2014.

[177] R. Minnes, M. Nissinmann, Y. Maizels, G. Gerlitz, A. Katzir, and Y. Raichlin, "Using attenuated total reflection fourier transform infra-red (atr, ftir) spectroscopy to distinguish between melanoma cells with a different metastatic potential," *Scientific reports*, vol. 7, no. 1, p. 4381, 2017.

List of abbreviations

MEMS	microelectromechanical devices
ECM	extra-cellular matrix
AFM	atomic force microscopy
MTC	magnetic twisting cytometry
PDMS	polydimethylsiloxane
PMMA	poly(methyl methacrylate
PC	polycarbonate
PS	polystyrene
PET	polyethylene terephthalate
PAA	poly(acrylic acid)
FEA	finite element analysis
DEA	dielectric elastomer actuators
CNT	carbon nanotubes
$SaOS_2$	Sarcoma osteogenic cell line
EDTA	ethylenediaminetetraacetic acid
MDCK	Madin-Darby Canine Kidney
DI	deionized water
CNC	computer numerical control
TFM	traction Force Microscopy
EMEM	Eagle's Minimum Essential Medium
BSA	bovine serum albumin
DAPI	4',6-diamidino-2-phenylindole
Zo-1	Zonula occludens-1
FTIR	Fourier transform infra-red spectroscopy
ATR	attenuated total reflection

List of publications

Journal articles

- **F. Sorba** and C. Martin-Olmos, 2018. High resolution polymer coated strain sensors for in-liquid operation. Microelectronic Engineering, 191, pp.38-41

- A. Poulin, M. Imboden, **F. Sorba**, S. Grazioli, C. Martin-Olmos, S. Rosset and H. Shea, 2018. An ultra-fast mechanically active cell culture substrate. Scientific reports, 8(1), p.9895.

- X. Ji, A. El Haitami, **F. Sorba**, S. Rosset, G.T. Nguyen, C. Plesse, F. Vidal, H. Shea, and S. Cantin, 2018. Stretchable composite monolayer electrodes for low voltage dielectric elastomer actuators. Sensors and Actuators B: Chemical, 261, pp.135-143.

- O.A. Araromi, A. Poulin, S. Rosset, M. Imboden, M. Favre, M. Giazzon, C. Martin-Olmos, **F. Sorba**, M. Liley and H. Shea, 2016. Optimization of thin-film highly-compliant elastomer sensors for contractility measurement of muscle cells. Extreme Mechanics Letters, 9, pp.1-10.

Submitted

- **F. Sorba**, A. Poulin, R. Isher, H. Shea and C. Martin-Olmos. Integrated elastomer-based device for measuring the mechanics of adhering cell monolayers. Submitted to Lab on Chip, January 2019.

In preparation

- **F. Sorba**, T. Kim, R. Ischer, A. Rowat and C. Martin-Olmos. Real time force measurements of cells through high sensitive in-liquid strain sensors

Conference proceedings

- **F. Sorba**, H. Shea, M. Despont, C. Martin-Olmos, "Determining the stiffness of cell monolayers with a pneumatically actuated microfluidic device", presented at the Twenty Second International Conference on Miniaturized Systems for Chemistry and Life Sciences (μTAS), Kaohsiung (Taiwan), November 11-15, 2018. (**Finalist for the best poster award, received Abstract Travel Award.**)

Oral presentations

- **F. Sorba**, A. Poulin, B. Dunan, M. Despont, H. Shea, C. Martin-Olmos, "Miniaturized elastomer-based pneumatic actuator to measure mechanical properties of cell monolayers", presented at the 10th European Solid Mechanics Conference (ESMC), Bologna (Italy), July 2-6, 2018.

Poster presentations

- **F. Sorba**, H. Shea, C. Martin-Olmos, "Viscoelastic response of epithelial cell monolayers", presented at the International Conference on Micro and Nano Engineering (MNE), Copenhagen, September 24-27, 2018.

- **F. Sorba**, H. Shea, C. Martin-Olmos, "Measuring cell population elastic response to stretch", presented at 7th European CellMech Meeting, Windermere (England), June 21–23 June 2017.

- M. Imboden, A. Poulin, **F. Sorba**, S. Rosset, C. Martin-Olmos, H. Shea, "High Speed Mechanical Stretching of in vitro cell cultures", presented at the 20th edition NanoBioTech-Montreux, Montreux (Switzerland), November 7-9, 2016.

- **F. Sorba**, M. Giazzon, M. Liley, O.A. Araromi, H. Shea, C. Martin-Olmos, "Ultra-thin PDMS substrates for high-resolution stiffness measurements with cell stretchers", presented at the International Conference on Micro and Nano Engineering (MNE), Vienna, September 19-23, 2016.

Francesca Sorba

Rue de la Pierre à Mazel, 11
2000 Neuchâtel
Switzerland

Phone: +41 32 720 5838
Mobile: +41 78 733 03 91
Email: fra.sorba@gmail.com
Nationality: Italian

Education

2015-2019	**PhD in Microsystems and Microelectronics**	
	Centre Suisse d'Électronique et Microtechnique (CSEM SA) and École Polytechnique Fédérale de Lausanne (EPFL), Soft Transducers Laboratory (LMTS), Switzerland.	
2013-2015	**MSc in Microengineering** (GPA 5.53/6.00)	
	École Polytechnique Fédérale de Lausanne (EPFL), Switzerland.	
	Specialization in Micro and Nano System.	
	Master project at CSEM, Switzerland.	
2009-2013	**BSc in Physic Engineering** (110/110)	
	Politecnico di Torino, Italy.	

Languages

English	Fluent, written and spoken
French	Fluent, written and spoken
Italian	Native
German	Basic knowledge

Technical skills

Engineering	SolidWorks, COMSOL, MATLAB, LabVIEW
Programming	C++, Phyton
Biomedical	Immunofluorescence imaging
Office	Microsoft Office, Latex, Origin, Inkscape, ImageJ